



Hassan First University of Settat
 Doctoral Studies Centre in Sciences,
 Techniques & Medical Sciences.



Faculty of Sciences & Techniques
 Settat

DOCTORAL THESIS

To obtain the Doctorate degree in Sciences & Techniques
 Doctoral discipline: **Biology, Health & Environment**
 Speciality: **Chemistry-Physics**

Thesis thematic:

Removal of some selected micropollutants in aqueous solution by advanced oxidation processes: case of Levafix blue dye, Difenconazole & Acibenzolar-S-Methyl fungicides

Presented by:

Hajar LAMKHANTER

Thesis Defended on 15/09/2022 at 10 am in front the examination committee members:

Pr. Jamal Naja	PES	FST, Hassan First University of Settat	President
Pr. Abdelhak Kherbeche	PES	EST, Sidi Med Ben Abdellah University, Fes	Reporter
Pr. Souad EL Hajjaji	PES	FS, Mohamed V University of Rabat	Reporter
Pr. Bouchaib Manoun	PES	FST, Hassan First University of Settat	Reporter
Pr. Mika Sillanpää	PES	Chemistry Department, Aarhus University, Denmark	Examiner
Pr. Hafida Mountacer	PES	FST, Hassan First University of Settat	Supervisor

Academic year: 2021-2022

Abstract

Over the last decades, Human consumption leads to massive industrial sector manufacturing. A regular utilization of micropollutants (dyes, pesticides, pharmaceuticals, and personal care products...etc) that end up the aquatic environment present real threat and considered ecosystem perturbators. Advanced oxidation processes are progressively applied for persistent pollutants degradation instead the conventional methods that have been confirmed inefficient. This research focused on Fenton-based processes using various categories of irradiations source in different type of reactors combined with commercial and synthesized material, and it has been tested on removal of three selected micropollutants, a dye and two pesticides. The degradation of Levafix Blue dye was investigated using Fenton and Visible light photo-Fenton processes. Under acidic medium, it has been observed that both processes, Fenton and Photo-Fenton, were able to eliminate roughly 99% of pollutant. However, the increase of iron concentration leads to the inhibition of reaction. The photodegradation of difenoconazole fungicide was carried out via Photo-Fenton process using synthesized α -Fe₂O₃ nanoparticles. The α -Fe₂O₃ was prepared using hydrothermal approach. Average crystallite size has been recorded to be 27 nm and the surface area was found to be $S_{Bet} = 24.82 \text{ m}^2/\text{g}$. DFL removal has been tested under diverse systems: UV photolysis, UV/H₂O₂, UV/ α - Fe₂O₃, Fenton and Photo-Fenton process. The kinetic has been monitored using High-Performance Liquid Chromatography. As a result, it was demonstrated that Photo-Fenton process (UV/ α - Fe₂O₃/ H₂O₂) as most effective for DFL removal. The optimal catalyst dose of α - Fe₂O₃ for high removal rate is about 0.5 g/l at initial solution pH. The mineralization efficiency attained 83.67%. A possible mechanism pathway was proposed based on detected intermediates using gas chromatography-mass spectrometry analysis. The last part of this work focused on comparative study between photo-Fenton and Sono-Fenton processes on degradation of fungicide Acibenzolar-S-Methyl. The investigation exhibited that ultrasound irradiation has accelerated the efficiency of Fenton process via increasing the hydroxyl radicals generation the removal rate achieved the complete degradation rate within 20 min compared to photo-Fenton, Fenton, photolysis, and sonolysis processes. An optimization of parameters was carried out. A transformation mechanism pathway of the sonochemical oxidation was suggested.

Key Words: Micropollutants, AOPs, Dyes, Pesticides, Fenton, Photo-Fenton, hematite, mechanism pathway.

Hajar
 LAMKHANTER

Removal of some selected micropollutants in aqueous solution by advanced oxidation processes: case of Levafix blue dye, Difenconazole & Acibenzolar-S-Methyl fungicides

2022, Biology, Health
 & Environment

Allah جل جلاله Said,

وَمَا بِكُمْ مِنْ نِعْمَةٍ فَمِنَ اللَّهِ

“And whatever of blessings and good things you have, it is from Allah.” An-Nahl (16:53)

Undertaking this doctoral degree has been a truly life-challenging experience for me and it would not have been possible to do without the reconciliation from Allah and the support and guidance that I received from many people.

الحمد لله



Résumé

Au cours des dernière décennies, l'industrialisation a mené à un changement profond du de la société vers un comportement de consommation massive. L'utilisation régulière des micropolluants (colorants, pesticides, produits pharmaceutique et produits de soin personnels ...etc) et qui finissent dans le compartiment environnemental aquatique et qui sont considérés des perturbateurs de l'écosystème aquatique. Depuis leurs découverte, les procédés d'oxydation avancées sont progressivement appliqués pour le traitement des eaux usées spécifiquement pour la dégradation des polluants persistants comme alternative des méthodes conventionnelles inapproprié pour l'élimination de cette nouvelle génération de polluants. Dans le cadre de ce travail, nous nous sommes intéressés à l'application des procédés d'oxydation avancées hybride basés sur le réactif de Fenton en se servant de différents types de source d'irradiation. L'objectif majeur de l'étude consiste à investiguer la performance catalytique des procédés utilisés pour la dégradation de deux catégories de micropolluants ; un colorant textile (Bleu Levafix) et deux fongicides (Difénoconazole et Acibenzolar-S-Méthyle). La dégradation du colorant bleu Levafix a été performé par le procédé Fenton et le Photo-Fenton en utilisant la lumière visible. Une optimisation des paramètres influençant la réaction a été étudié pour les deux procédés. Dans un milieu acide, les deux procédés ont démontré une réelle efficacité du processus avec une capacité d'élimination de 99% du polluant. Cependant, l'augmentation de la concentration des ions ferreux inhibe la réaction. La photodégradation du fongicide difénoconazole a été réalisé par le procédé photo-Fenton en utilisant des nanoparticules de l'hématite synthétisées $\alpha\text{-Fe}_2\text{O}_3$ par voie hydrothermale. La taille moyenne des cristallites est de 27 nm et la surface spécifique est $S_{\text{Bet}} = 24,82 \text{ m}^2/\text{g}$. L'étude cinétique du Difénoconazole a été suivie par HPLC. Les résultats ont montré que le procédé photo-Fenton est le plus efficace pour la dégradation du polluant avec une dose optimal du catalyseur de 0.5g/L sans ajustement du pH. Un mécanisme réactionnel des voies de transformation possible du fongicide a été proposé en se basant sur la détection des photo-produits par GC/MS. La dernière partie de ce travail a été consacré à une étude comparative entre le procédé photo-Fenton et sono-Fenton pour la dégradation du fongicide Acibenzolar-S-Méthyle. L'investigation a démontré que les ultrasons ont accéléré l'efficacité de la réaction du Fenton via l'augmentation de la génération des radicaux hydroxyles. Après 20 min de traitement son-Fenton, une dégradation complète du polluant a été achevé en comparaison aux autres procédés. Une optimisation des paramètres impactant la réaction à été effectuée ainsi que la suggestion d'un mécanisme réactionnel de la voie d'oxydation sonochimique.

Mots clés : Micropolluants, procédés d'oxydation avancés, Fenton, Photo-Fenton, hématite, voie mécanistique de transformation.

DEDICATION

*A very special thank you to my **grandmother**, my mentor, for building a family of love, kindness, generosity, the knowledge and joy you bring to the lives of everyone around you. I would also like to say a heartfelt thank you to my **Mum & Dad** for always believing in me and encouraging me to follow my dreams. Moreover, I would like to thank also all members of my two families for helping in whatever way they could during this challenging period.*

I also would like to thank my friends for their friendship and emotional support through all these last years.



Thank you...

ACKNOWLEDGEMENTS

This work was conducted within the Engineering, Industrial Management and innovation (IMII) laboratory at Faculty of Sciences technologies, Hassan First University of Settat in collaboration with Separation Sciences Department, Lut-Lappeenranta University in Finland.

First and foremost, I am extremely grateful to Professor **Hafida Mountacer**, my main supervisor, who started by proposing this project and believing in my capacity to accomplish it. I am very grateful for her permanent support, scientific guidance, constant optimism and encouragement throughout this long walk with all its “ups and downs”. I deeply appreciate her careful revision of all work. I also would like to thank her friendship.

I would like to express my sincere gratitude for having met and worked with Professor **Mika Sillanpää** at Separation Sciences Department, Lut-Lappeenranta University in Finland, for his collaboration and providing all the necessary means for project experiments, his cheerful mood and support whenever needed.

I would also to thank Professor **Yuri Park** from Department of Environmental Engineering, Seoul National University of Science and Technology, Seoul, Korea. For her important considerations, suggestions and scientific guidance and for advices offering a valuable interdisciplinary view.

I deeply express a special appreciation to Dr **Sana Frindy** Post-doctoral researcher at Department of Chemical and Metallurgical Engineering, School of Chemical Engineering, Aalto University in Finland for her relevant contributions that enriched our work, all the dedication, patience and support.

Finally, my profound appreciation is extended to the examination committee members, Pr. **Souad EL HAJJAJI**, Pr. **Abdelhak KHERBECHE**, Pr. **Bouchaib MANOUN**, Pr. **Jamal NAJA** & Pr. **Abdelmalek DAHCHOUR** (as invited guest) for accepting to evaluate, and being part of the main dissertation.

LIST OF FIGURES

Figure 1: Sources and pathways of micropollutants	7
Figure 2: Sources and pathway of synthetic dyes to aquatic mediums.	11
Figure 3: Pesticide's contamination routes	16
Figure 4: Global world consumption of pesticides since 1990 to present (Food and Agriculture Organisation of United Nations 2021).	18
Figure 5: Advanced Oxidation Processes application.	23
Figure 6: History of ozone and ozonation in water treatment.	24
Figure 7: Propagation of electromagnetic wave in free space with electric and magnetic field components.	29
Figure 8: Schematic representation of electromagnetic spectrum range on the wavelength and frequency scale.	30
Figure 9: a) electronic transition between HOMO and LUMO levels. b) Energy levels showing the different types of electronic transitions within organic molecules from the more energetic $\sigma \rightarrow \sigma^*$ to the less energetic orbital $n \rightarrow \pi^*$.	33
Figure 10: Franck-Condon principle energy diagram, the vibronic transitions.	34
Figure 11: example of electronic structure of singlet and triplet states	35
Figure 12: Jablonski diagram for an organic molecule illustrating the photophysical processes.	37
Figure 13: The four pillars that have had a great impact in the development of heterogeneous photocatalysis.	39
Figure 14: Mechanism photocatalysis	40
Figure 15: Ultrasound frequency range	41
Figure 16: longitudinal wave graphic representation	42
Figure 17: Sonocatalytic mechanism of micropollutants removal.	43
Figure 18: Reaction sites in sonochemistry.	44
Figure 19: Absorption spectra of Levafix Blue in UV-Visible domain	56
Figure 20: Schematic diagram of hematite synthesis protocol.	59
Figure 21: Irradiation UV light system	60
Figure 22: Photoreactor with polychromatic irradiation system	61
Figure 23: ultrasonic irradiation system	62
Figure 24: schematic presentation of X-ray diffraction system	65
Figure 25: Schematic presentation of FT-IR spectroscopy analysis	66
Figure 26: In a gas adsorption measurement, the pores of the sample progressively fill with the adsorptive gas as pressure is increased.	67
Figure 27: Diffuse reflectance measurement principal	68
Figure 28: illustration of SEM analysis system	69
Figure 29: Schimatic explination of Raman analysis system	70
Figure 30: Calibration curve of Levafix Blue dye	71
Figure 31: Configuration of HPLC analysis system.	72
Figure 32: Calibration curve of difenoconazole fungicide	73
Figure 33: Calibration curve of Acibenzolar-S-Methyl fungicide	73
Figure 34: Absorption spectrum of Levafix Blue at different pH, [BL]=10 mg/L	78
Figure 35: the dye absorbance versus their pH solution	79
Figure 36: FT-IR spectrum of Levafix Blue dye	80
Figure 37: Irradiation intensity effect on BL degradation, pH=5,58, [BL]=10 mg/L	81
Figure 38: Degradation of BL under different systems, [BL]=10 mg/L, pH=3.0,	82
Figure 39: Effect of initial pH of solution, [BL]=10 mg/L, [H ₂ O ₂]=0.8M, and [Fe ²⁺]=10mM	83
Figure 40: Effect of initial dye concentration, pH=3.0, [H ₂ O ₂]=0.8M, and [Fe ²⁺]=10mM	84
Figure 41: Effect of hydrogen peroxide, [BL]=10 mg/L, pH=3.0, and [Fe ²⁺]=10mM	85
Figure 42: Effect of ferrous ions concentration, [BL]=10 mg/L, pH=3.0, [H ₂ O ₂]=0.8M.	86
Figure 43: Effect of Humic acid on BL degradation, pH=3.0, [BL]=10 mg/L, [H ₂ O ₂]=0.8M, and [Fe ²⁺]=10mM	87
Figure 44: UV-Vis diffuse reflectance spectra of hematite	94
Figure 45: Tauc plot for hematite bandgap determination	95
Figure 46: Nitrogen adsorption-desorption spectra	96
Figure 47: X-ray diffraction pattern of hematite α -Fe ₂ O ₃ .	97
Figure 48: SEM & TEM micrographs of hematite	98
Figure 49: RAMAN spectra of α -Fe ₂ O ₃	99

Figure 50: Photodegradation of DFL under different system(UV/ α - Fe ₂ O ₃ / H ₂ O ₂ , UV/ α - Fe ₂ O ₃ , UV/H ₂ O ₂ , UV, and α - Fe ₂ O ₃ / H ₂ O ₂), pH=5, [H ₂ O ₂]=9.79 M, [α - Fe ₂ O ₃]=0.5 g/l	100
Figure 51: pH effect, at 20 min of reaction,[H ₂ O ₂]=9.79M,[α - Fe ₂ O ₃]=0.5 g/l, UV	101
Figure 52: Hydrogen peroxide effect, pH=5, [α - Fe ₂ O ₃]=0.5 g/l ,UV	102
Figure 53: Effect of catalyst dosage, pH=5, [H ₂ O ₂]=9.79 M, UV.	103
Figure 54: pH=5, [H ₂ O ₂] =9.79 M, [α -Fe ₂ O ₃]=0.5 g/L, scavengers study	104
Figure 55: reusability of catalyst.	105
Figure 56: pH=5, [H ₂ O ₂] =9.79 M, [α -Fe ₂ O ₃]=0.5 g/L, kinetic study Ln(C ₀ /C)=f(time)	106
Figure 57: Representative HPLC chromatogram of Difenoconazole	107
Figure 58: HPLC chromatogram of photoproductes generated from the photocatalytic degradation of DFL	107
Figure 59: Mass spectrum of Difenoconazole at 15.76 min.	108
Figure 60: Mass spectrum of different identified photoproducts at various retention time.	109
Figure 61: Proposed transformation pathway of difenoconazole under Photo-Fenton process treatment.	111
Figure 62: Degradation and TOC removal rate under different used systems.	112
Figure 63: Intersection between ASM UV-Vis spectra and UV-C emission spectrum	120
Figure 64: ASM removal under different processes Photolysis, Sonolysis, Fenton (pH= 3.0, [H ₂ O ₂]=3.25 M, [Fe ²⁺]= 10 mmol/L), Photo-Fenton & Sono-Fenton.	121
Figure 65: Effect of pH on Photo-Fenton and Sono-Fenton processes, [H ₂ O ₂]=3.25 M, [Fe ²⁺]= 10 mmol/L.	123
Figure 66: Hydrogen peroxide concentration effect, pH= 3.0, [Fe ²⁺]= 10 mmol/L.	124
Figure 67: Ferrous ions concentration effect on (a) Photo-Fenton process (b) Sono-Fenton.	125
Figure 68: kinetic study Ln(C ₀ /C)= f(time)	126
Figure 69: Mass spectrum of ASM eluted at 9.87 min	127
Figure 70: Mass spectrum of different identified Sonoproducts at various retention time.	128
Figure 71: Proposed pathway of sonochemical transformation of ASM	131

LIST OF TABLES

Table 1: Principal chromophores and auxchromes group dyes.	9
Table 2: Classification of pesticides.	12
Table 3: Classification of organic pesticides.	14
Table 4: Hydroxyl radicals standard oxidation-reduction potential.	22
Table 5: Interaction of electromagnetic matter with matter according to spectrum range.	31
Table 6: the electronic excitation reactions after photon absorption.	32
Table 7: Physico-chemical properties of Difenconazole.	57
Table 8: Physico-chemical properties of Acibenzolar-S-Methyl.	58
Table 9: Textural characteristic of hematite.	96
Table 10: The photoproducts generated from DFL fungicide degradation obtained by GC/MS analysis.	110
Table 11: Metabolites of sono-Fenton degradation of ASM according to GC/MS analysis.	129

ABBREVIATIONS

<i>CI</i>	Colour index number
<i>DDT</i>	Dichloro-Diphenyl-Trichloroethane
<i>UNEP</i>	United Nations Environment Programme
<i>FAO</i>	Food and Agriculture Organization
<i>PIC</i>	Prior informed consent
<i>MRL</i>	Maximum residue limit
<i>ONSSA</i>	National Office of Food Safety
<i>•OH</i>	Hydroxyl radicals
<i>AOPs</i>	Advanced Oxidation Processes
<i>TCE</i>	Trichloroethylene
<i>PCE</i>	Perchloroethylene
<i>TNT</i>	2,4,6-trinitrotoluene
<i>RDX</i>	Research Department Explosive
<i>HMX</i>	High Melting eXplosive
<i>EM</i>	Electromagnetic matter
<i>HOMO</i>	Highest occupied molecular orbital
<i>LUMO</i>	Lowest occupied molecular orbital
<i>IUPAC</i>	International Union of Pure and Applied Chemistry
<i>XRD</i>	Powder X-ray Diffraction
<i>BET</i>	Brunauer-Emmett Teller
<i>UV-Vis DRS</i>	UV-Vis Diffuse Reflectance spectroscopy
<i>SEM</i>	Scanning electron microscopy
<i>TEM</i>	Transmission electron microscopy
<i>HPLC</i>	High performance liquid chromatography
<i>E_g</i>	Bandgap Energy
<i>GC/MS</i>	Gas chromatography combined with mass spectroscopy
<i>TOC</i>	Total organic carbon
<i>S_{BET}</i>	Surface area
<i>BL</i>	Levafix Blue
<i>DFL</i>	Difenoconazole
<i>ASM</i>	Acibenzolar-S-Methyl
<i>WWTP</i>	Wastewater treatment plan
<i>UV</i>	Ultraviolet
<i>US</i>	Ultrasound
<i>JCPS-ICCD</i>	Joint Committee on Powder Diffraction Standards- International Centre for Diffraction Data.

TABLE OF CONTENTS

Résumé.....	I
DEDICATION	II
ACKNOWLEDGEMENTS	III
LIST OF FIGURES.....	IV
LIST OF TABLES	VI
ABBREVIATIONS.....	VII
TABLE OF CONTENTS	VIII
GENERAL INTRODUCTION	1
CHAPTER I : Literature review.....	5
1 Introduction.....	6
2 Micropollutants occurrence in the aquatic environment.....	6
2.1 Dyes	7
2.1.1 Dyes history.....	7
2.1.2 Dyes classification.....	8
2.1.2.1 Azo dyes.....	9
2.1.2.2 Nitro and Nitroso dyes	9
2.1.2.3 Anthraquinone dyes	9
2.1.2.4 Indigo dyes.....	9
2.1.2.5 Phtalocyanine dyes.....	10
2.1.2.6 Sulfur dyes	10
2.1.3 Dyes Toxicity and their impact on the environment	10
2.2 Pesticides	11
2.2.1 Pesticides history.....	11
2.2.2 Pesticide's classification	12
2.2.2.1 Classification of pesticides based on target pests	12
⇒ Insecticides	12
⇒ Herbicides.....	13
⇒ Fungicides	13
2.2.2.2 Chemical classification of pesticides	13
2.2.3 Pesticides routes in the environment.....	16
2.2.4 Pesticides toxicity.....	17
2.2.4.1 Acute toxicity.....	17
2.2.4.2 Chronic toxicity	17

2.2.5	Regulations of pesticides.....	18
2.2.5.1	International regulation.....	18
2.2.5.2	Moroccan regulations.....	20
3	Advanced oxidation processes.....	20
3.1	Ozonation.....	23
3.1.1	Direct reaction.....	24
3.1.1.1	Oxidation-reduction reaction.....	24
3.1.1.2	Cycloaddition reaction.....	25
3.1.1.3	Electrophilic substitution reaction.....	25
3.1.1.4	Nucleophilic reaction.....	25
3.1.2	Indirect reaction.....	25
3.1.2.1	Ozone-based water treatment processes.....	26
3.1.2.2	Peroxone process.....	26
3.1.2.3	Catalytic ozonation process.....	26
3.2	Fenton reaction.....	26
3.3	Photochemical processes.....	28
3.3.1	Fundamentals of photochemistry.....	28
3.3.1.1	Definition.....	28
3.3.1.2	Basic laws of photochemistry.....	28
3.3.1.3	Electromagnetic radiation.....	29
3.3.1.4	Interaction of electromagnetic radiation with matter.....	30
3.3.1.5	Reaction pathways.....	31
3.3.1.6	Light Absorption – Formation of the Excited State.....	32
3.3.1.7	Singlet and triplet states.....	34
3.3.1.8	Photophysical processes.....	35
3.3.2	Photochemistry application in AOPs treatments.....	37
3.3.2.1	Direct photolysis.....	37
3.3.2.2	Photolysis of ozone/ H ₂ O ₂	38
3.3.2.3	Homogeneous photocatalysis: photo-Fenton process.....	38
3.3.2.4	Heterogeneous photocatalysis.....	39
3.4	Sonochemical processes.....	40
3.4.1	Sonolysis and Sonocatalytic processes.....	42
3.4.2	Application of sonocatalysis in environmental remediation.....	44
4	References.....	46
	CHAPTER II : Materials & Methods.....	55

1. Introduction.....	56
2. Materials.	56
2.1 Chemicals and reagents:	56
2.1.1 Levafix Blue:.....	56
2.1.2 Difenoconazole.....	57
2.1.3 Acibenzolar-S-Methyl.....	57
2.2 Other chemicals	58
2.3 Synthesized materials:	59
2.3.1 Catalyst:.....	59
2.3.2 Ferrioxalate actinometer.....	60
3. Methods.....	60
3.1 Irradiation system	60
3.1.1 Monochromatic light irradiation at 254 nm wavelength.....	60
3.1.2 polychromatic irradiation light source with maximum of 365 nm.....	61
3.1.3 Ultrasonic radiation system.....	61
3.1.4 Photonic flux determination	62
3.1.5 Actinometry.....	62
3.1.6 Ferrioxalate actinometry	62
3.1.7 Photonic flux intensity	63
3.1.8 Quantum yield measurement.....	64
3.2 Analytical methods	64
3.2.1 Characterization techniques used for synthesized hematite.....	64
3.2.1.1 Powder X-ray Diffraction	64
3.2.1.2 Fourier Transform Infrared Spectroscopy (FT-IR).....	66
3.2.1.3 Brunauer-Emmett Teller (BET).....	66
3.2.1.4 UV-Vis Diffuse Reflectance spectroscopy (UV-Vis DRS).....	67
3.2.1.5 Scanning electron microscopy (SEM)	68
3.2.1.6 Transmission Electron Microscopy (TEM)	69
3.2.1.7 Raman spectroscopy	69
3.2.2 Photocatalytic monitoring techniques	70
3.2.2.1 UV-Vis spectroscopy	70
3.2.2.2 High Performance Liquid Chromatography (HPLC)	71
3.2.2.3 Gas Chromatography coupled with Mass Spectroscopy (GC/MS)	73
3.2.2.4 Total Organic Carbon (TOC).....	74
4. References.....	74

CHAPTER III: Visible light degradation of Levafix blue dye using Fenton & Photo-Fenton processes.....	76
1 Introduction.....	77
2 Materials & methods.....	77
2.1 Photolysis system	77
2.2 Fenton and Photo-Fenton processes	77
3 Results & Discussion	78
3.1 Spectral characteristics of Levafix Blue	78
3.2 Radiation intensity effect on photolysis	80
3.3 Photocatalytic discoloration of Levafix Blue dye	81
3.4 Effect of initial pH.....	82
3.5 Initial dye concentration effect	83
3.6 H ₂ O ₂ concentration effect.....	84
3.7 Ferrous ions concentration effect	85
3.8 Humic acid effect.....	86
4 Conclusion	87
5 References.....	88
CHAPTER IV: Photocatalytic degradation of fungicide difenoconazole via Photo-Fenton process using α -Fe ₂ O ₃	91
1 Introduction.....	92
2 Materials & methods.....	93
2.1 Synthesis protocol.....	93
2.2 Characterization of synthesized α -Fe ₂ O ₃	93
2.3 Photochemical degradation activity.....	93
3 Results & discussion	94
3.1 Characterization of α -Fe ₂ O ₃	94
3.1.1 DRS analysis	94
3.1.2 BET analysis	95
3.1.3 X-ray diffraction analysis.....	96
3.1.4 SEM & TEM analysis	97
3.1.5 Raman analysis.....	98
3.2 Photocatalytic activity	99
3.2.1 Photodegradation under different systems	99
3.2.2 pH effect.....	100
3.2.3 Hydrogen Peroxide concentration effect.....	101
3.2.4 The effect of catalyst dosage.....	102

3.2.5	Scavenger study.....	103
3.2.6	Reusability efficiency.....	104
3.2.7	Kinetic analysis	105
3.2.8	Quantum yield.....	106
3.3	Identification of photoproducts of Difenconazole photodegradation.....	106
3.4	Mineralization study	112
4	Conclusion	112
5	References.....	114
CHAPTER V: Photochemical and sonochemical removal of Acibenzolar-S-Methyl fungicide: transformation mechanism pathway.....		
1	Introduction.....	118
2	Materials & methods.....	119
2.1	Experimental Design	119
2.2	Analytical Methods.....	119
3	Results & Discussion	120
3.1	Spectral characteristic of ASM.....	120
3.2	Degradation of ASM by various processes	121
3.3	pH effect	122
3.4	Effect of hydrogen peroxide concentration	123
3.5	Ferrous ions concentration effect	124
3.6	Kinetic analysis.....	126
3.7	Proposed mechanism of ASM degradation by Sono-Fenton reaction.....	126
4	Conclusion	132
5	References.....	133
GENERAL CONCLUSION		
SCIENTIFIC CONTRIBUTIONS		
1	List of publications	140
2	List of communications.....	140

GENERAL INTRODUCTION

During the last decades, the planet is experiencing a significant population growth that is accompanied by the excessive human consumption. Human has shown a great need to improve his living conditions through the increasing production of chemicals. This development had a high cost resulting the voluntary or accidental introduction of exogenous substances into environment.

The anthropogenic activities are perturbing the ecosystem everyday more than expected, the environmental pollution concern has arisen with the variety and high concentration levels of contaminants found in environment. Water resources are one of the impacted environmental compartments involving the overuse and the degradation of its quality.

In principle, the increase of population is necessarily in parallel with the rise of wastewater effluents. In addition, a sustainable management of water resources requires an effective planification and efficient treatment processes. The conventional wastewater treatment technologies including coagulation, flocculation, sedimentation, filtration, chlorination, and membrane separation have been proven inefficient to remove persistent organic pollutants (dyes, pesticides, pharmaceuticals, and personal care products...etc.). Hence, Advanced Oxidation Processes (AOPs) has known an enhancing interests from researchers as promising alternative treatment technologies for industrial and hazardous effluents specifically removal of micropollutants and pathogens.

Homogeneous and heterogeneous catalysis as part of AOPs technologies provide many advantages and is considered as low-cost and eco-friendly processes. These methods demonstrate to be the most effective for degradation of organic pollutants due to the powerful oxidising agents generated during the process leading to the complete mineralization stage of compounds. Basic Fenton and Fenton-based processes are also confirmed as a simple and convenient methods for wastewater treatment. The combination of Fenton method with optical radiation (Visible or Ultraviolet light sources), ozone, ultrasound radiations, and electricity have been exploited to give birth of many valuable studies and it have proven higher efficient than the basic Fenton for removal of various micropollutants.

In particular, optical and ultrasound radiation supply a strong stimulation for hydroxyl radicals species based on the Fenton process fundamentals. The photocatalytic performance of Photo-Fenton process is affected by the category of the used light source. Furthermore, the common developed optical radiation that is used in photo-Fenton process is UV radiation source as a

powerful energy and the large wavelength coverage indeed. However, visible light source is the more sustainable option from the economic and environment protection overview.

The first part of this thesis investigated the suitability of basic Fenton and visible light Photo-Fenton processes for the degradation of the commonly used textile dye Levafix Blue via evaluating the comparative degradation kinetics for photolysis, Fenton, and photo-Fenton oxidation, the optimization of reaction and the investigation of humic acid effect on degradation reaction. On the other hand, the second part of our research focused on the photo-Fenton like and sonochemical removal of two selected fungicides (Difenoconazole (DFL), and Acibenzolar-S-Methyl (ASM)) that are widely used as plant control agents in crops. A synthesized hematite was used in photo-Fenton process for DFL treatment. A comparative study of photochemical and sonochemical removal of ASM was carried out. Finally, the reaction metabolites formation has been investigated and transformation mechanism pathways of both pesticides were suggested.

This manuscript is divided into five chapters:

Chapter one provides two sections, the first part gives an overview about micropollutants precisely dyes and pesticides. It reports on their historical discovery, the classification, the use, and their environment contamination. The second section is devoted to the background of wastewater treatment technologies specifically the Advanced Oxidation Processes. This part describes various processes with special focus on the fundamentals of Photochemistry and its diverse application.

The second chapter is concerned with materials, analytical methods, and experimental procedure used in this study. It gives all details related to the chemicals and reagents that have been used in our study including the physico-chemical properties of the investigated micropollutants, a dye (Levafix Blue) and two pesticides (Difenoconazole and Acibenzolar-S-Methyl).

Chapter three describes the promising ability of visible light combined to Fenton process in Blue Levafix dye removal. In order to optimise the photocatalytic performance of processes, different experiments were carried out under various parameters conditions.

Chapter four summarises the experimental results of difenoconazole pesticide degradation using synthesized hematite. The chapter includes a part of material characterization and a

second part of photocatalytic application with an investigation on the transformation mechanism pathway of difenoconazole.

Chapter Five compares the photochemical and sonochemical degradation of Acibenzolar-S-Methyl including discussion of the optimisation of results obtained from the conducted experiments of Fenton-based processes

The last part of the thesis is dedicated to the general conclusion of this study and, provides recommendations, and outlooks for further research opportunities.

CHAPTER I : Literature review.

1 Introduction

Persistent organic pollutants are toxic, non-biodegradable molecules, and cannot be eliminated by conventional physico-chemical and biological treatment. New techniques have been developed over last decades that can lead to complete mineralisation of these micropollutants such as advanced oxidation processes.

In relevance to the investigation about the micropollutants and their impact on environment, this first literature review chapter is divided into two parts. The first part describes the occurrence of emerging pollutants in environment with focus on dyes and pesticides history, classification, toxicity, and their routes in environment. Furthermore, the second part of this work is devoted to advanced oxidation processes on global basis spotlighting light on photochemistry fundamentals and the application of photochemical processes in micropollutants degradation.

2 Micropollutants occurrence in the aquatic environment

Since life's creation, water has been considered a vital element for human existence. It plays a crucial role in a nation's development and ecosystems equilibrium. The exponential world's population growth associated with rapid urbanization and industrialization has resulted in an overexploitation of natural resources [1]. The extensive anthropogenic activities and the unsustainable use of resources have increased pollution and present real threats to our environment. The agricultural sector, industrial manufacturing, mining, and power generation are some puzzle pieces that contributed to the ecosystem contamination [2]. At present, climate change, food insecurity, and water scarcity have become an urgent global concern. Due to poor management strategies, various toxic compounds found in different environmental compartments are derived directly from domestic and industrial effluent[3]. Among these substances, micropollutants are emerging contaminants, including dyes, pesticides, pharmaceuticals, personal care products, and steroid hormones. Their presence in water resources is persistent with very low concentrations (ng/μg) and specific behaviour that affects their detection and removal from aquatic medium [4].

The appearance of these persistent pollutants presents a real challenge for the scientific community. The massive implementation of wastewater treatment plants (WWTPs) was not efficient enough to deal with the problem. The conventional chemical and biological treatments

were unable to get rid of these substances. Consequently, the micropollutants end up in the aquatic environment, as illustrated in figure 1 [5].

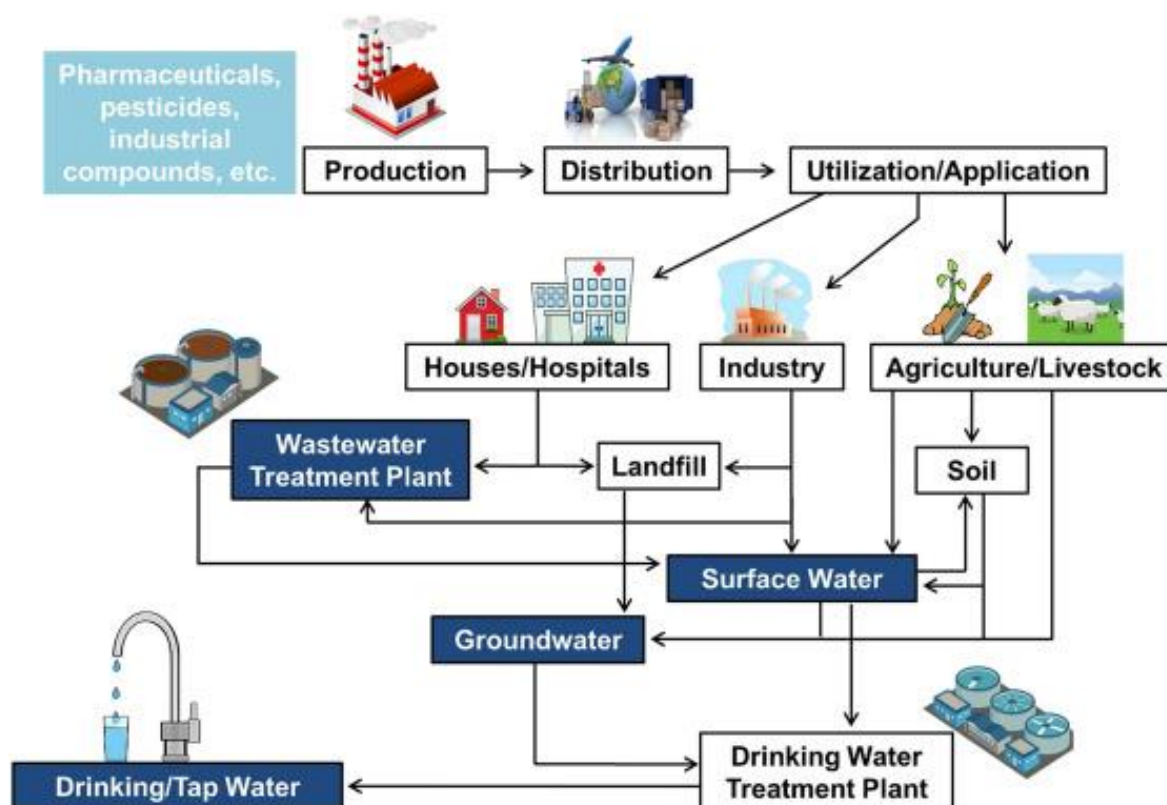


Figure 1: Sources and pathways of micropollutants [6]

2.1 Dyes

Dyes are organic compounds, natural or synthetic, that are able to colour fabrics, leather, plastic, paper, food, and cosmetic products. Generally, natural dyes are from natural resources extracted from plants, animals, minerals, and microbial dyes. Synthetic dyes are chemical substances based on petroleum compounds. A dyed substrate should be resistant to cleansing procedure and stable to light. Dyes possess at least one chromophore, auxochrome group. These chemical groups ensure the stability of dyes due to their capacity to absorb light in the visible spectrum (400-700 nm)[7].

2.1.1 Dyes history

Ever since prehistoric time, human has been fascinated by colors. Dyes were for daily use for the primitive population in body arts and in the ancient Egyptian civilization for rocks and pottery art with natural pigments. The experience with natural dyeing has given an insight into exploring natural resources and discovering diverse fiber plant colors [8]. Due to their brightness and non-toxic composition, natural dyes were the preferred compounds to use. With

the great demand and the industrial revolution and after the creation of the first synthetic dye mauveine by the British chemist William Henry Perkins in 1856, the use of natural dyes has gradually gone out of existence around all parts of the world [9]. This discovery was the success-catalyzed activity that synthesized of new and better chemical dyes. The global dyes production is estimated at 800 000 tons per year which azo-dyes are 60% of production [10].

Nowadays, the dye industry has become a massive chemical sector. The dyes have been employed in the printing, textile sector, wood, and plastic industry. They are also used in the food industry and pharmaceutical production as an additive, in cosmetics, in biology for microscopic samples preparation, and chemistry as indicators. The use of dyes is still a large to account that the textile industry was considered the principal dominant sector [11]. However, the food industry has known a significant increase in dye utilization, notably in cans, soft drinks, candies, and fat (oil, butter, and cheese). They are used to improve the flavor and consistency of products that, unfortunately, could be toxic in overdoses and threaten human health.

The wastewater effluents derived from the textile industry are categorized to be the most polluted wastewater due to the large quantity of water consumed in manufacturing processes and the inefficient dyeing operation; up to 200,000 tons of dyes are lost in effluents. The conventional wastewater treatment processes are ineffective in treating these persistent compounds that present a real threat to human health and the environment [12].

2.1.2 Dyes classification

In the dye industry, all commercialized dyes and pigments are identified according to their method and application via color index number (CI), a unique digit number. The CI number permits the easy recognition of the dye chemical specification, mode of action, and behaviour details. In addition, chemists classify synthetic dyes according to their chemical structures[13]. The chemical classification consists of two groups: the chromophores and auxochromes as described in Table1.

Table 1:Principal chromophores and auxchromes group dyes[14]

Chromophores group	Auxchromes group
Azo (-N=N-)	Amino (-NH ₂)
Nitroso (-NO or -N-OH)	Methylamino (-NHCH ₃)
Carbonyl (=C=O)	Dimethylamino (-N(CH ₃) ₂)
Vinyl (-C=C-)	Hydroxyl (-HO)
Nitro (-NO ₂ or =NO-OH)	Alkoxy (-OR)
Sulfur (>C=S)	Electron's donor group

2.1.2.1 Azo dyes

For their simplicity, high stability, and intensity of color, azo dyes are reported to be the largest synthesized category, approximately (60-70%) of total dye industry production [15]. Azo dyes are characterized by one, two (di) or more (poly) azo groups that play an essential role in ensuring the solubility of the dyes in water. Their chemical structures consist on the attachment of azo groups with aromatic or heterocyclic compounds [16].

2.1.2.2 Nitro and Nitroso dyes

The nitro and nitroso dyes are among the old school production, and they are a limited commercial class of dyes at present. The characteristic feature of this category is the combination of an electron-donating group with one or more nitro or nitroso groups via an aromatic system. These substrates have no ability to dye themselves without forming metal complexes that acquire pigments properties [17].

2.1.2.3 Anthraquinone dyes

After azo dyes, the anthraquinone dyes are considered the second most important, and the oldest classes. They have been found to be one of the elements in the mummification process. Anthraquinone dyes have a high molar extinction coefficient, strong absorption bands, and excellent photostability. Structurally, these dyes are formed by carbonyl groups related to the quinonoid system [18].

2.1.2.4 Indigo dyes

Indigoid dyes are one of the oldest types. They are known for their extinctive blue color and have been almost used for denim jeans and jacket dyeing. The indigo dyes were essentially

obtained from natural sources once discovered. However, with the development of the chemical industry, indigoid dyes are the first natural molecules to be synthesized [19].

2.1.2.5 Phthalocyanine dyes

Phthalocyanine dyes are aromatic, macrocyclic compounds. This dyes class consists formally of a porphirazine core to which four nitrogen-containing heterocycles are condensed. Compared to other classes, the Phthalocyanine materials have unique properties due to their high stability, architectural flexibility, diverse coordination, and improved spectroscopic characteristics. These compounds have the ability to form coordination complexes with an extensive list of elements, specifically metals (Cu, Fe, Si...etc.)[20].

2.1.2.6 Sulfur dyes

Sulfur dyes are complex heterocyclic molecules; they are insoluble compounds in water mostly used for dyeing cellulosic fabrics. These substances are synthesized by heating aromatic amines, phenols, or nitro compounds with sulfur or specifically alkali polysulfides. Unlike most other types of dyes, the chromogen is hardly defined, consisting of the macromolecular structure of phenthiazonethianthrone type which sulfur is present as sulfide bridging links and as thiazine groups. The sulfur dyes are considered an important dyes category for producing cost-effective tertiary shades [21].

2.1.3 Dyes Toxicity and their impact on the environment

Being an indispensable element in various industrial sectors to ensure the wide choices demand human life basic needs satisfaction, dyes are hazardous chemicals that are carcinogenic and mutagenic to organisms, human health, and the environment. Globally, environmental problems related to the dyeing industry are those associated with water pollution caused by the direct discharge of untreated effluents in aquatic ecosystems, as shown in figure 2. The toxicity of those compounds has been performed by acute and enrichment toxicity tests that confirmed the high persistence of dyes; the results revealed that algae were more sensitive to dyes than other organisms, *vibrio fischeri* and *tetrahymena pyriformis* toxicity tests have shown growth inhibition and cells deformation [22]. The high thermal and photo-stability of dyes inhibit oxygenation and sunlight absorption that impact and troubles the natural food chain [23].

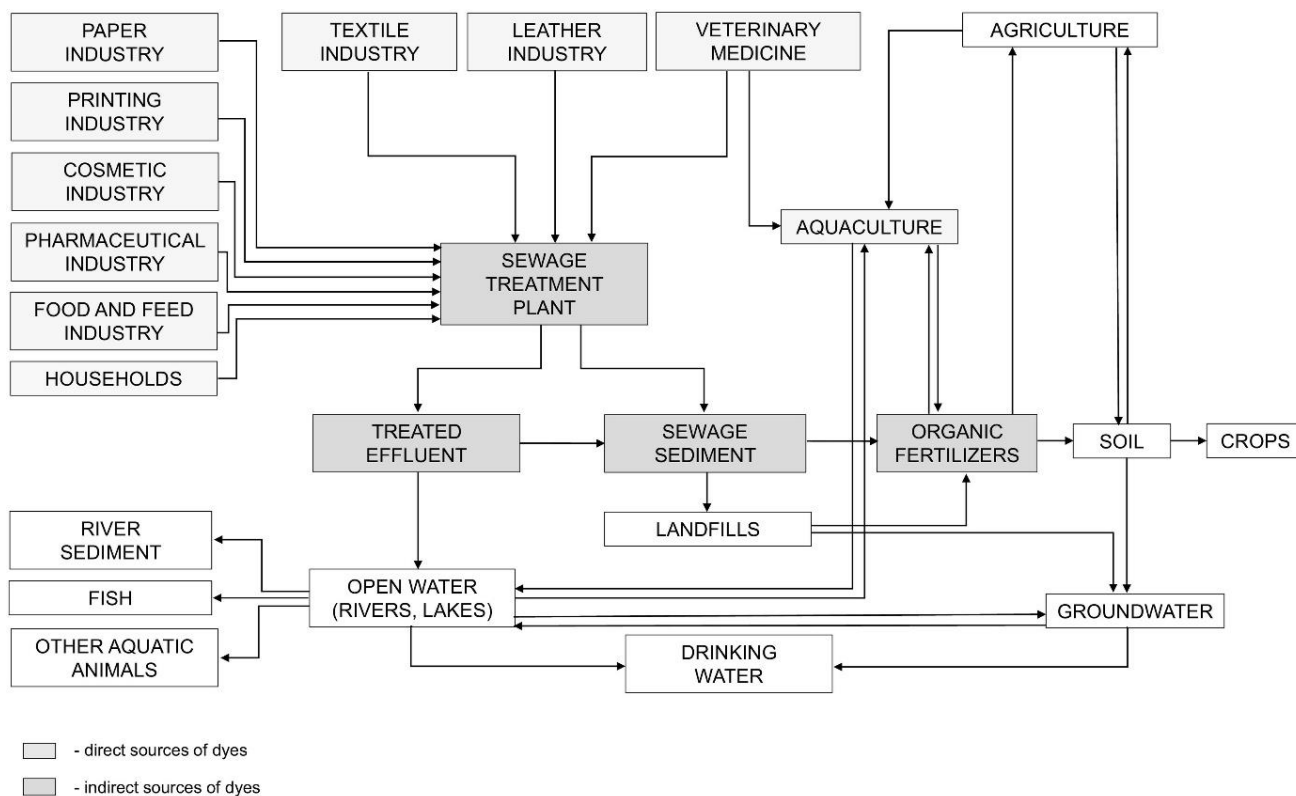


Figure 2: Sources and pathway of synthetic dyes to aquatic mediums [22].

2.2 Pesticides

Pesticides are defined as a chemical substance or a mixture of substances intended for preventing, destroying, repelling, or mitigating pests (insects, nematodes, weeds, bacteria, virus, and others). Since their creation, pesticides have become a necessity in agricultural production that generate large product yields to ensure worldwide food security [24]. These compounds are also considered plant growth regulators, defoliants, and desiccants. The word pesticide comprises herbicides, insecticides, fungicides, and nematicides used for specific pests' treatment. They are classified according to the target pest and their chemical structure.

2.2.1 Pesticides history

Since ancient civilizations, various agents have been employed in crops for pest control (Sulphur, salt, fire, olive oil, nicotine, arsenic, and mercury). These compounds were used for centuries until the creation of chemical pesticides in the 1940s, specifically with the growth of international trade relations between all parts of the world and the second World War. The Dichloro-Diphenyl-Trichloroethane (DDT) was the first modern synthetic pesticide by the Scientist Paul Muller to combat malaria, typhus, and other insects [25].

In 1950, the second world war led to the shortage of copper and sulfur that stimulated researcher for new pesticides discovery (fungicides for seeds treatment). Day after day, the pesticides industries have been competitively introducing a large variety of pesticides [26].

After many years of DDT use and others, Rachel Carson raised the alarm in 1962s with her book “*silent spring*” which discussed the harmful effects of DDT on human health and the environment [27]. Numerous states have immediately banned this substance's use to minimize the risk in forthcoming years. However, the immense exponential population growth imposed the continuity of the pesticide industry. In the 1970s, the environmental protection and human health agencies have strived for a strict new law regulation that require the decrease of pesticides production and sustainable use of these substances in crops [28].

2.2.2 Pesticide’s classification

Pesticides are classified according to various criteria: target pest, chemical composition, mode of action, mode of entry, and source of origin Table 2.

Table 2:Classification of pesticides [29]

Classification	Examples
Target pest	Insecticides, fungicides and herbicides
Chemical structure	Carbamates, organophosphorus, and pyrethrums
Mode of action	Chitin synthesis inhibitors and anticholinesterase

2.2.2.1 Classification of pesticides based on target pests

The most common classification of pesticides is based on target organisms they kill and their functions. The three major families are cited below:

⇒ **Insecticides**

In chronological order of appearance, insecticides are the first generation of pesticides used by our primitive ancestors in food crops[30]. The insecticides are intended to destroy insects in the agricultural sector, horticultural industry, and forestry. They are also present in a domestic environment, offices, gardens, workplaces, aircraft, or throughout the contaminants in food [31].

Insecticides are chemical or biological agents that manage or prevent the insect from engaging its destructive behaviours [32]. These compounds affect the nervous system disorder of pests,

oxygen metabolism, insect's maturation process, or other aspects of physiology. The mode of action of insecticides makes them the most powerful used chemicals.

⇒ **Herbicides**

Herbicides are phytocides used to destroy or interrupt weed's growth. This category presents 48% of pesticides used worldwide. They are used in agriculture, aquatic, forest, and wildland ecosystems to reduce the density of unwanted vegetation species. These organic substances are classified according to the method and timing of application, including oil and foliage treatments, depending on their specific absorption area in the plant [33]. The crucial and useful characteristic of any herbicide is its high selectivity that hits the target weeds without risk to crops. The herbicides selectivity is also related to many factors (herbicide chemistry, the plant physiology details, and the environment area). In addition, the herbicides are also classified by plant response, their movement in plant, systemic herbicides are those that occur in the phloem and xylem or both. These chemicals are also categorized by their action mechanism, including growth regulators, photosynthesis inhibitors, pigments, lipid synthesis, and cell membrane destroyers. Contact herbicides are named to those having effect at the application site without movement in the plant [34].

⇒ **Fungicides**

Fungicides are chemical agents used to prevent or eradicate fungal plants or seeds infections. Historically, the earliest compounds were inorganic materials (sulfur, copper, lime, and others). Fungicides are classified according to their chemical structure, mode of action (agriculture and horticulture), and mode of application. The fungicides application mode is divided to three major categories; foliar fungicides that are liquids or powders for cuticular surface protection, soil fungicides that act either through the vapor phase or systemic properties, and dressing fungicides that are used in the post-harvest to prevent infections specifically if the temperature and humidity storage conditions are less than optimum [35].

Fungicides application is considered indispensable when the crops know the development of specific disease to point to lost yield. The dose rate of fungicides is used depending on the disease variety and risk. The technology development makes the decision easier via the computational models designs that give the precise threshold doses [36].

2.2.2.2 Chemical classification of pesticides

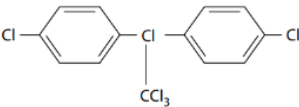
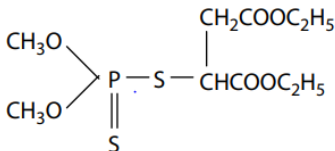
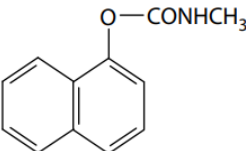
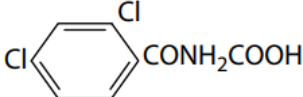
⇒ **Mineral pesticides**

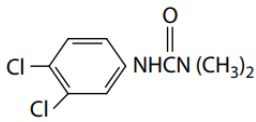
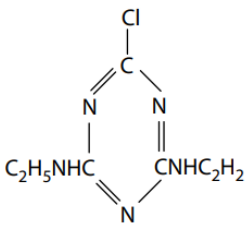
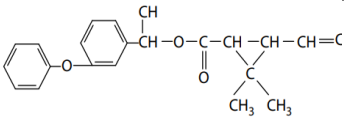
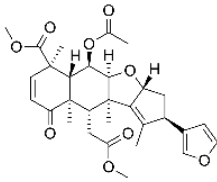
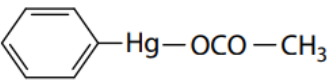
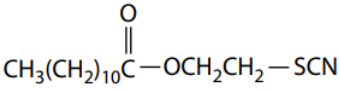
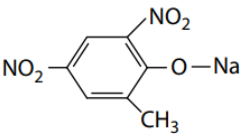
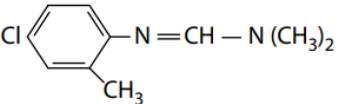
The inorganic pesticides commonly contain arsenic, copper, boron, mercury, sulfur, or zinc. These are considered the earlier used chemicals, specifically in the second World war period. Until today, some of these compounds are still used as herbicides and for wood preservation. They are also known for their toxicity to a wide range of organisms (low selectivity) that affect their efficiency. In addition, as their composition is based on heavy metals (mercury, arsenic, ...etc.), they have generated widespread health and environmental concerns that lead authorities to ban or severely curtail their use [37].

⇒ Organic pesticides

Nowadays, organic pesticides are a widely used class. The majority of these substances are synthetic, and a limited series are extracted directly from plants. Their simple use and the high effectiveness with their accessible price make these compounds the highlighted part of the pesticides industry and customers. However, it has been proven that they also have hazardous risks on human health and the environment. The organic pesticides are classified based on their chemical structure as described in table 3, with some examples of each family [38].

Table 3: Classification of organic pesticides

Chemical Type	Example	Structure	Typical Action
Organochlorines	DDT		Insecticide
Organophosphates	Malathion		Insecticide
Carbamates	Carbaryl		Insecticide
Dithiocarbamates	Thiram	$(\text{CH}_3)_2 \text{N-CS-S-CNS} (\text{CH}_3)_2$	Fungicide
Carboxylic acid derivatives	2,4-D		Herbicide

Substituted ureas	Diuron		Herbicide
Triazines	Simazine		Herbicide
Pyrethroids	Cypermethrin		Insecticide
Neem products	Nimbin		Insecticide
Organometallics	Phenylmercury acetate		Fungicide
Thiocyanates	Lethane 60		Insecticide
Phenols	Dinitroresol		Insecticide
Formamides	Chlordimeform		Insecticide

2.2.3 Pesticides routes in the environment

After their application, pesticides have the potential to move from the threatened site zone to contaminate the different environmental compartments. They have the ability to drift easily by the wind to the atmosphere as vapor, spray droplets, dust, or solid particles. However, the water resources are widely contaminated via the runoff water that transport pesticides into a drainage system, streams, ponds, or other surface water. In addition, pesticides could simply leach downward through the soil, which reaches the groundwater. Pesticides application is related to an important range of human health and environmental damage. Figure 3 illustrates an example of the multidimensional environmental impact of pesticides. The use of these chemical substances presents real concern since the aquatic and terrestrial biodiversity have been affected, which caused an ecosystem's disequilibrium. Many reports insist on the seriousness of the situation as many workers in the agricultural sector have been poisoned [39][39].

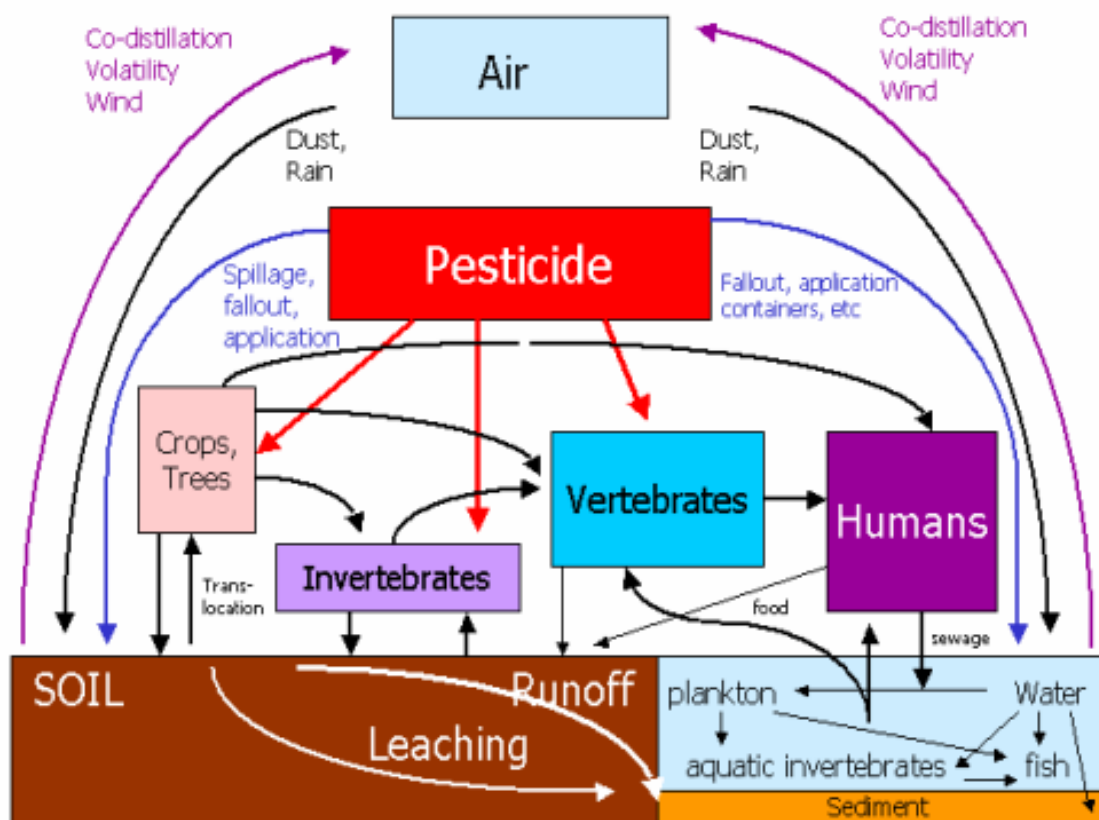


Figure 3: Pesticide's contamination routes[40]

2.2.4 Pesticides toxicity

Pesticides are designed to improve agricultural production, but unfortunately, their toxicity is not limited to the target pests. They could be harmful to human health and the environment [41]. The toxicity of any compound depends on the used dose except the highly toxic substances that can, with a small dose, causes severe symptoms of poisoning. Toxicity tests are generally divided into two levels, acute or chronic, which are defined as below:

2.2.4.1 Acute toxicity

The acute toxicity tests are short-term tests that measured the adverse effects resulting from a single exposure to the substance. The ability of a substance to develop fast harmful effects after exposure. The acute toxicity is quantified depending on two values measurements; the first value is the Lethal Dose (**LD₅₀**) which is the amount of compound that kills 50% of the tested microorganism after dermal or oral exposure. The value is given in milligrams per kilogram of body weight of the tested microorganism. The second value is the Lethal Concentration (**LC₅₀**), where the concentration is used instead of dose because it is related to the amount of substance inhaled in the air. The value is expressed as a ratio of substance to air, in parts per million (ppm). For both tests, the lower the **LD₅₀/LC₅₀** values, the more toxic the substance [42].

2.2.4.2 Chronic toxicity

Chronic toxicity is related to repeated or long-term exposure to a substance that causes effects within a week to years following the exposure. Less known about chronic toxicity of harmful substances than is known about their acute toxicity as it is developed gradually, which makes the monitoring complicated. Contrarily to acute toxicity, there is no specific standard test measurement in chronic toxicity. It is evaluated depending on studied substances and their chronic adverse effects defined as carcinogenic, mutagenic, endocrine disruption, hemotoxic, infertility, and teratogenic effect [43].

Numerous studies have confirmed the toxicity level of pesticides and their impact on human health and the environment. Pesticides manufactures are required to investigate and demonstrate the safety of their products and inform the users via signal words on each product label. The signal words are divided into four categories depending on the toxicity level of pesticides (highly toxic, moderately, slightly, and relatively non-toxic) [44].

2.2.5 Regulations of pesticides

The fast increase of pesticides utilization around the world urges the authorities to establish strict standards and legislation to control this sector. In most countries, there are government agencies responsible for regulating the sale and distribution of pesticides. Registration with these agencies is a crucial protocol, a required step from industries before any pesticide product can be marketed and used. The registration is a good way to limit the fraudulent claims and it could control and warranted the consumer safety and product effect on environment. The product label is the bottom line of registration process. The label should contain specific details with use instructions and also about the toxicity level of product and all adverse effects on human health and environment.

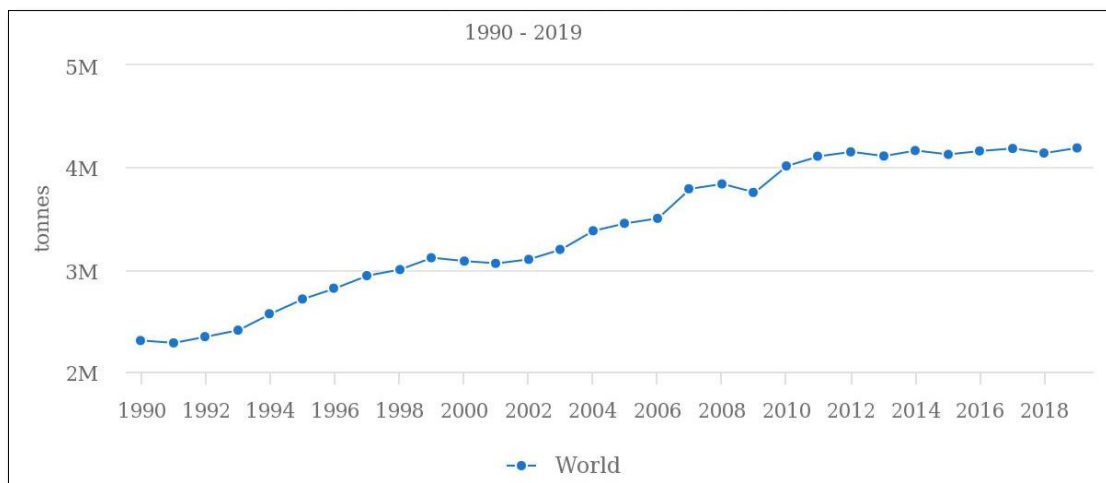


Figure 4: Global world consumption of pesticides since 1990 to present (Food and Agriculture Organisation of United Nations 2021).

2.2.5.1 International regulation

The enormous growth in chemical production has expanded considerably the international concerns with human health and environment protection in the past several decades. In response to these concerns, the international community has adopted a vast array of actions. UNEP and FAO started developing and promoting voluntary information exchange programs in the mid-1980s. FAO launched its international code of conduct on the distribution and use of pesticides in 1985, and UNEP established the London Guidelines for the exchange of information on chemicals in international trade in 1987 [45].

In 1989, the two organizations jointly introduced the voluntary prior informed consent (PIC) procedure into these two instruments. Together, these instruments helped to ensure that

governments had the necessary information to enable them to assess the risks of hazardous chemicals and to take informed decisions on their future import. Seeing the need for mandatory controls, officials attending the 1992 Rio earth summit adopted chapter 19 of Agenda 21, which called for a legally binding instrument on the PIC procedure by the year 2000. Consequently, the FAO Council (in 1994) and the UNEP governing council (in 1995) mandated their executive heads to launch negotiations. Talks started in March 1996 and concluded in March 1998 with the finalization of the convention's text on the prior informed consent procedure for certain hazardous chemicals in international trade. As clear testimony to the urgency attributed to addressing international trade of dangerous chemicals, governments completed the negotiations of the convention in only two years, which was also two years in advance of the deadline set by the Rio Earth Summit.

The Rotterdam Convention was adopted at the diplomatic conference held in Rotterdam on 10 September 1998. It entered into force on 24 February 2004, 90 days after the 50th instrument of ratification deposition. Between the convention's adoption and its entry into force, it has been operated on a voluntary basis as the interim prior informed consent procedure whose purpose was to continue the original PIC procedure and prepare for the effective operation of the convention upon its entry into force. During the interim period, over 170 countries have designated some 265 national authorities (DNAs) to act on their behalf to perform the administrative functions required by the convention. On entry into force, the Convention became legally binding for its Parties.

At the Stockholm Convention on persistent organic pollutants in 2001, the parties and regional economic integration organizations committed to reduce and eliminate the persistent pollutants. The objective of the Convention is to promote shared responsibility and cooperative efforts among parties in the international trade of certain hazardous chemicals to protect human health and the environment from potential harm and to contribute to their environmentally sound use by facilitating information exchange about their characteristics, providing for a national decision-making process on their import and export and disseminating these decisions to Parties.

The European Commission has implemented numerous directives to regulate the pesticides production and use, the directive NO 396/2005 of the European Parliament and of the Council of 23 February 2005 on maximum residue levels of pesticides in or on food and feed of plant and animal origin and amending the directive 91/414/EEC related to the pesticides marketing on the basis on the substance's physicochemical properties and their toxicity level.

2.2.5.2 Moroccan regulations

Since 1979, as an agricultural country, Morocco has performed numerous laws and directives relating to the control and organization of trade of pesticides products. Starting with law NO 42-95 that governed the conditions for the pesticide's products approval activities of manufacture, import, distribution, and sale.

The Directive N° 2-10-473 of 7th Chaoual 1432 (6th September 2011) expressly proclaimed food safety is a priority and related to the usage of pesticides that are restricted via setting the maximum residue limit (MRL). The concentration of substances in crops should be approved and authorized in accordance with the legislation and must be controlled by authorities by regular monitoring of pesticides level present in food products.

Recently, the Moroccan government council has adopted a new law project N° 35-19 related to the pesticides. with its coming into force, the new law will repeal and replace the law 42-95 related to the control and organization of pesticides production and usage. Due to the agricultural sector techniques advances, and the necessity of pesticides use for crops protection to increase the yield, the National Office of Food Safety (ONSSA) and the Ministry of Agriculture and Fisheries suggested a new legislation to keep up with the recent food safety and environmental protection challenges. The law project includes 84 articles divided into five titles and ten chapters. This law project aims to reinforce authorities' capacity and competence to evaluate the risks, to control and, to minimize the usage of the more toxic pesticides or promising new safe ecological alternatives. In addition, the law tends to improve the organization of trade of these substances, reducing the danger associated with their distribution and sale, and rationing the sector by imposing the need of agreement delivered by authorities to qualified persons to exclusively distribute or sale pesticides.

3 Advanced oxidation processes

Water pollution is one of major priorities for society and public authorities, the multiplicity of contamination sources (industrial wastes, mining activities, urban wastewater, micropollutants, and radioactive waste) impose a variety of treatment methods before discharging into the environment [46]. Conventional wastewater treatment is a combination of physical and biological processes to remove organic matter. Generally, the treatment process is categorized in four stages: pre-treatment, primary treatment, secondary treatment, and tertiary or advanced treatment that is considered as an additional step depending on the quality required of final effluents [47]. The preliminary treatment is a crucial step that maintains the wastewater

treatment plant equipment; it permits the control of flow measurement, screening, and grit removal. Primary treatment builds on the pre-treatment via removing all suspended inert materials. In this stage, numerous processes occur simultaneously as sedimentation, flocculation, and adsorption process where flow is known as settled sewage, then proceeds to secondary treatment. The biological treatment consists of activated sludge using aerobic microorganisms (bacteria, algae, protozoa, and fungi) that oxidize biological carbon and nitrogen for the removal of BOD. The settled sewage is aerated in the reactor and to the removal of organic matter with continuous stirring to be mixed with the new entering sewage. Commonly, effluents are discharged into the environment after the secondary treatment. However, the new persistent pollutants generation imposes a tertiary treatment that improves the quality of effluents via removing the inorganic compounds, bacteria, viruses, and all harmful substances that make the water safe to reuse, recycle, or discharge into the environment [48].

In order to improve the conventional wastewater treatment techniques that are classified to be ineffective for persistent organic pollutants (POPs) elimination, the advanced oxidation processes (AOPs) were launched in 1970 as promising, efficient, and environmental- friendly methods by scientists [49].

AOPs are based on the in-situ generation of oxidizing agents; oxidation is the transfer of one or more electrons from an electron donor (reductant) to an electron acceptor (oxidant). An oxidant attracts electrons, resulting in a chemical transformation in both the reductant and the oxidant. This can produce chemical species with an odd number of valence electrons called “radicals”. These radicals are highly unstable, hence highly reactive, as one of the electrons is unpaired. The produced electrons follow additional oxidation until stable products are formed [50]. The ability of an oxidant to initiate chemical reactions is measured by its oxidation potential. Hydroxyl radicals ($^{\circ}\text{OH}$) are one of the most powerful oxidizing agents that are non-selective, and they have the ability to effectively decontaminate wastewater at low concentration table 4. In addition to hydroxyl radicals, oxygen species such as superoxide radical anions ($\text{O}_2^{\bullet-}$), and hydroperoxyl radicals (HO_2^{\bullet}) are involved in the reactions. The choice of hydroxyl radicals for wastewater treatment processes referred to a series of criteria that meet the needs of treatments circumstances exigence, level of toxicity of used chemicals, non-corrosive, simplicity in application, and being effective without generation of new and/or more persistent pollutants [51]. However, hydroxyl radicals are the primary oxidant in most cases. Different AOP techniques have different possible ways of hydroxyl radical formation. The AOPs are divided

into various categories based on chemical, photochemical, electrochemical, and sonochemical reactions [52].

Table 4:Hydroxyl radicals standard oxidation-reduction potential [53].

Couple redox	Réaction	Potentiel, V/ENH)
Cl_2/Cl^-	$\text{Cl}_2(\text{g}) + 2 \text{e}^- \rightarrow 2\text{Cl}^-$	1,36
Br_2/Br^-	$\text{Br}_2(\text{g}) + 2 \text{e}^- \rightarrow 2\text{Br}^-$	1,06
I_2/I^-	$\text{I}_2(\text{g}) + 2 \text{e}^- \rightarrow 2\text{I}^-$	0,53
$\text{HO}^\bullet/\text{H}_2\text{O}$	$\text{HO}^\bullet + \text{H}^+ \text{e}^- \rightarrow \text{H}_2\text{O}$	2,81
O_3/O_2	$\text{O}_3 + 2\text{H}^+ + 2\text{e}^- \rightarrow \text{O}_2 + \text{H}_2\text{O}$	2,07
$\text{H}_2\text{O}_2/\text{H}_2\text{O}$	$\text{H}_2\text{O}_2 + 2\text{H}^+ + 2\text{e}^- \rightarrow 2\text{H}_2\text{O}$	1,77
$\text{MnO}_4^-/\text{Mn}^{2+}$	$\text{MnO}_4^- + 8\text{H}^+ + 5\text{e}^- \rightarrow \text{Mn}^{2+} + 4\text{H}_2\text{O}$	1,51
HClO/Cl^-	$\text{HClO} + \text{H}^+ + 2\text{e}^- \rightarrow \text{Cl}^- + 2\text{H}_2\text{O}$	1,49
$\text{ClO}_2/\text{ClO}_2^-$	$\text{ClO}_2 + \text{e}^- \rightarrow \text{ClO}_2^-$	0,95
$\text{S}_2\text{O}_8^{2-}/\text{SO}_4^{2-}$	$\text{S}_2\text{O}_8^{2-} + 2\text{e}^- \rightarrow 2\text{SO}_4^{2-}$	2,05

The AOPs present a large range of decontamination applications, any organic contaminant that is reactive with the hydroxyl radical can potentially be treated. These include petroleum hydrocarbons, aromatic hydrocarbons (toluene, benzene, xylene, etc.), phenols, chlorinated hydrocarbons (TCE, PCE, vinyl chloride, etc.), dyes, pesticides, pharmaceuticals, explosives (TNT, RDX, and HMX), and many more. Some other applications of AOPs are given in figure5 [54] .

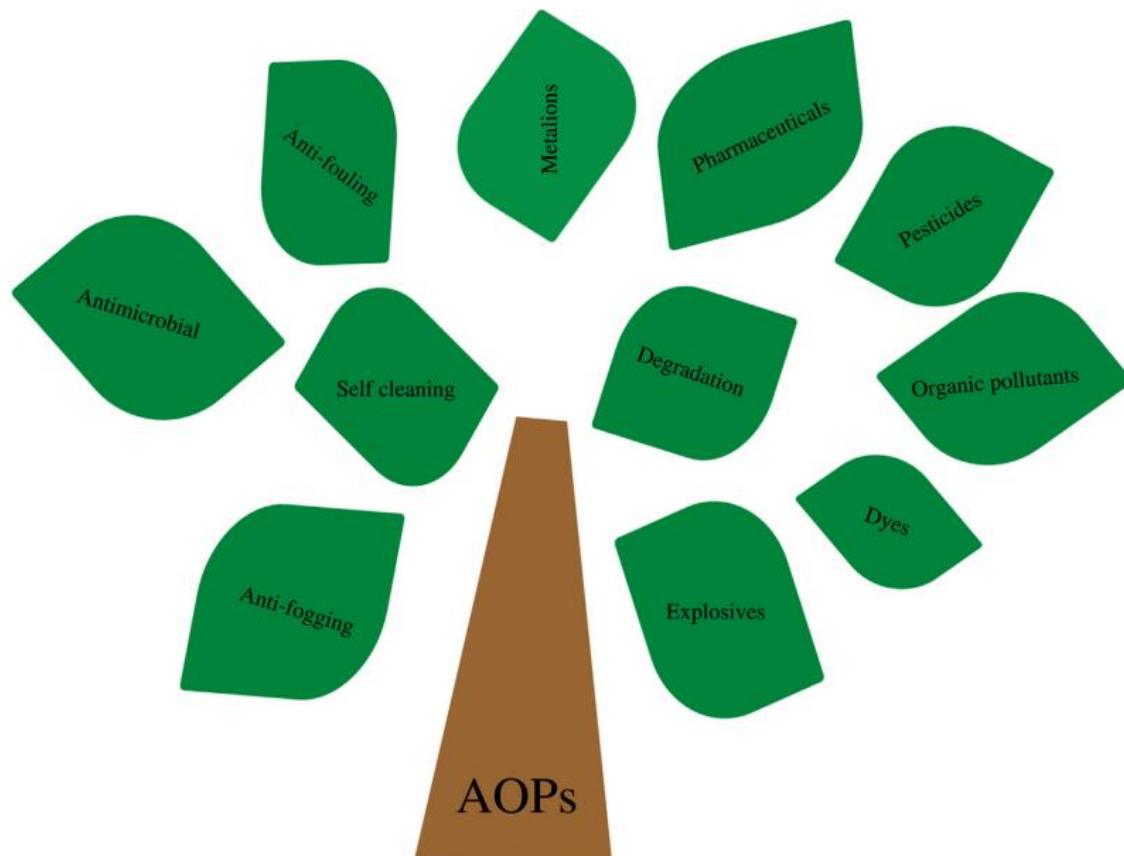


Figure 5:Advanced Oxidation Processes application [49].

3.1 Ozonation

Ozone (O_3) is normally known to be the stratosphere gas composition that protect earth against the ultraviolet (UV) radiations. However, this is one of numerous properties that can be addressed to ozone molecule. Ozone is powerful oxidant (2.07V) that has been widely used in industrial processes in chemical synthesis, food beverage, agriculture, medical dental application, air pollution, drinking water disinfection, and wastewater treatment [55]. Its high reactivity is derived from its inherent instability due to the molecule's readiness to accept electron; reducing ozone to O_2 , the electron donor becomes oxidized. Particularly, ozone has been used for more than hundred years figure 6 in drinking water treatment throughout the world, and also in wastewater treatment for effluent disinfection, odor control, color removal, oxidation of inorganic and organic contaminants [56].

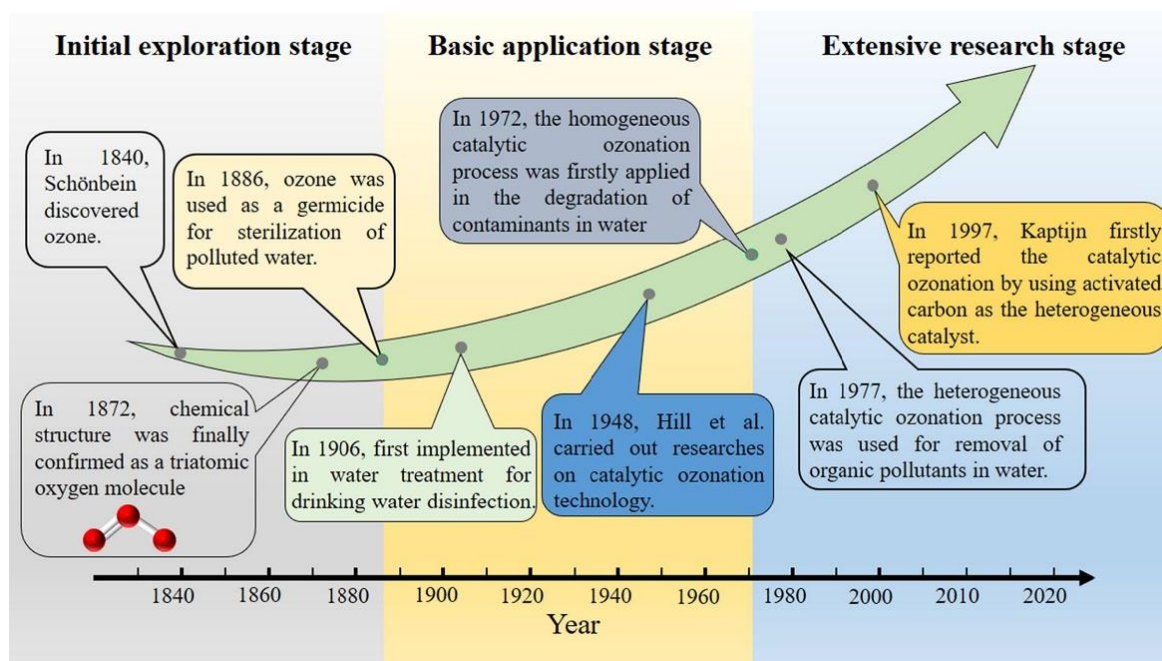


Figure 6:History of ozone and ozonation in water treatment [57].

Ozone is a highly reactive gas with limited solubility in water. Therefore, the ozone reactions are highly complicated in the aqueous solution system, that impose the involvement of gas-liquid mass transfer, self-decomposition, reactions dissolved and suspended inorganic and organic constituents. Ozone behaves as an oxidant once dissolved in water, it reacts with dissolved inorganic and organic matters. Ozonation of contaminants can proceed via two ways: a direct reaction by ozone molecule with high selectivity and indirect via the generated hydroxyl radicals ($^{\circ}\text{OH}$) [58].

3.1.1 Direct reaction

Due to its unique chemical structure that involves four possible resonance forms with three oxygen atoms, ozone possesses both electrophilic and nucleophilic characters that lead the direct reaction with pollutants to be divided into four categories [59]:

3.1.1.1 Oxidation-reduction reaction

Ozone has a high redox potential that is responsible for its capacity to oxidize a large array of compounds in which the reactions mostly proceed through the electron transfer process as described in Eq (1,2).



3.1.1.2 Cycloaddition reaction

A reaction in which two or more unsaturated molecules combine and forming new compound. However, the addition reaction between ozone and compound could be different types which can be defined as cycloaddition reaction. Ozone is known to attack the carbon double bonds in organic molecules as aromatics to form a cyclic intermediate called ozonide, which subsequently undergoes a series of ozonolysis reactions and generates ketones, aldehydes, or carboxylic acids [60].

3.1.1.3 Electrophilic substitution reaction

Electrophilic Substitution reaction is one the useful tools commonly researched in organic chemistry area. As electrophilic agent, ozone has the capacity to attack the nucleophilic position of organic substances and substitute one part of the organic molecule. Furthermore, a significant influence on the reactivity of aromatic ring with ozone has been observed and proved. Various substitution group would develop based on the property of the substitution group. The deactivating groups will facilitate the substitution of hydrogen from meta position, while the activating groups would promote the substitution into ortho- and para-hydroxylation of aromatic compounds such as phenol that is a typical example of electrophilic substitution reactions [61].

3.1.1.4 Nucleophilic reaction

Owing to its resonance structure, ozone molecule has negative charge in on of terminal oxygen atoms. Hence, it explains the nucleophilic property that can react with other substances at their electrophilic positions specifically with compounds contains carbonyl or double and triple nitrogen carbon bonds. Nevertheless, this was confirmed in non-aqueous solution system [62].

3.1.2 Indirect reaction

The indirect reaction is defined as the decomposition of ozone molecules into various reactive oxygen species that otherwise called the hydroxyl radicals pathway. The hydroxyl radicals are non-selective and they have the ability to oxidize organic substrates, microorganisms, and nitrogen. Unfortunately, the indirect reaction is constrained by reaction limited conditions (pH, Temperature, presence of chemical scavengers...etc) [63].

3.1.2.1 Ozone-based water treatment processes

Ozonation process is a powerful developed technology with large range of use around the world. As strong oxidant, ozone has been an attractive substance to be used in various areas. Environment pollution specifically water contamination is a serious concern of all authorities around the world that lead to improve the wastewater treatments technologies for more effective and low-cost processes. Ozone is used alone or combined with other oxidant or energy in water treatment.

3.1.2.2 Peroxone process

The ozone combined with hydrogen peroxide is the most studied and best implemented ozone based AOP water treatment. The addition of H₂O₂ boost the reaction and increase the generation of hydroxyl radicals, it leads to fast consumption of O₃. The optimum stoichiometry for an effective reaction in this process is 2ml of Ozone per mol of hydrogen peroxide [59]. It has been found that hydrogen radicals react with ozone following the Eq (3,4,5). However, like other AOPs, in peroxone process, the enhancement of hydroxyl radicals formation is restricted to reaction conditions.



3.1.2.3 Catalytic ozonation process

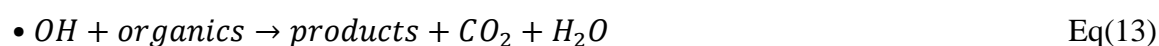
A diverse homogeneous and heterogeneous catalytic ozonation processes have been reported and tested in water and wastewater treatment [64]. The catalytic performance of ozone-metal system (iron (II), cobalt (II), zinc (II), nickel (II), and copper (II)) has been investigated and found to enhance the removal rate of pollutants from aqueous solution [65]. In addition to dissolved metal ions, the metal oxides as titanium, manganese, iron oxide, and activated carbon were also found to act as heterogeneous catalysts of ozone decomposition. The ozone-based AOPs treatments have proven to be useful and efficient to remove various array of pollutants.

3.2 Fenton reaction

In 1894, Henry John Horstman Fenton discovered and described for the first time an oxidation reaction of tartaric acid by hydrogen peroxide in the presence of ferrous ions that was attributed his own name to it until today [66]. Later, in 1960, the Fenton reaction was employed in

wastewater treatment to the destruction of hazardous organic compounds [67]. The Fenton process involves the combination of iron salts and hydrogen peroxide for hydroxyl radicals production. Ferrous ions are oxidized by hydrogen peroxide to ferric ions, a hydroxyl radical, and a hydroxyl anion. For after, the ferric ions are reduced back to ferrous ions, a peroxide radical, and a proton in presence of irradiation.

The Fenton reaction requires a specific set of conditions to achieve the highest degradation rate of organic matter. Hence, the efficiency of the process is related and defined by various parameters including temperature, pH, hydrogen peroxide, and ferrous ions concentrations. To avoid the precipitation of iron, the reaction must be carried out in acidic medium. As it was reported in various studies, the reaction achieves its maximum catalytic activity at pH 3, after which the performance of reaction decreases obviously owing to the precipitation of iron as $Fe(O)_3$ simultaneously with the consumption of hydrogen peroxide into O_2 and H_2O [68]. The optimum temperature of reaction has been found close to the room temperature. The ratio and dosage of reagents is the most important consideration part in the treatment process, as it will not only affect the efficiency but also the cost of treatment. It is generally recommended that an optimal dose of reagents is tailored to meet the desired removal of pollutants for a specific effluent using experimental trials and mathematical optimization techniques. The Equations (6,7,8,9,10,11,12, and 13) describe the possible steps of Fenton reaction [69].



3.3 Photochemical processes

3.3.1 Fundamentals of photochemistry

3.3.1.1 Definition

Photochemistry is a sub-discipline of chemistry that refers to interactions between light or other electromagnetic radiations and matter. Photochemical reactions are occurring in the living systems and in environment since life existence, underlaying the processes of vision, photosynthesis, atmospheric chemistry (the ozone layer) that helped and increased the understanding of the phenomenon. The power and versatility of photochemistry is becoming increasingly important in improving the quality of lives, through health care (neonatal jaundice treatment, photodynamic therapy for cancer treatment), energy production, synthesis of materials (photography, photopolymerization, photocopying, and photochromism in sunglasses production process), and wastewater treatment.

3.3.1.2 Basic laws of photochemistry

There are two principle basic laws that govern the effects of radiation on chemical reactions. The first law of photochemistry was formulated in 1818s by Christian von Grotthus and was later reaffirmed in 1841 by John Draper. The law has been defined as:

“When light falls on any substance, only a fraction of it absorbed whereas the rest is either reflected or transmitted. It is only the absorbed light which is effective in bringing about a chemical reaction”

The law states that only light that is absorbed by a molecule can produce a photochemical change in that molecule. In addition, the law relates photochemical activity to the fact that each chemical substance absorbs only certain wavelengths of light, the set of which is unique to that substance. Therefore, the presence of light alone is not sufficient to induce a photochemical reaction which means that the radiation should be in the right range of wavelength to be absorbed by the reactant species. Moreover, the absorbed light could be transformed into thermal energy or may stimulate another phenomenon to happen such as fluorescence, phosphorescence, etc. The law also states that in few cases, the light is transferred into the reacting substances indirectly via other existing substances, this phenomenon is called photosensitization [70].

In 1900s, the concept of light absorption in mystery packets of energy called photons led to the extension of photochemistry laws and to the development of quantum theory of light. The second law of photochemistry was firstly developed by Johannes Stark and it has been

enunciated in 1913 by Einstein. The law of photochemical equivalence which defined as:

“Every atom or molecule which takes part in a chemical reaction absorbs one quantum of the radiation which induces the reaction”

The second law states that only one photon of light is absorbed by each molecule undergoing a photochemical reaction. The law explains the equivalence and correspondence between the number of absorbed photons and the number of excited species. The second law had also permit to calculate the quantum yield of reaction that reveals the reaction efficiency [71].

3.3.1.3 Electromagnetic radiation

Electromagnetic radiation is presented in classical physic as combination of oscillating electric and magnetic fields. At right angles to each other to the direction of propagation, the electric and magnetic field vectors oscillate as sinusoidal vibration which it is called a transverse wave figure 7. These electromagnetic waves are characterized by: wavelength, frequency, diffraction, interference, extension in time and space, reflection, and polarisation.

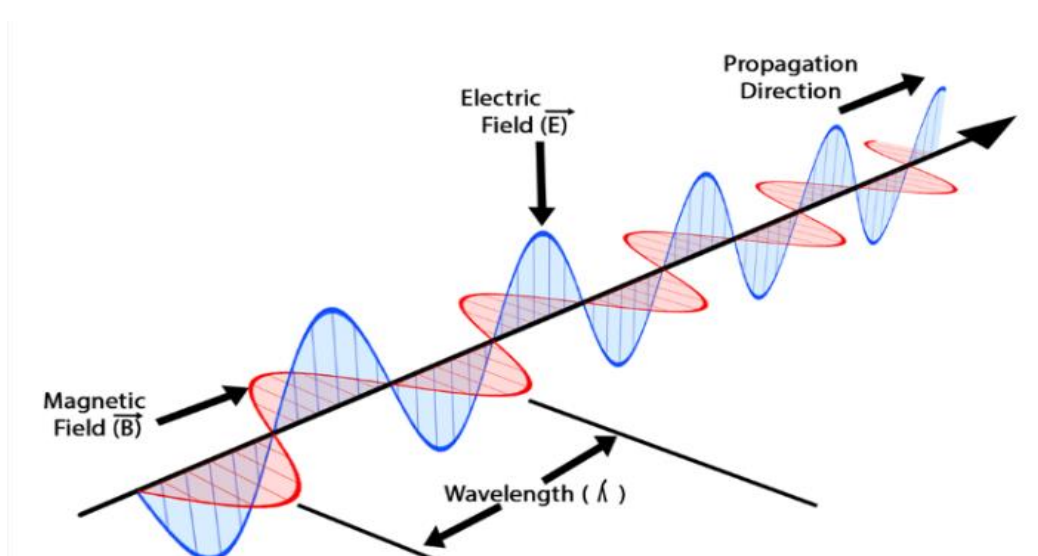


Figure 7: Propagation of electromagnetic wave in free space with electric and magnetic field components [72].

In photochemistry, the electromagnetic radiation is described to be an amount of energy that consist on photons. The electromagnetic spectrum is the range of all possible frequencies, wavelength of electromagnetic radiation. The spectrum covers as displayed in figure 8 radio waves, microwave, infrared, the visible region (light), ultraviolet, X-rays, and gamma rays. The wavelength and also the amount of energy play important rule in electromagnetic radiation behaviour in interaction with atoms and molecules [73].

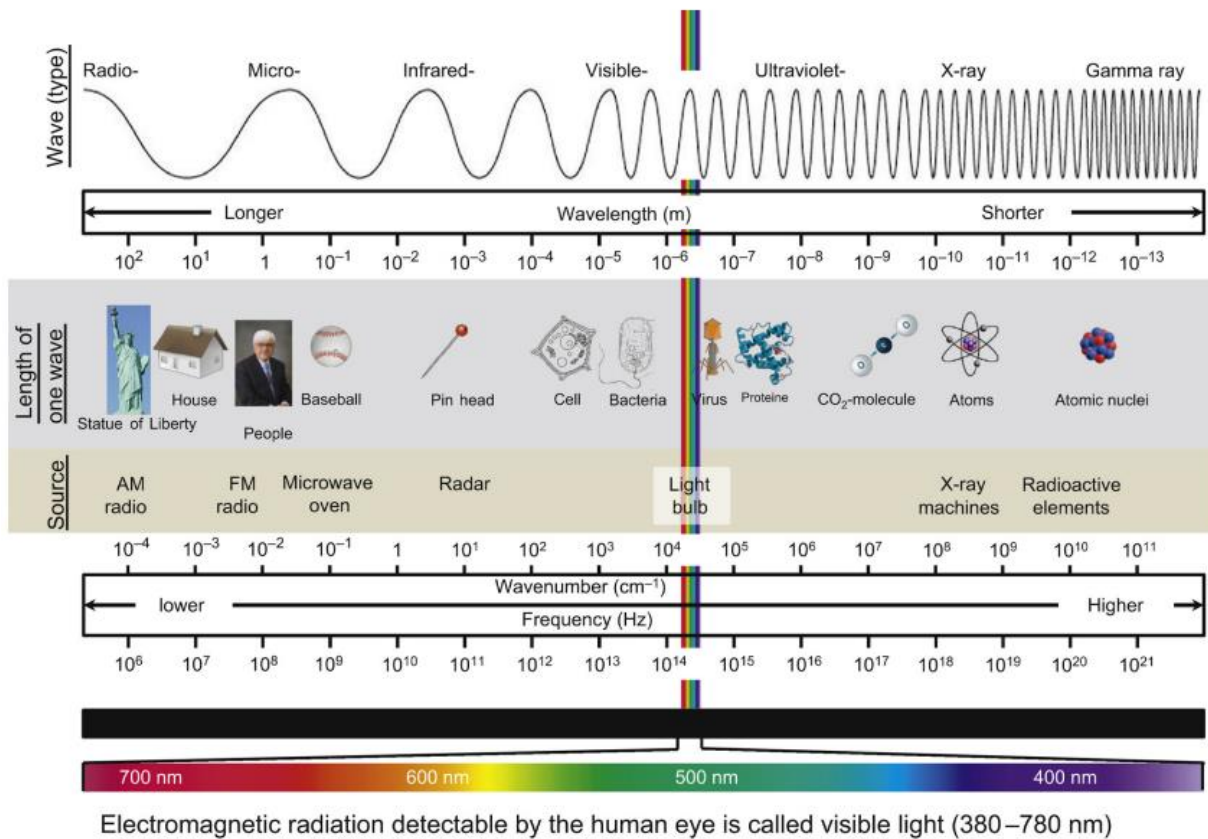
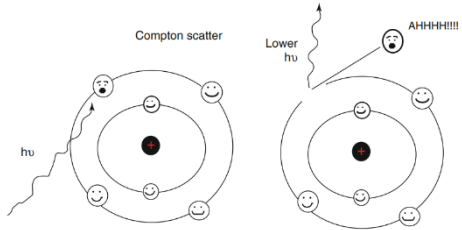


Figure 8: Schematic representation of electromagnetic spectrum range on the wavelength and frequency scale [74].

3.3.1.4 Interaction of electromagnetic radiation with matter

For many years, the atom nature and the particles and matter interaction were considered as a mystery. However, the spectroscopy and other discovered experiments revealed the atomic structure and incorporate new concept of energy levels. In addition, in twentieth century, the chemical physics scientific world knew a revolution of theories that leads to understand more the atomic and molecule structure. The theories gave birth to the new concept called “*quantum*” that uncovers the mysterious nature of electronic transitions in atoms and removes the theory of distinction between waves and particles. Moreover, the exploration of the other electromagnetic radiation beside the visible range enlightened new light perspectives and provided an advanced tools in EM technological application [74]. The EM-matter interaction proceeds in various way according to electromagnetic radiation nature referred to spectrum range. Table 5 describes all possible interaction of between the different type of electromagnetic radiation and matter.

Table 5: Interaction of electromagnetic matter with matter according to spectrum range [75].

EM nature according to spectrum range	Interaction with matter
Radio	Transmission in collective oscillation of charge carriers in bulk material (example of oscillation of the electrons in an antenna).
Microwave	Oscillation, molecular rotation and production of heat as result of that molecular motion.
Infrared	-Molecular vibration, -Plasma oscillation (in metals only).
Visible	Molecular electron excitation (including molecules found in human retina), Plasma oscillation in metals only.
Ultraviolet	-Excitation of molecular and atomic valence electrons, including ejection of the electrons (photoelectric effect).
X-rays	-Excitation and ejection of core atomic electrons, -Compton scattering for low atomic numbers. 
Gamma-rays	-Energetic ejection of core electrons in heavy elements, -Compton scattering (for all atomic numbers), -Excitation of atomic nuclei.

3.3.1.5 Reaction pathways

A photochemical process involves two crucial steps, the absorption of a photon followed by the reaction. The absorbed energy stimulates the excitation of electrons, in which the photon loses

its entire energy to an atomic electron that is in turn liberated from the atom. The electronically excited species lead to new products and tried to reach their normal state. Table 6 defines the process of all possible photochemical reactions [76].

Table 6:the electronic excitation reactions after photon absorption

Reaction	Name of phenomenon
$AB^* \rightarrow A+B$	Dissociation
$AB^* \rightarrow AB^+ + e^-$	Ionization
$AB^* \rightarrow BA$	Isomerization
$AB^* + C \rightarrow AC+B$	ABC reaction
$AB^* + DE \rightarrow AB+DE^*$	Energy transfer (intermolecular)
$AB^* + M \rightarrow AB+ M$	Physical quenching
$AB^* \rightarrow AB$	Energy transfer (intramolecular)
$AB^* \rightarrow AB+ h\nu$	Luminescence

3.3.1.6 Light Absorption – Formation of the Excited State

After light absorption, molecules induce sufficient energy to break or reorganize the most covalent bonds. The position of electrons in a molecule can be explained by assuming that they occupy molecular orbitals which are a linear combination of atomic orbitals. The energy levels can be determined by substituting the wavefunctions of the molecular orbitals in the time dependent Schrödinger equation. The wavefunctions used to describe many electron atoms are analytical functions but approximate the true wavefunctions enough to represent the electronic structure of a molecule. A molecular orbital can be, in order of increasing energy, bonding, non-bonding or anti-bonding. The photochemically interesting orbitals are described as n orbitals depending on the geometry and symmetry of their wavefunctions. Frontier orbitals are the most important orbitals in molecules for reactivity, HOMO which is defined as the highest occupied molecular orbital and the lowest unoccupied molecular orbital LUMO. The electronic excitation of molecule M^* leads to HOMO-LUMO transition as described in figure 9 [77].

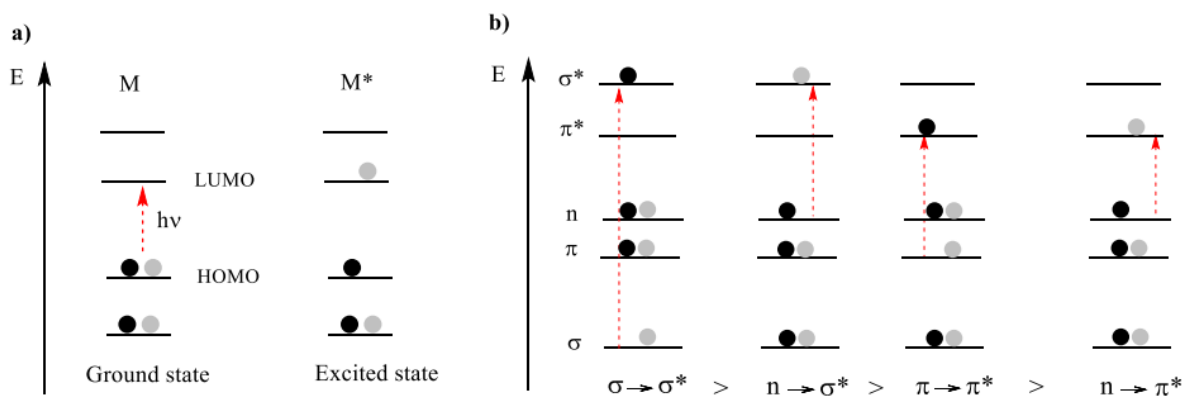


Figure 9: a) electronic transition between HOMO and LUMO levels. b) Energy levels showing the different types of electronic transitions within organic molecules from the more energetic $\sigma \rightarrow \sigma^*$ to the less energetic orbital $n \rightarrow \pi^*$ [78].

In 1927, Max Born and J. Robert Oppenheimer introduced the Born-Oppenheimer approximation which consists on the separation of the electrons in a molecule from the motion of the nuclei based on the mass and movement of the nuclei which is considered as the heavier and slow part compared to electrons. The nuclei is defined as stationary in a given arrangement that helps to solve the Schrödinger equation for the electrons [79]. In addition, Franck Condon principle is another concept that plays an important role in understanding the nature of optical transitions. The principle states that the electronic transitions are rapid in a fast timescale in femtoseconds at fixed nuclear position that permit to calculate the transition probability. The readjustment of charge in a molecule that follows an electronic transition leads to changes in the vibrational state of the molecule. Excitation according to Franck-Condon principle is not to the lowest vibrational level, but somewhere higher and the transition involved a vertical transition figure 10. The molecule after absorption of light, finds itself in non-equilibrium state with thousands of vibrations. The vibration mode is so short 9 to 10 seconds and the equilibrium can be established through a non-radiative relaxation to the non-vibrational state v_0 [80].

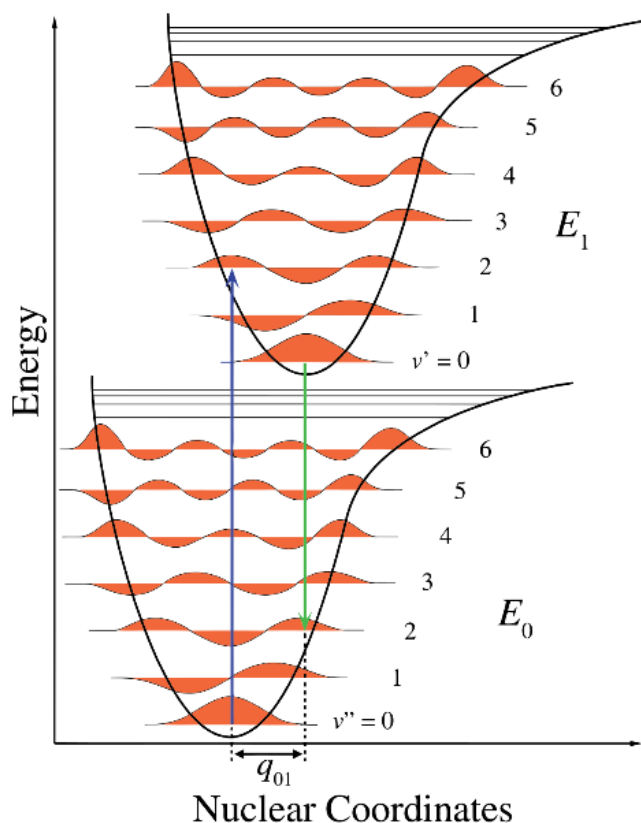


Figure 10: Franck-Condon principle energy diagram, the vibronic transitions [81].

3.3.1.7 Singlet and triplet states

The absorption or scattering of photons induces the excited states of molecule, the electron finds itself in the highest energy molecular orbital. The electronic arrangement results various combinations of electron spin and orbital angular momentum that have the capacity to generate atomic energy levels of different spin (*spin multiplicity*), orbital and angular momenta. An electronic transition takes place with no change in the case that the total electron spin $S=0$ means the spins of the electrons are paired, this is known as singlet state. In the other hand, the triplet state is defined as a system with two parallel and unpaired electrons, the total electron spin is $S=1$ which allows three values of the angular momentum as -1, 0, and +1 that results the split of three spectral lines, and thus, got the name of triplet state figure 11 [82].

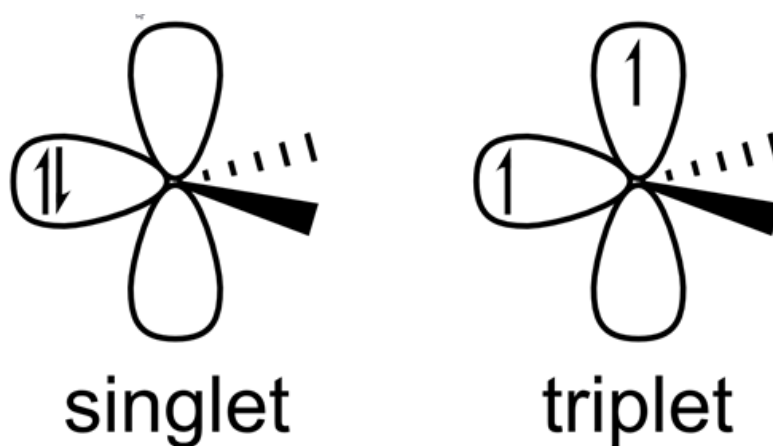


Figure 11: example of electronic structure of singlet and triplet states

3.3.1.8 Photophysical processes

The photophysical processes are the consequences of molecular absorbance and emission of light. Aleksander Jablonski developed a schematic energy diagram as illustrated in figure 12 that generally explain the energy of photoluminescent molecule in its different energy states. The lowest horizontal line represents the ground-state electronic energy of molecule (singlet state) which is labelled as S_0 . The upper lines represent the energy state of the three excited states; the two electronic singlet states S_1 and S_2 in the left and the first electronic triplet state T_1 in the right of diagram. Within each electronic energy state are multiple vibronic energy states that may be coupled with the electronic state. The photophysical processes are listed as below [83]:

⇒ **Vibrational relaxation**

The vibrational relaxation is an association of electronically-excited species with an excess of vibrational energy. The vibrational relaxation involves transitions between a vibrationally-excited state ($v>0$) and the $v=0$ state once the excited molecule collides with other species. the process is of the order of nanoseconds and the energy of molecule is eventually degraded as heat to the surroundings.

⇒ **Internal conversion**

The internal conversion is a non-radiative process that explained as the relaxation from an upper excited electronic state to a lower electronic excited state with the same multiplicity. The process is mechanistically identical to the vibrational relaxation process. The internal conversion occurs as result of the overlap of vibrational and electronic energy states. This overlap gives a higher degree of probability of electron transition between vibrational levels

that will decrease the energy of electronic state. In internal conversion, the electron takes much time to return to the ground state which permit the complete of other transitive processes at the same time.

⇒ **Fluorescence**

Fluorescence is considered as one of the molecules energy pathways once absorbed a photon. This phenomenon as indicated on the Jablonski diagram is a radiative process, it involves a radiative transition (photon emission) between states of the same multiplicity. The fluorescence emission is of the order of 10^{-9} . The process is commonly observed between the first excited electron state and the ground state as at higher energies levels, the energy is dissipated through internal conversion and vibrational relaxation processes. In addition, the emitted energy is less than the absorbed energy, the loss can be explained via the energy transfer to other processes mechanism.

⇒ **Intersystem crossing**

The intersystem crossing involves the intramolecular spins, the process is the connection as electronic change from the excited singlet state to the excited triplet state. The process is the slower event in the Jablonski diagram, the slow transition is a forbidden transition based directly on electronic selection. Intersystem crossing leads to several routes once returning to the ground state, a direct transition which gives birth to the phosphorescence phenomenon, and another possible pathway that delayed fluorescence via returning to the first excited singlet level followed by emission of transition to the ground electronic state.

⇒ **Phosphorescence**

Phosphorescence is radiative transition, a spin-forbidden in which the electron in the excited orbital has the same spin orientation as the ground electron. The emission of light by phosphorescence phenomenon is of order of nanoseconds 10^{-3} [84].

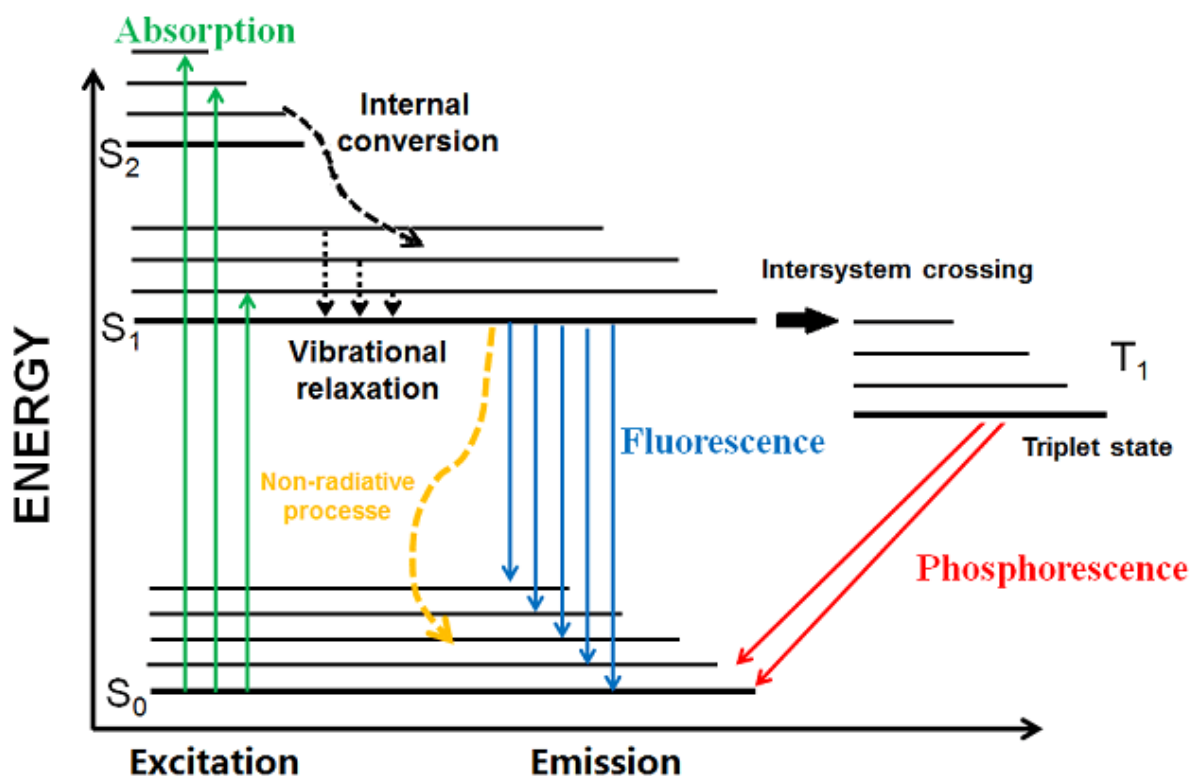


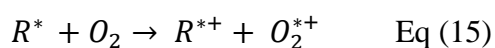
Figure 12:Jablonski diagram for an organic molecule illustrating the photophysical processes [85].

3.3.2 Photochemistry application in AOPs treatments

A various array of wastewater chemical treatments methods specifically the oxidation processes including ozonation and chlorination have shown their efficiency in POPs removal. However, the efficiency of any process is always related to the molecular nature of treated pollutant and the dosage of oxidant agent during the treatment. In addition, the generation of processes based on photochemical oxidation using UV or visible light source have also investigated to be effective [86].

3.3.2.1 Direct photolysis

The direct photolysis involves that the treated micropollutant has the capacity to absorb photons. The absorbed energy must be enough to induce the photochemical reaction. The direct irradiation stimulates the excitation of molecules, leading to the promotion of a molecules from ground state to an excited singlet state, that may then intersystem crossing to produce triplets state excitation. Generally, the photolytic process occurs when the excited molecules react with dissolved oxygen leading to the photo-transformation of organic pollutant Eq(14, 15, 16)[87].



The rate photodegradation of direct photolysis depends on the absorbed light intensity, the irradiation wavelength, and the quantum yield of reaction. Furthermore, the process was rapidly abandoned due to numerous reasons including the high cost of energy, the low reliability and the maintenance difficulties of equipment. However, the photolysis technology process is widely combined with other conventional or chemical methods [88].

3.3.2.2 Photolysis of ozone/ H₂O₂

Ozone has a strong absorption ability of UV light, the irradiated ozone in aqueous solution generates a large concentration of hydrogen peroxide that proceeds in micropollutants decomposition via inducing the hydroxyl radicals. The addition of hydrogen peroxide accelerates the decomposition of ozone in hydroxyl radicals. Hence, the process reaction occurs because of a synergic effect due to the combination of three principal reactions; the ozonation, the direct photodecomposition, and the radical decomposition. The efficiency of process depends on the quantity of ozone and hydrogen peroxide and proven any previous work a high removal rate of organic micropollutants. However, the economic viability of this technique is limited due to the high costs of the system elements [89].

3.3.2.3 Homogeneous photocatalysis: photo-Fenton process

The photo-Fenton process alone still inefficient with no capacity of pollutants mineralization. The light source is known as accelerator of Fenton reaction for hydroxyl radicals production, the irradiation induces the reduction of dissolved Fe³⁺ to Fe²⁺ and contributes in the direct decomposition of hydrogen peroxide molecules into hydroxyl radicals. the photo-Fenton process is one of AOPs technologies that has proven a high efficiency in micropollutants removal which is related essentially to the concentration of iron ions, hydrogen peroxide, and light intensity, the process elements concentration boosts the hydroxyl radical generation leading to high performance of process. According to the literature, the photo-Fenton process was investigated for degradation and mineralization of diverse categories of micropollutants (dyes, pharmaceuticals, and pesticides). However, the process is limited by the necessity of identification of photoproducts after each treatment [90].

3.3.2.4 Heterogeneous photocatalysis

The heterogeneous photocatalysis is defined as an intersection of multidisciplinary fields of sciences. It is based on four crucial pillars (heterogeneous catalysis, photochemistry, spectroscopy, and material sciences) figure 13. The semiconductors are activated by the light absorption with energy above its bandgap. The heterogeneous refers to the fact that the reaction is a combination between two phases liquid (the contaminants in aqueous solution) and solid (the semiconductor as powder, films or any solid state). The mainly used semiconductors are the metal oxides, the most commonly used is titanium dioxide TiO_2 because of its high chemical stability, economic cost, and the high effectiveness compared to other processes.

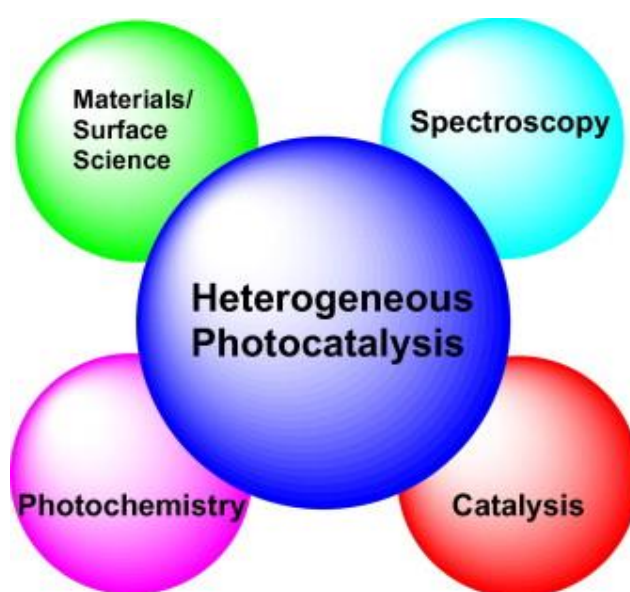


Figure 13:The four pillars that have had a great impact in the development of heterogeneous photocatalysis [91].

The photocatalytic reaction is initiated by light harvesting process based mainly on the surface morphology and structure of catalyst. The absorbed energy must be the same or more than the photocatalyst bandgap energy to provoke the photonic excitation that implies an electronic transition from the valence band which is saturated to the conduction band. The electronic transition generates electron e^- /hole h^+ pairs in the conduction and valence band respectively figure 14. The electron and hole have the ability to recombine and without any chemical reaction they could realising the absorbed energy as heat. In addition, they can contribute in redox reactions with absorbed species, dissolved oxygen in aqueous medium, and generate the hydroxide ions. These series of reactions lead to high photocatalytic performance to degrade the organic pollutants to a complete mineralization [92].

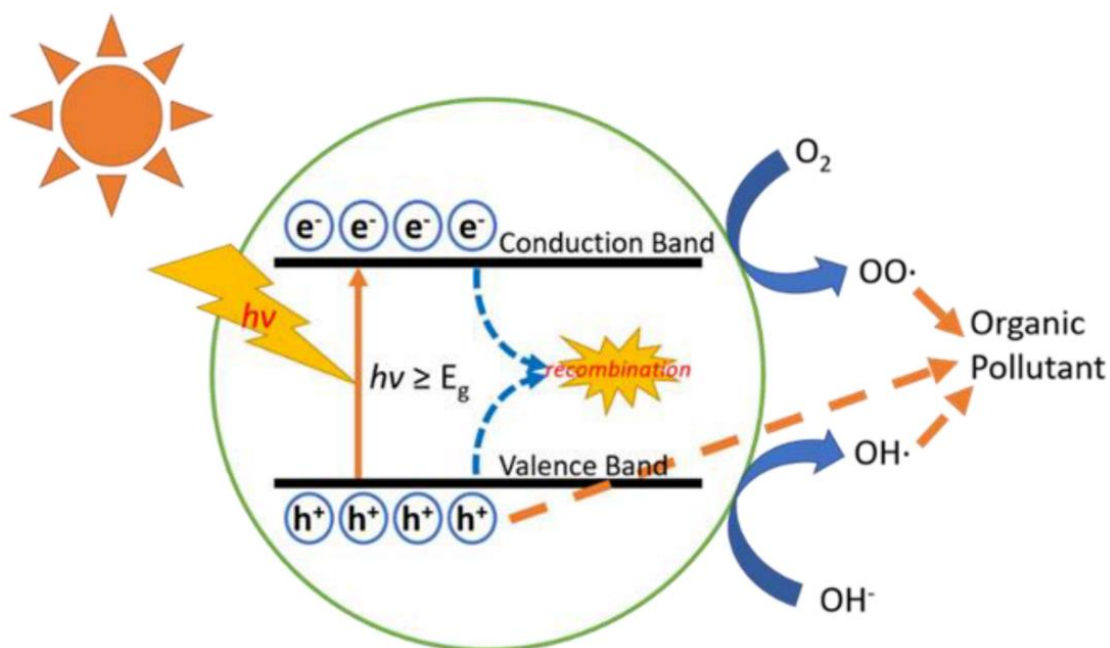


Figure 14:Mechanism photocatalysis [93]

In literature, a various semiconductors were investigated as powerful photocatalysts (TiO₂, ZnO, WO₃, Fe₂O₃, and some nanocomposite materials)[94-97]. The low-cost, high chemical stability, availability, easy use of these materials, and also the light absorption spectrum that is aligned with solar spectrum range this all circumstance increases the interest of researches on these materials.

3.4 Sonochemical processes

Sonochemistry is a discipline of chemistry studying the properties of sonic cavitation and its effect and interaction on chemical systems. The sonochemical processes are part of AOPs that have been investigated to be effective in organic pollutants degradation. Figure 15 presents the ultrasounds frequency range, as the ultrasounds are defined to be a mechanical wave that need an elastic medium to have the capacity to spread by the wave frequency over and differ from sounds. From 16 to 20 Hz frequencies are defined the sounds, human hearing level. In addition, the high frequencies range from 5 to 10 MHz are used in different sectors as medical imaging or in industries to detect for example defect material products.

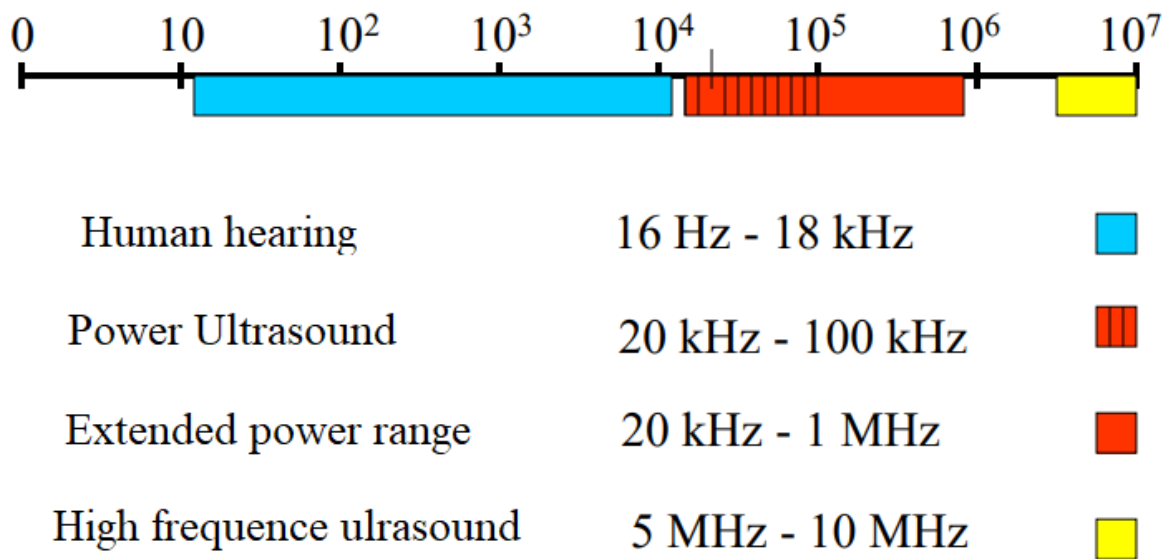


Figure 15: Ultrasound frequency range

The ultrasound is defined as a result of vibration of an oscillating body in an elastic medium causing a local movement of the particles called wave. The wave is generally described in terms of frequency and intensity of sonic properties. There are two basic types of waves, transverse and longitudinal, differentiated by the way in which the wave is propagated. The transverse wave is generated in the medium by perpendicular oscillation to the direction of propagation. The longitudinal wave that is the most existing in nature, generated by parallel movement of particles to the direction of propagation, leading to formation of acoustic impulse that compresses (high pressure) and rarefying (low pressure) the particles depending on the elasticity of medium as displayed in figure 16.

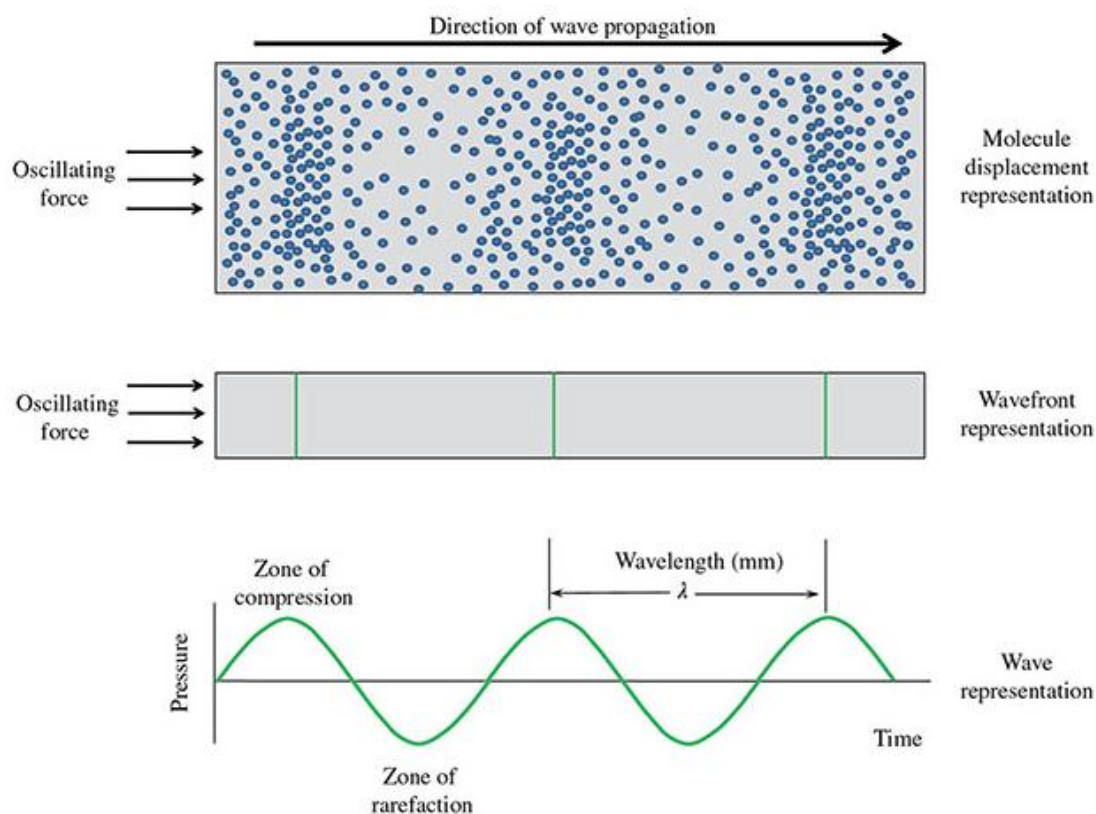


Figure 16:longitudinal wave graphic representation

3.4.1 Sonolysis and Sonocatalytic processes

Sonochemical oxidation is one of the most recent used process, ultrasound irradiation generates the hydroxyl radicals by the water pyrolysis. Alone or coupled with other techniques, sonocatalytic processes have been proven efficient, and also considered as a green technique to eradicate toxic pollutants figure 17.

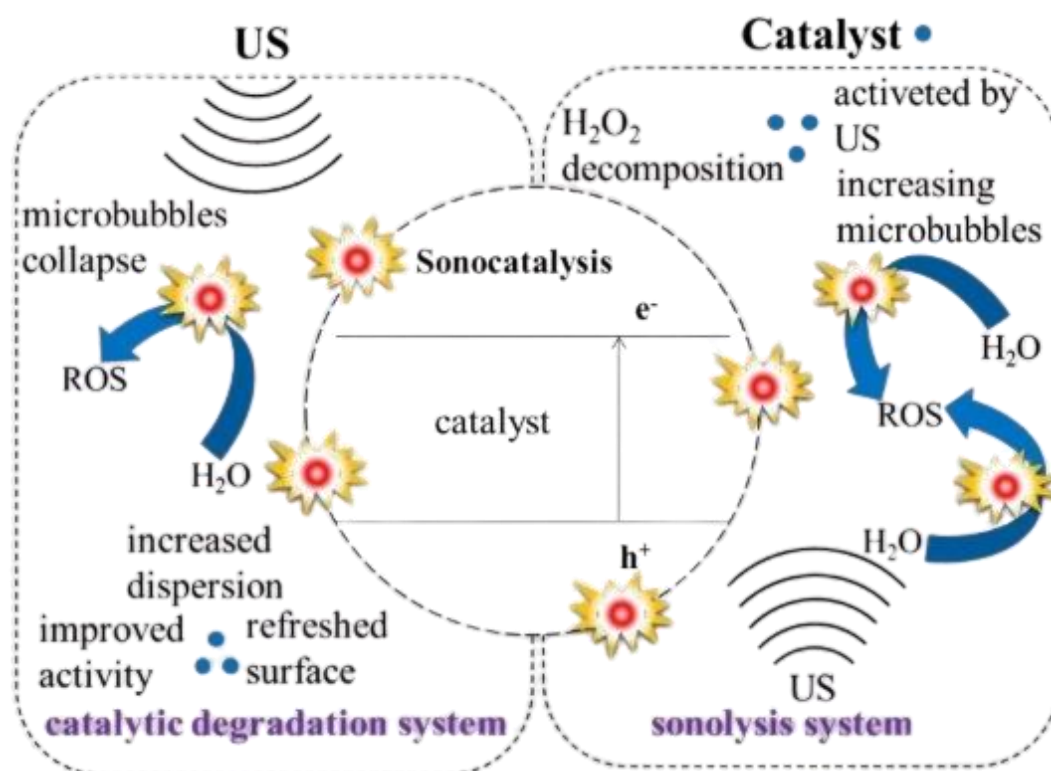


Figure 17: Sonocatalytic mechanism of micropollutants removal [98].

The formation and the subsequent collapse of bubbles in aqueous solution once ultrasound irradiation take place is defined as cavitation, which induces a high energy amount. The sonocatalytic performance involves the hydroxyl radicals as result of chemical transformation of water, where the organic micropollutants are removed via oxidation, and the volatile compounds are thermally degraded [99]. In homogeneous sonochemistry, there are three reaction sites responsible of organic pollutant oxidation as described in figure 18, the interior bubble cavitation, the interfacial bubble region, and the bulk solution. The chemical removal of organic molecules occurs inside the bubble depending on volatility of compound. Generally, the oxidation reactions in the bulk solution still limited due to the restricted amount of hydroxyl radicals coming from the collapsing cavities and interfacial region. The predominant of the three sites that conduct the water medium contamination is the gas-liquid interface site which induces the high concentration of $\bullet\text{OH}$.

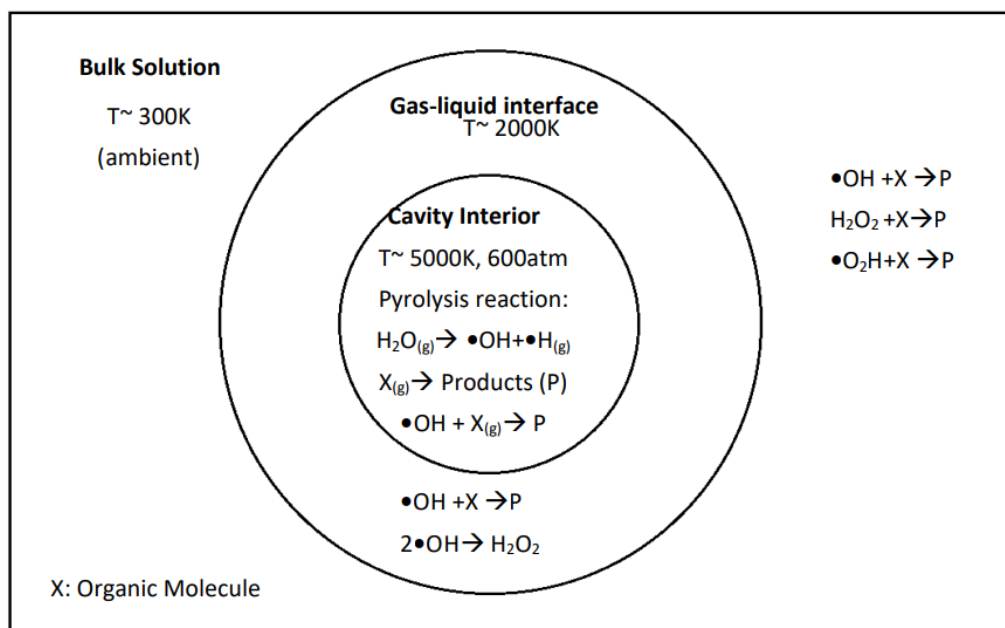
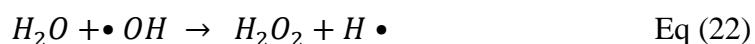


Figure 18:Reaction sites in sonochemistry [100].

A various array of micropollutants have been oxidized by sonolysis alone as described in Eq(17,18,19, 20, 21, and 22) [101]. However, the sonication has limited efficiency and requires a huge amount of energy which is economically disadvantageous. Furthermore, in order to improve the process efficacy and cost reduction, the sonochemical technique has been combined with other processes, the sonocatalysis, sono-Fenton, sono-ozonation, sono-electrochemical degradation, and other AOPs processes.



3.4.2 Application of sonocatalysis in environmental remediation

Environmental remediation is the biggest challenge motivating scientists to find out the simple, low cost, and the effective environmental treatment. Recently, the application of ultrasound as an AOPs for decontamination of water has attract a considerable interest of researchers. As mentioned before, the sonolysis process induces the pollutants degradation via hydroxyl

radicals and thermal decomposition. A series of organic pollutants including persistent micropollutants (pesticides, pharmaceuticals, azo dyes, and personal care products) degradation have been investigated with these radicals and direct pyrolysis [101-103]. Moreover, beside the removal characteristic of ultrasound, it has been used also in synthesis of materials and as microorganism's disinfectant. Generally, many studies have explored the ultrasonic irradiation combined to other various treatments such as ozonation, chlorination, electrolysis, adsorption, and with semiconductors that have been able to degrade the pollutants and achieved an excellent removal efficiency [105-106].

4 References

- [1] S. Kumar *et al.*, “Water resources pollution associated with risks of heavy metals from Vatukoula Goldmine region, Fiji,” *Journal of Environmental Management*, vol. 293, October 2020, p. 112868, 2021, doi: 10.1016/j.jenvman.2021.112868.
- [2] Md. K. Hasan, A. Shahriar, and K. U. Jim, “Water pollution in Bangladesh and its impact on public health,” *Heliyon*, vol. 5, no. 8, p. 02145, 2019, doi:10.1016/j.heliyon.2019.e02145.
- [3] A. Li, C. Kroeze, T. Kahil, L. Ma, and M. Strokal, “Water pollution from food production: lessons for optimistic and optimal solutions,” *Current Opinion in Environmental Sustainability*, vol. 40, pp. 88–94, 2019, doi: 10.1016/j.cosust.2019.09.007.
- [4] H. B. Quesada, A. T. A. Baptista, L. F. Cusioli, D. Seibert, C. de Oliveira Bezerra, and R. Bergamasco, “Surface water pollution by pharmaceuticals and an alternative of removal by low-cost adsorbents: A review,” *Chemosphere*, vol. 222, pp. 766–780, 2019, doi: 10.1016/j.chemosphere.2019.02.009.
- [5] N. A. Oladoja and I. E. Unuabonah, “The pathways of microplastics contamination in raw and drinking water,” *Journal of Water Process Engineering*, vol. 41, no. December 2020, p. 102073, 2021, doi: 10.1016/j.jwpe.2021.102073.
- [6] M. O. Barbosa, N. F. F. Moreira, A. R. Ribeiro, M. F. R. Pereira, and A. M. T. Silva, “Occurrence and removal of organic micropollutants: An overview of the watch list of EU Decision 2015/495,” *Water Research*, vol. 94, pp. 257–279, 2016, doi: 10.1016/j.watres.2016.02.047.
- [7] J. Sharma, S. Sharma, and V. Soni, “Classification and impact of synthetic textile dyes on Aquatic Flora: A review,” *Regional Studies in Marine Science*, vol. 45, 2021, doi: 10.1016/j.rsma.2021.101802.
- [8] P. S. Vankar, *Natural Dyes for Textiles* book, ISBN:978-0-08-101274-1, Elsevier Editor, 2017. doi: 10.1016/c2015-0-01885-8.
- [9] T. M. Baldwinson and J. Shore, “Colorants and Auxiliaries,” *J. Shore (Ed.)*, vol. 2, pp. 338–339, 1990.
- [10] H. Ben Mansour, O. Boughzala, D. Barillier, and R. Mosrati, (2011). Les colorants textiles sources de contamination de l’eau : CRIBLAGE de la toxicité et des méthodes de traitement. *Revue des sciences de l’eau / Journal of Water Science*, 24(3), 209–238. <https://doi.org/10.7202/1006453ar>
- [11] G. R. Chatwal, *Synthetic Dyes*. ISBN: 978-81-84882-20-9, Himalaya publishing house, 2009. doi: 10.1201/noe0824727857.ch355.
- [12] F. M. D. Chequer, G. A. R. de Oliveira, E. R. A. Ferraz, J. C. Cardoso, M. V. B. Zanoni, and D. P. de Oliveira, “Textile Dyes: Dyeing Process and Environmental Impact”, in *Eco-Friendly Textile Dyeing and Finishing*. London, United Kingdom: IntechOpen, 2013 [Online]. Available: <https://www.intechopen.com/chapters/41411> doi: 10.5772/53659

- [13] L. M. G. Jansen, Doctoral Thesis “Photochemistry and photophysics of Azo dyes,” Loughborough University, 1998.
- [14] É. Guivarch and M. A. Oturan, “Le problème de la contamination des eaux par les colorants synthétiques : Comment les détruire ? Application du procédé électro-Fenton,” *Actualite Chimique*, no. 277–278, pp. 65–69, 2004.
- [15] H. Ben Slama *et al.*, “Diversity of synthetic dyes from textile industries, discharge impacts and treatment methods,” *Applied Sciences (Switzerland)*, vol. 11, no. 14, 2021, doi: 10.3390/app11146255.
- [16] K. Hunger, *Industrial Dyes : Chemistry, Properties, Applications*. WILEY-VCH Verlag GmbH & Co. KGaA, Weinheim, 2003.
- [17] K. Basuki, “A Handbook of Dyes, Stains and Fluorochromes for Use in Biology and Medicine,” *ISSN 2502-3632 (Online) ISSN 2356-0304 (Paper) Jurnal Online Internasional & Nasional Vol. 7 No.1, Januari – Juni 2019 Universitas 17 Agustus 1945 Jakarta*, vol. 53, no. 9, pp. 1689–1699, 2019.
- [18] K. Itoh, C. Yatome, and T. Ogawa, “Biodegradation of anthraquinone dyes by *Bacillus subtilis*,” *Bulletin of Environmental Contamination and Toxicology*, vol. 50, no. 4, pp. 522–527, 1993, doi: 10.1007/BF00191240.
- [19] P. O. Bankole, A. A. Adekunle, O. F. Obidi, O. D. Olukanni, and S. P. Govindwar, “Degradation of indigo dye by a newly isolated yeast, *Diutina rugosa* from dye wastewater polluted soil,” *Journal of Environmental Chemical Engineering*, vol. 5, no. 5, pp. 4639–4648, 2017, doi: 10.1016/j.jece.2017.08.050.
- [20] J. Kröger, N. Néel, R. Berndt, Y. F. Wang, and T. G. Gopakumar, “Exploring the organic-inorganic interface with a scanning tunneling microscope,” *Encyclopedia of Interfacial Chemistry: Surface Science and Electrochemistry*, pp. 81–98, 2018, doi: 10.1016/B978-0-12-409547-2.14144-7.
- [21] J. N. Chakraborty, *Sulphur dyes*, vol. 1. Woodhead Publishing Limited, 2011. doi: 10.1533/9780857093974.2.466.
- [22] A. Tkaczyk, K. Mitrowska, and A. Posyniak, “Synthetic organic dyes as contaminants of the aquatic environment and their implications for ecosystems: A review,” *Science of the Total Environment*, vol. 717, p. 137222, 2020, doi: 10.1016/j.scitotenv.2020.137222.
- [23] G. Samchetshabam, A. Hussan, T. G. Choudhury, and S. Gita, “Impact of Textile Dyes Waste on Aquatic Environments and its Treatment Wastewater Management View project Tribal Sub Plan View project,” *Environment & Ecology*, vol. 35, no. September, pp. 2349–2353, 2017.
- [24] R. M. de Souza, D. Seibert, H. B. Quesada, F. de Jesus Bassetti, M. R. Fagundes-Klen, and R. Bergamasco, “Occurrence, impacts and general aspects of pesticides in surface water: A review,” *Process Safety and Environmental Protection*, vol. 135. Institution of Chemical Engineers, pp. 22–37, Mar. 01, 2020. doi: 10.1016/j.psep.2019.12.035.
- [25] J. Beard, “DDT and human health,” *Science of the Total Environment*, vol. 355, no. 1–3, pp. 78–89, Feb. 2006, doi: 10.1016/j.scitotenv.2005.02.022.

- [26] Oussama SAASANE, Doctoral thesis N°127 : the impact of pesticides on environment & human health, & alternative methods, Faculty of pharmacy, University Mohammed V of Rabat, 2018.
- [27] W. M. Jarman and K. Ballschmiter, “From coal to DDT: The history of the development of the pesticide DDT from synthetic dyes till Silent Spring,” *Endeavour*, vol. 36, no. 4. Elsevier Ltd, pp. 131–142, 2012. doi: 10.1016/j.endeavour.2012.10.003.
- [28] Y. Abubakar *et al.*, “Pesticides, history, and classification,” in *Natural Remedies for Pest, Disease and Weed Control*, Elsevier, 2019, pp. 29–42. doi: 10.1016/B978-0-12-819304-4.00003-8.
- [29] A. Maria and G. Martins, “Development of a Surface Acoustic Wave Micromixer for Enhanced Chemiluminescence Microanalysis: Application to Pesticides,” 2016.
- [30] R. C. Gupta, I. R. Miller Mukherjee, J. K. Malik, R. B. Doss, W.-D. Dettbarn, and D. Milatovic, “Insecticides,” in *Biomarkers in Toxicology*, Elsevier, 2019, pp. 455–475. doi: 10.1016/B978-0-12-814655-2.00026-8.
- [31] A. Ghosal, Mode of Action of Insecticides Network Project on Organic Farming (NPOF) View project Creation of Seed Hub for increasing production of indigenous pulse project View project. 2018. [Online]. Available: <https://www.researchgate.net/publication/327580308>
- [32] P. K. Gupta, “Herbicides and Fungicides,” in *Reproductive and Developmental Toxicology*, Elsevier, 2011, pp. 503–521, doi: 10.1016/B978-0-12-382032-7.10039-6.
- [33] J. S. Holt, “Herbicides,” in *Encyclopedia of Biodiversity: Second Edition*, Elsevier Inc., 2013, pp. 87–95. doi: 10.1016/B978-0-12-384719-5.00070-8.
- [34] P. K. Gupta, “Toxicity of Fungicides,” in *Veterinary Toxicology: Basic and Clinical Principles: Third Edition*, Elsevier, 2018, pp. 569–580. doi: 10.1016/B978-0-12-811410-0.00045-3.
- [35] H. J. S. Finch, A. M. Samuel, and G. P. F. Lane, “Diseases of farm crops,” in *Lockhart & Wiseman’s Crop Husbandry Including Grassland*, Elsevier, 2014, pp. 119–157. doi: 10.1533/9781782423928.1.119.
- [36] G. W. A. Milne, Handbook of Pesticides Editor, 1st edition, *CRC press*, 1998.
- [37] Nollet, L.M.L., & Rathore, H.S. (Eds.). (2009). Handbook of Pesticides: Methods of Pesticide Residues Analysis (1st edition). *CRC Press*. <https://doi.org/10.1201/9781420082470>.
- [38] D. Beale, Doctoral thesis “Development Towards a Portable Instrument for the Determination of Pesticide Residue in Water”, *School of Applied Sciences, RMIT university*, 2011.
- [39] S. Gouma, Doctoral thesis “Biodegradation of mixtures of pesticides by bacteria and white rot fungi school of health”, *School of health, Grandfield University*, 2009.
- [40] R. Mesnage and G.-E. Séralini, “Editorial: Toxicity of Pesticides on Health and Environment,” *Frontiers in Public Health*, vol. 6, Sep. 2018, doi: 10.3389/fpubh.2018.00268.

- [41] L. Hanson and L. Ritter, "Toxicity and Safety Evaluation of Pesticides," in *Hayes' Handbook of Pesticide Toxicology*, Elsevier Inc., 2010, pp. 333–336. doi: 10.1016/B978-0-12-374367-1.00126-9.
- [42] D. Ramsingh, "The Assessment of the Chronic Toxicity and Carcinogenicity of Pesticides," in *Hayes' Handbook of Pesticide Toxicology*, Elsevier Inc., 2010, pp. 463–482. doi: 10.1016/B978-0-12-374367-1.00014-8.
- [43] V. I. Lushchak, T. M. Matviishyn, V. v. Husak, J. M. Storey, and K. B. Storey, "Pesticide toxicity: A mechanistic approach," *EXCLI Journal*, vol. 17. Leibniz Research Centre for Working Environment and Human Factors, pp. 1101–1136, 2018. doi: 10.17179/excli2018-1710.
- [44] F. W. Kopisch-Obuch, "Pesticide management under the international code of conduct on the distribution and use of pesticides," *Journal of Environmental Science and Health - Part B Pesticides, Food Contaminants, and Agricultural Wastes*, vol. 31, no. 3. Taylor and Francis Inc., pp. 293–305, 1996. doi: 10.1080/03601239609372991.
- [45] G. Crini and E. Lichtfouse, "Advantages and disadvantages of techniques used for wastewater treatment," *Environmental Chemistry Letters*, vol. 17, no. 1. Springer Verlag, pp. 145–155, Mar. 01, 2019. doi: 10.1007/s10311-018-0785-9.
- [46] A. Jelić, M. Gros, M. Petrović, A. Ginebreda, and D. Barceló, "Occurrence and Elimination of Pharmaceuticals During Conventional Wastewater Treatment," in *Handbook of Environmental Chemistry*, vol. 19, Springer Verlag, 2012, pp. 1–23. doi: 10.1007/978-3-642-25722-3_1.
- [47] M. Clara, B. Strenn, M. Ausserleitner, and N. Kreuzinger, "Comparison of the behaviour of selected micropollutants in a membrane bioreactor and a conventional wastewater treatment plant," 2004. [Online]. Available: <https://iwaponline.com/wst/article-pdf/50/5/29/46823/29.pdf>
- [48] S. C. Ameta, "Introduction," in *Advanced Oxidation Processes for Wastewater Treatment: Emerging Green Chemical Technology*, Elsevier Inc., 2018, pp. 1–12. doi: 10.1016/B978-0-12-810499-6.00001-2.
- [49] Y. Deng and R. Zhao, "Advanced Oxidation Processes (AOPs) in Wastewater Treatment," *Current Pollution Reports*, vol. 1, no. 3. Springer, pp. 167–176, Sep. 01, 2015. doi: 10.1007/s40726-015-0015-z.
- [50] V. K. Saharan, D. v. Pinjari, P. R. Gogate, and A. B. Pandit, "Advanced Oxidation Technologies for Wastewater Treatment: An Overview," in *Industrial Wastewater Treatment, Recycling and Reuse*, Elsevier Inc., 2014, pp. 141–191. doi: 10.1016/B978-0-08-099968-5.00003-9.
- [51] M. A. Oturan and J. J. Aaron, "Advanced oxidation processes in water/wastewater treatment: Principles and applications. A review," *Critical Reviews in Environmental Science and Technology*, vol. 44, no. 23. pp. 2577–2641, Dec. 02, 2014. doi: 10.1080/10643389.2013.829765.

- [52] S. Dalhatou, Doctoral thesis “Application des techniques d’oxydation avancée pour la dépollution des effluents organiques dans les eaux de rejets industriels : Cas des savonneries”, *Grenoble University*, 2014.
- [53] Janusz. Pawliszyn, J. M. Bayona, H. L. Lord, X. Chris. Le, and Luigi. Mondello, *Comprehensive sampling and sample preparation: analytical techniques for scientists* Book, ISBN: 978-0123877710 *Elsevier*, 2012.
- [54] C. M. Thompson and J. A. Drago, “North American installed water treatment ozone systems,” *Journal - American Water Works Association*, vol. 107, no. 10, pp. 45–55, Oct. 2015, doi: 10.5942/jawwa.2015.107.0157.
- [55] A. Chavoshani, M. Hashemi, M. Mehdi Amin, and S. C. Ameta, “Pharmaceuticals as emerging micropollutants in aquatic environments,” in *Micropollutants and Challenges*, Elsevier, 2020, pp. 35–90. doi: 10.1016/b978-0-12-818612-1.00002-7.
- [56] J. Wang and H. Chen, “Catalytic ozonation for water and wastewater treatment: Recent advances and perspective,” *Science of the Total Environment*, vol. 704. Elsevier B.V., Feb. 20, 2020. doi: 10.1016/j.scitotenv.2019.135249.
- [57] C. von Sonntag and U. von Gunten, *Chemistry of ozone in water and wastewater treatment: from basic principles to applications*, Book, *IWA Publishing*, 2012.
- [58] F. J. Fernando J. Beltrán, *Ozone reaction kinetics for water and wastewater systems*, Book. *Lewis Publishers*, 2004.
- [59] Creigee Rudolf, “Mechanism of Ozonolysis,” *Angewandte Chemie International Edition*, vol. 14, no. 11, pp. 745–752, 1975.
- [60] N. Stamenković, N. P. Ulrih, and J. Cerkovnik, “An analysis of electrophilic aromatic substitution: a ‘complex approach,’” *Physical Chemistry Chemical Physics*, vol. 23, no. 9. Royal Society of Chemistry, pp. 5051–5068, Mar. 07, 2021. doi: 10.1039/d0cp05245k.
- [61] Y. Guo, L. Yang, and X. Wang, “The Application and Reaction Mechanism of Catalytic Ozonation in Water Treatment,” *Journal of Environmental & Analytical Toxicology*, vol. 02, no. 06, 2012, doi: 10.4172/2161-0525.1000150.
- [62] Y. P. Chiang, Y. Y. Liang, C. N. Chang, and A. C. Chao, “Differentiating ozone direct and indirect reactions on decomposition of humic substances,” *Chemosphere*, vol. 65, no. 11, pp. 2395–2400, 2006, doi: 10.1016/j.chemosphere.2006.04.080.
- [63] A. Rodríguez *et al.*, “Ozone-based technologies in water and wastewater treatment,” *Handbook of Environmental Chemistry, Volume 5: Water Pollution*, vol. 5 S2, pp. 127–175, 2008, doi: 10.1007/698_5_103.
- [64] A. M. Gorito *et al.*, “Ozone-based water treatment (O₃, O₃/UV, O₃/H₂O₂) for removal of organic micropollutants, bacteria inactivation and regrowth prevention,” *Journal of Environmental Chemical Engineering*, vol. 9, no. 4, Aug. 2021, doi: 10.1016/j.jece.2021.105315.
- [65] Henry John Fenton, “Oxidation of tartaric acid in presence of iron,” *Journal of the Chemical Society, Transactions*, vol. 65, no. 0, pp. 899–910, 1894.

- [66] S. M. Aramyan, "Advances in Fenton and Fenton Based Oxidation Processes for Industrial Effluent Contaminants Control-A Review," *International Journal of Environmental Sciences & Natural Resources*, vol. 2, no. 4, Jun. 2017, doi: 10.19080/ijesnr.2017.02.555594.
- [67] R. Ameta, A. K. Chohadia, A. Jain, and P. B. Punjabi, "Fenton and Photo-Fenton Processes," in *Advanced Oxidation Processes for Wastewater Treatment: Emerging Green Chemical Technology*, Elsevier Inc., 2018, pp. 49–87. doi: 10.1016/B978-0-12-810499-6.00003-6.
- [68] N. Masomboon, C. Ratanatamskul, and M. C. Lu, "Chemical oxidation of 2,6-dimethylaniline in the fenton process," *Environmental Science and Technology*, vol. 43, no. 22, pp. 8629–8634, Nov. 2009, doi: 10.1021/es802274h.
- [69] A. Albini, "The Framework of Photochemistry: The Laws," in *Photochemistry*, Springer Berlin Heidelberg, 2016, pp. 9–40. doi: 10.1007/978-3-662-47977-3_2.
- [70] J. R. Bolton, I. Mayor-Smith, and K. G. Linden, "Rethinking the Concepts of Fluence (UV Dose) and Fluence Rate: The Importance of Photon-based Units - A Systemic Review," *Photochemistry and Photobiology*, vol. 91, no. 6. Blackwell Publishing Inc., pp. 1252–1262, Nov. 01, 2015. doi: 10.1111/php.12512.
- [71] J. Zwinkels, "Light, Electromagnetic Spectrum," in *Encyclopedia of Color Science and Technology*, Springer Berlin Heidelberg, 2015, pp. 1–8. doi: 10.1007/978-3-642-27851-8_204-1.
- [72] R. C. Evans, P. Douglas, and H. D. Burrows, *Applied photochemistry*, vol. 9789048138302. Springer Netherlands, 2014. doi: 10.1007/978-90-481-3830-2.
- [73] A. Braeuer, "Interaction of Matter and Electromagnetic Radiation," *Supercritical Fluid Science and Technology*, vol. 7, pp. 41–192, Jan. 2015, doi: 10.1016/B978-0-444-63422-1.00002-X.
- [74] Pérez-Juste, I. and Nieto Faza, O. (2015). Interaction of Radiation with Matter. In *Structure Elucidation in Organic Chemistry (eds M.-M. Cid and J. Bravo)*. <https://doi.org/10.1002/9783527664610.ch1>.
- [75] E. M. A. Hussein, "Radiation Mechanics, ISBN: 978-0-08-045053-7, pp. 1–65, Jan. 2007, doi: 10.1016/B978-008045053-7/50002-1.
- [76] G. v. Loukova, "The first experimental approach to probing frontier orbitals and HOMO–LUMO gap in bent metallocenes," *Chemical Physics Letters*, vol. 353, no. 3–4, pp. 244–252, Feb. 2002, doi: 10.1016/S0009-2614(02)00031-3.
- [77] A. Nano, "Towards optical memories : switchable optical systems for electron and energy transfer processes Antibody-drug conjugates View project," strasbourg, 2015. [Online]. Available: <https://www.researchgate.net/publication/280793112>
- [78] I. R. McNab, "Rotational Spectroscopy, Theory," *Encyclopedia of Spectroscopy and Spectrometry*, pp. 978–987, Jan. 2017, doi: 10.1016/B978-0-12-803224-4.00273-9.

- [79] R. Poli, "Spin Crossover Reactivity," *Comprehensive Inorganic Chemistry II (Second Edition): From Elements to Applications*, vol. 9, pp. 481–500, Jan. 2013, doi: 10.1016/B978-0-08-097774-4.00919-0.
- [80] V. V. Ter-Mikirtychev, "Optical Spectroscopy of Rare-Earth Ions in the Solid State," *Encyclopedia of Spectroscopy and Spectrometry*, pp. 481–491, Jan. 2017, doi: 10.1016/B978-0-12-409547-2.12095-5.
- [81] C. Karunakaran and M. Balamurugan, "Electron Paramagnetic Resonance Spectroscopy," *Spin Resonance Spectroscopy: Principles and applications*, pp. 169–228, Jan. 2018, doi: 10.1016/B978-0-12-813608-9.00004-6.
- [82] T. C. Corcoran, "Laser-induced fluorescence spectroscopy (LIF)," *Laser Spectroscopy for Sensing: Fundamentals, Techniques and Applications*, pp. 235–257, Jan. 2014, doi: 10.1533/9780857098733.2.235.
- [83] K. G. Fleming, "Fluorescence Theory," *Encyclopedia of Spectroscopy and Spectrometry*, pp. 647–653, Jan. 2017, doi: 10.1016/B978-0-12-803224-4.00357-5.
- [84] S. N. Iyer, N. Behary, V. Nierstrasz, J. Guan, and G. Chen, "Study of photoluminescence property on cellulosic fabric using multifunctional biomaterials riboflavin and its derivative Flavin mononucleotide," *Scientific Reports*, vol. 9, no. 1, Dec. 2019, doi: 10.1038/s41598-019-45021-5.
- [85] P. Sadeghpour, E. Jalilnejad, and K. Ghasemzadeh, "Achievements in ultraviolet irradiation and in advanced oxidation technologies for wastewater and water treatment," in *Current Trends and Future Developments on (Bio-) Membranes*, Elsevier, 2020, pp. 1–39. doi: 10.1016/b978-0-12-817378-7.00001-x.
- [86] C. G. Silva, W. Wang, P. Selvam, S. Dapurkar, and J. L. Faria, "Structured TiO₂ based catalysts for clean water technologies," *Studies in Surface Science and Catalysis*, vol. 162, pp. 151–158, Jan. 2006, doi: 10.1016/S0167-2991(06)80902-X.
- [87] K.-Y. Show, Y.-G. Yan, and D.-J. Lee, "Biohydrogen production from algae: Perspectives, challenges, and prospects," *Biofuels from Algae*, pp. 325–343, Jan. 2019, doi: 10.1016/B978-0-444-64192-2.00013-5.
- [88] G. K. Moortgat and A. R. Ravishankara, "OZONE DEPLETION AND RELATED TOPICS | Photochemistry of Ozone," *Encyclopedia of Atmospheric Sciences: Second Edition*, pp. 370–379, Jan. 2015, doi: 10.1016/B978-0-12-382225-3.00292-9.
- [89] M. I. Litter, "Introduction to Photochemical Advanced Oxidation Processes for Water Treatment," in *Environmental Photochemistry Part II*, Springer-Verlag, 2005, pp. 325–366. doi: 10.1007/b138188.
- [90] A. v. Emeline, V. N. Kuznetsov, V. K. Ryabchuk, and N. Serpone, "Heterogeneous Photocatalysis: Basic Approaches and Terminology," *New and Future Developments in Catalysis: Solar Photocatalysis*, pp. 1–47, Jan. 2013, doi: 10.1016/B978-0-444-53872-7.00001-7.
- [91] J. Wen, J. Xie, X. Chen, and X. Li, "A review on g-C₃N₄-based photocatalysts," *Applied Surface Science*, vol. 391, pp. 72–123, Jan. 2017, doi: 10.1016/J.APSUSC.2016.07.030.

- [92] Z. Gao, C. Pan, C.-H. Choi, and C.-H. Chang, "Continuous-Flow Photocatalytic Microfluidic-Reactor for the Treatment of Aqueous Contaminants, Simplicity, and Complexity: A Mini-Review," *Symmetry*, vol. 13, no. 8, 2021, doi: 10.3390/sym13081325.
- [93] H. Mountacer, S. M. Nemmaoui, S. Rafqah, G. Voyard, and M. Sarakha, "TiO₂ Photocatalysis of the Organophosphorus Fenamiphos: Insight into the Degradation Mechanism," *ISRN Environmental Chemistry*, vol. 2013, pp. 1–8, 2013, doi: 10.1155/2013/319178.
- [94] Y. Ye, H. Yang, H. Zhang, and J. Jiang, "A promising Ag₂CrO₄/LaFeO₃ heterojunction photocatalyst applied to photo-Fenton degradation of RhB," *Environmental Technology (United Kingdom)*, vol. 0, no. 0, pp. 1–45, 2018, doi: 10.1080/09593330.2018.1538261.
- [95] G. Li *et al.*, "Graphene-bridged WO₃/MoS₂ Z-scheme photocatalyst for enhanced photodegradation under visible light irradiation," *Materials Chemistry and Physics*, vol. 246, no. September 2019, p. 122827, 2020, doi: 10.1016/j.matchemphys.2020.122827.
- [96] P. K. Labhane, V. R. Huse, L. B. Patle, A. L. Chaudhari, and G. H. Sonawane, "Synthesis of Cu Doped ZnO Nanoparticles: Crystallographic, Optical, FTIR, Morphological and Photocatalytic Study," *Journal of Materials Science and Chemical Engineering*, vol. 03, no. 07, pp. 39–51, 2015, doi: 10.4236/msce.2015.37005.
- [97] P. Liu, Z. Wu, A. v. Abramova, and G. Cravotto, "Sonochemical processes for the degradation of antibiotics in aqueous solutions: A review," *Ultrasonics Sonochemistry*, vol. 74, p. 105566, Jun. 2021, doi: 10.1016/J.ULTSONCH.2021.105566.
- [98] Y. Choi *et al.*, "Investigation of the synergistic effect of sonolysis and photocatalysis of titanium dioxide for organic dye degradation," *Catalysts*, vol. 10, no. 5, May 2020, doi: 10.3390/catal10050500.
- [99] Y. G. Adewuyi, "Sonochemistry: Environmental Science and Engineering Applications," *Industrial & Engineering Chemistry Research*, vol. 40, no. 22, pp. 4681–4715, Oct. 2001, doi: 10.1021/ie010096l.
- [100] M. H. Abdurahman, A. Z. Abdullah, and N. F. Shoparwe, "A comprehensive review on sonocatalytic, photocatalytic, and sonophotocatalytic processes for the degradation of antibiotics in water: Synergistic mechanism and degradation pathway," *Chemical Engineering Journal*, vol. 413, p. 127412, Jun. 2021, doi: 10.1016/J.CEJ.2020.127412.
- [101] S. Thomas, M. P. Rayaroth, S. P. M. Menacherry, U. K. Aravind, and C. T. Aravindakumar, "Sonochemical degradation of benzenesulfonic acid in aqueous medium," *Chemosphere*, vol. 252, p. 126485, Aug. 2020, doi: 10.1016/J.CHEMOSPHERE.2020.126485.
- [102] K. Yasuda, "Sonochemical green technology using active bubbles: Degradation of organic substances in water," *Current Opinion in Green and Sustainable Chemistry*, vol. 27, p. 100411, Feb. 2021, doi: 10.1016/J.COAGSC.2020.100411.
- [103] W. Xiang *et al.*, "Efficient degradation of carbamazepine in a neutral sonochemical FeS/persulfate system based on the enhanced heterogeneous-homogeneous sulfur-iron

- cycle,” *Separation and Purification Technology*, vol. 282, p. 120041, Feb. 2022, doi: 10.1016/J.SEPPUR.2021.120041.
- [104] L. L. He *et al.*, “Synthesis of CaMoO₄ microspheres with enhanced sonocatalytic performance for the removal of Acid Orange 7 in the aqueous environment,” *Separation and Purification Technology*, vol. 276, p. 119370, Dec. 2021, doi: 10.1016/J.SEPPUR.2021.119370.
- [105] Y. Areerob, J. Y. Cho, W. K. Jang, and W. C. Oh, “Enhanced sonocatalytic degradation of organic dyes from aqueous solutions by novel synthesis of mesoporous Fe₃O₄-graphene/ZnO@SiO₂ nanocomposites,” *Ultrasonics Sonochemistry*, vol. 41, pp. 267–278, Mar. 2018, doi: 10.1016/J.ULTSONCH.2017.09.034.

CHAPTER II : Materials & Methods.

1. Introduction.

This chapter describes the experimental framework that consists of three basic parts. The first part is devoted to chemicals and reagents including the selected micropollutants studied in our project with their physico-chemical properties details. In addition, the part involves the protocol of synthesized catalyst. The second part of this chapter presents the photocatalytic activity performance: the Irradiation source systems and the photochemical treatment process. The final part incorporates analytical techniques used for characterization of studied material in order to investigate the optical properties, the monitoring of photocatalytic degradation for process efficiency evaluation, the detection of metabolites for mechanism pathway suggested and finally the mineralization study of micropollutants.

2. Materials.

Milli-Q water was used for all solutions preparation. All chemicals were utilized as received without any purification.

2.1 Chemicals and reagents:

2.1.1 Levafix Blue:

Levafix Blue is a synthetic azo dye for textile sector. The substrate was obtained from DyStar industry. Unfortunately, the chemical structure of compound has been not revealed. The figure19 shows the absorption spectra that presents a maximum absorption at wavelength 613nm.

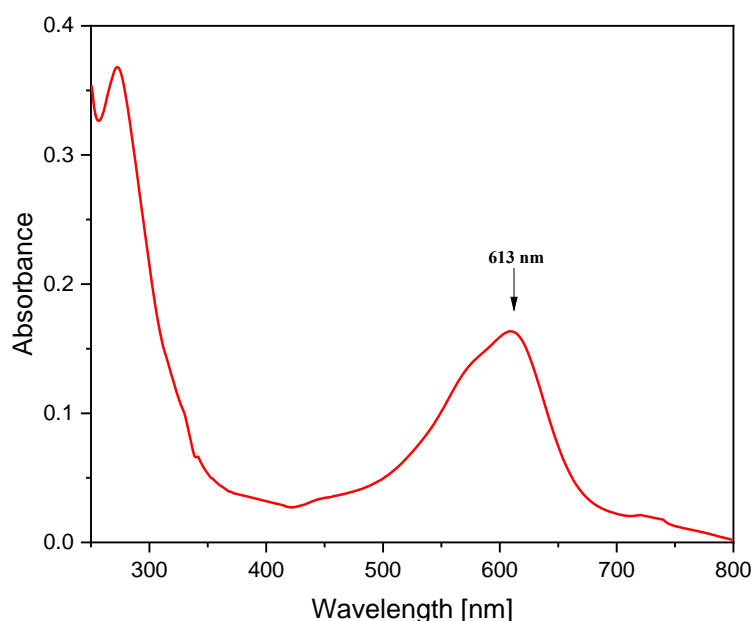
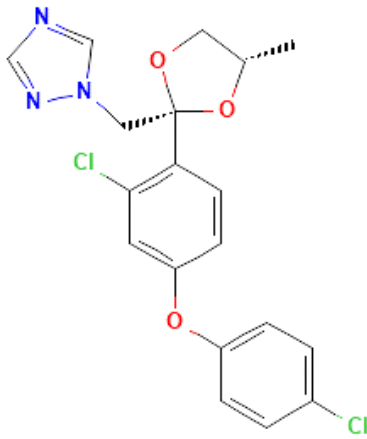


Figure 19: Absorption spectra of Levafix Blue in UV-Visible domain

2.1.2 Difenoconazole

Difenoconazole (DFL) analytical grade was obtained from Sigma Aldrich. Table 5 summarizes the physico-chemical description of compound.

Table 7:Physico-chemical properties of Difenoconazole

IUPAC Name	1-((2-(Chloro-4-(4-chlorophenoxy)phenyl)-4-methyl-1,3-dioxolan-2-yl)methyl)-1H-1,2,4-triazole
Chemical structure	 The chemical structure of Difenoconazole consists of a 1,2,4-triazole ring (blue) attached via a methylene group to a 1,3-dioxolane ring (red). The dioxolane ring has a methyl group (dotted line) and a 2-(4-chlorophenoxy)phenyl group (green) attached to its 2-position. The phenyl ring has a chlorine atom at the 4-position and a 4-chlorophenoxy group at the 2-position.
Formula	C ₁₂ H ₁₇ Cl ₂ N ₃ O ₃
Molecular weight	406.26 g/mol
Physical state	Powder
Solubility	In water at 25 °C 15 mg/L

Difenoconazole is a triazole fungicide, widely used for fruit, vegetables, and cereals disease control. It is considered a toxic product in an exceeded dose; a deterioration of environment and human health is expected in long term use.

2.1.3 Acibenzolar-S-Methyl

Acibenzolar-S-methyl (ASM) obtained from Sigma Aldrich analytical grade. The ASM is a functional analogue of salicylic acid and systemic acquired resistance elicitor that is categorized as a control agent of fungal plant diseases (Table 6). ASM is the most commonly used fungicide to protect vegetables and fruits crops as well as post-harvest products [1-2].

Table 8:Physico-chemical properties of Acibenzolar-S-Methyl

IUPAC Name	S-methyl1,2,3-benzothiazole-7-carbothioate
Chemical structure	
Formula	C ₈ H ₆ N ₂ OS ₂
Molecular weight	210.28 g.mol ⁻¹
Physical state	Powder
Solubility	In water at 25°C 7.7 mg/L

2.2 Other chemicals

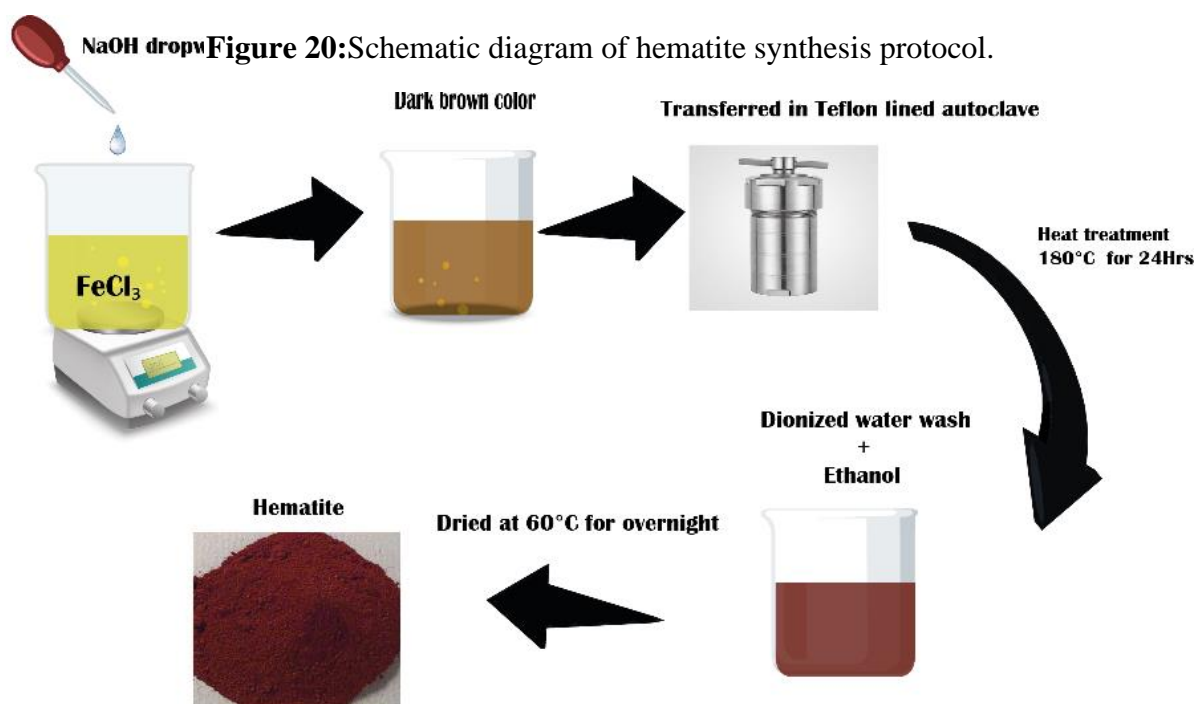
- Hydrogen peroxide (30%) (H₂O₂): Fluka, M= 34.01 g.mol⁻¹
- Iron(II) sulfate heptahydrate (FeSO₄ .7H₂O): Merck, M= 278.01 g.mol⁻¹
- Ferric chloride hexahydrate ≥ 99,9% (FeCl₃.6H₂O): Sigma Aldrich, M= 270.30 g/mol
- Sulfuric acid (95-97%) (H₂SO₄): Sigma Aldrich, M= 98.8 g.mol⁻¹
- Sodium hydroxide 99% (NaOH): Riedel-de Haën, M = 40,0 g.mol⁻¹,
- Ethanol (C₂H₆O) : Merck, M= 46.07 g.mol⁻¹
- Acetonitrile (C₂H₃N) (99.9%) HPLC grade: Sigma Aldrich, M= 41.05 g.mol⁻¹
- Methanol (CH₃OH) (99.9%) HPLC grade: Sigma Aldrich, M= 32.04 g.mol⁻¹
- Potassium oxalate (C₂O₄K₂. H₂O) (98.5%): Riedel-de Haën, M= 134.23 g.mol⁻¹
- Ammonium ferric sulfate (NH₄)Fe(SO₄)₂ . 12 H₂O: Merck, M= 482.19 g.mol⁻¹
- 1,10-Phenanthroline monohydrate (C₁₂H₈N₂. H₂O): Sigma Aldrich, M= 198.22 g.mol⁻¹
- Sodium acetate anhydrous (C₂H₃NaO₂): Sigma Aldrich, M= 82.03 g.mol⁻¹

2.3 Synthesized materials:

2.3.1 Catalyst:

Hematite is one of the abundant existing metals; it knows via its expanded application in multidisciplinary fields. Water treatment, oncology, material sciences research projects have revealed appealing results of iron oxide activity.

In the present work, we reported the synthesis of α - Fe_2O_3 nanoparticles using the hydrothermal method described by Frindy et al.; [3], as illustrated in Figure 20, to 80 ml of ferric chloride poured, 80 ml of the sodium hydroxide is added dropwise to the solution over 15 min until dark brown color appeared. The mixture is vigorously stirred for 30 min during the preparation process. The mixture was transferred in Teflon-lined autoclave and was hydrothermally treated for 24 hrs at 180 °C. The hydrothermally treated and prepared hematite was washed with deionized water several times as well as ethanol and dried subsequently at 60 °C overnight before use.



2.3.2 Ferrioxalate actinometer

In order to quantifying the photocatalytic process efficiency, the quantum yield has been calculated using the ferrioxalate actinometer method. The potassium ferrioxalate $K_3[Fe(C_2O_4)_3]$ prepared following the method described by Goldstein and al;[4]. A mixture of equal volumes of 0.02M ammonium ferric sulfate with 0.06M Potassium oxalate both in 0.1N sulfuric acid stirred until green color appeared. The complex ions are light sensitive, to separate the potassium ferrioxalate from the by-product; the solution has been letting in the dark. After formation of crystals, the mixture filtered and the material washed for several time. The prepared sample has been confirmed with 1,10-phenanthroline solution test that manifests a full red color.

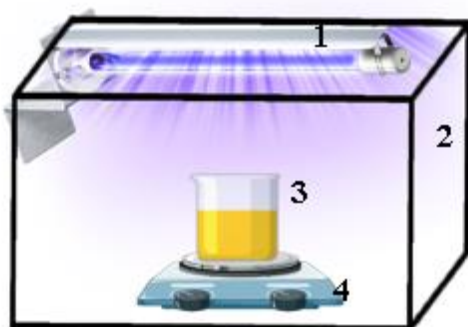
3. Methods

3.1 Irradiation system

The irradiation was performed using different systems depending on the objective of the study.

3.1.1 Monochromatic light irradiation at 254 nm wavelength.

The monochromatic source light has been used in order to evaluate the quantum yield of photochemical degradation reaction of difenoconazole. A UV Philips lamp 254 nm (8W) fixed in the top of a rectangular enclosure as shown in figure 21 in a quartz beaker, the substrate solution was placed with a continuous stirring at fixed distance of 6cm from the lamp.



- 1: UV Lamp (254 nm)
- 2: Rectangular enclosure
- 3: Quartz beaker
- 4: Magnetic stirrer

Figure 21:Irradiation UV light system

3.1.2 polychromatic irradiation light source with maximum of 365 nm.

The polychromatic irradiation system was used for photodegradation of Levafix Blue azo dye. The irradiation experiments were performed as illustrated in figure 22 in a home-made photoreactor placed in a cylindrical stainless steel container. The reaction device consists of four tubes light (Philips TLD 15W) emitting from 300 nm to 450 nm with a maximum irradiation at 365 nm. These four tubes were separately placed in the four different axes in symmetrical way. A water-jacketed Pyrex tube was placed in the center of the setup. The solution (100 ml) was magnetically stirred during the treatment to insure its homogeneity.

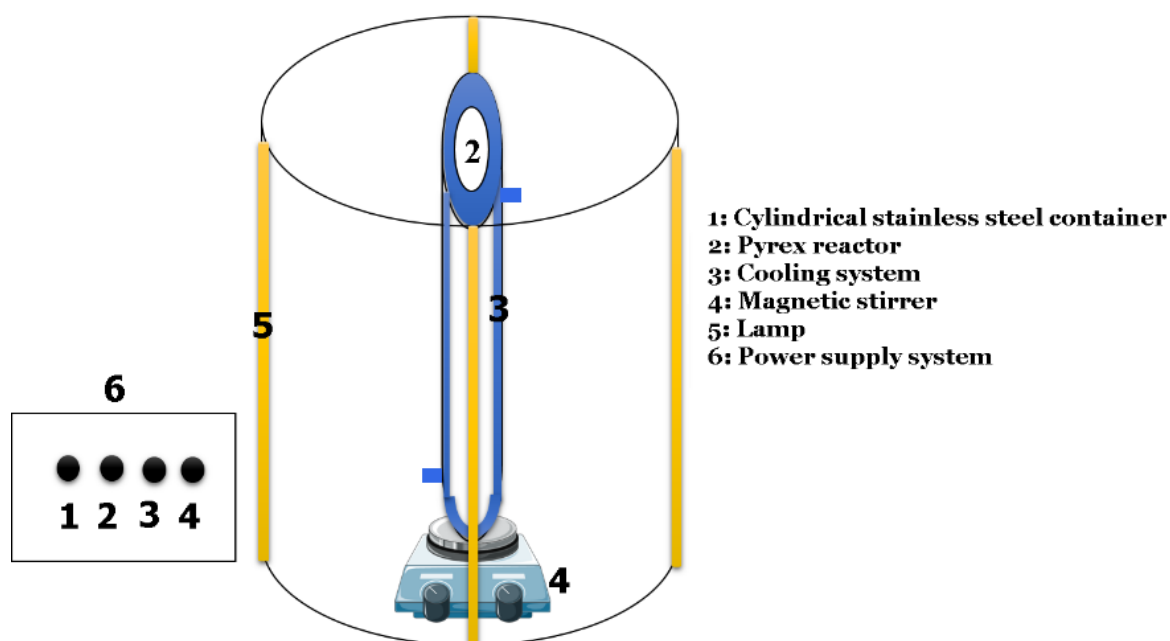


Figure 22:Photoreactor with polychromatic irradiation system

3.1.3 Ultrasonic radiation system

Sonochemistry is now well recognized as technique for micropollutants degradation. In the present work, we investigated the sonocatalytic removal of Acibenzolar-S-Methyl in aqueous solution. Ultrasonic experiments were performed in programmable sonicator at an ultrasound frequency of 20 kHz (Sonics & Materials, Inc., VCX750) with a titanium alloy probe with a tip diameter of 13 mm and maximum power output 125W. A quartz double jacket reactor filled with 100 ml of substrate solution with a water circulation that was used for reaction temperature maintain. A schematic diagram of experimental setup is shown in figure 23.

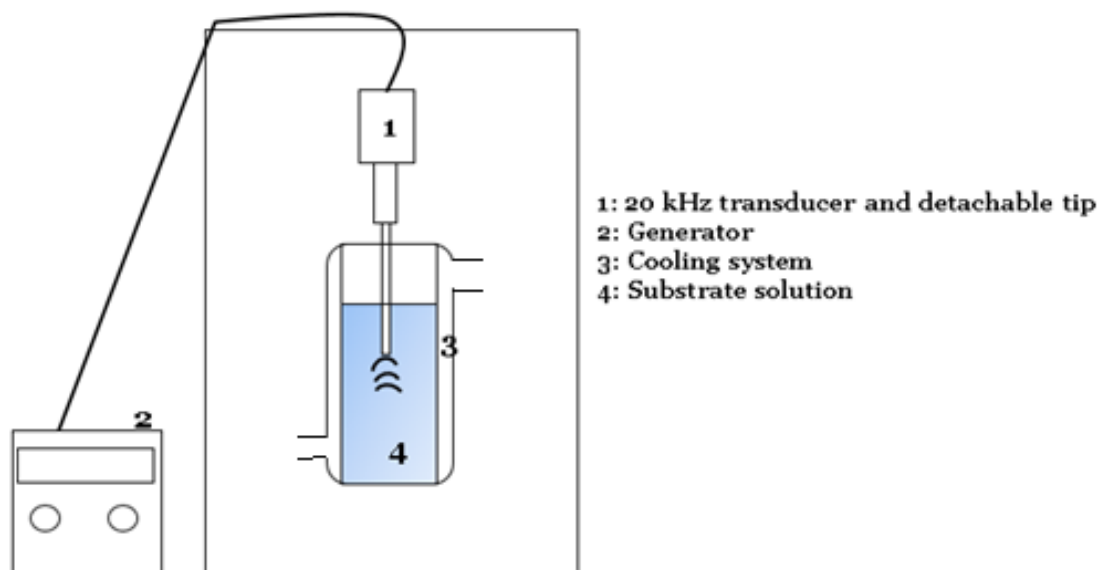


Figure 23:ultrasonic irradiation system

3.1.4 Photonic flux determination

The Photonic flux determination is an indispensable element for photochemical reaction. Indeed, the rate of degradation or transformation of the studied compound depends on the quantity of photons absorbed by the reagents. In addition, the photonic flux detection is necessary to determine the quantum yield of the photochemical reaction. The incident photon flux is quantified using the actinometry method.

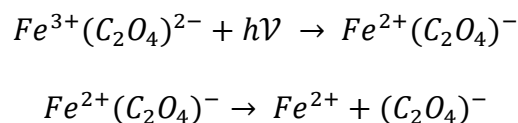
3.1.5 Actinometry

Actinometry is an old approach developed in order to estimate the amount of absorbed photons in photochemical reaction. Actinometers are defined as chemical or physical measurement devices that converts the energy of number of incident photons in quantifiable electrical signal. However, the most commonly used method is based on a chemical actinometer, a reference substance undergoing a photochemical reaction whose quantum yield is known.

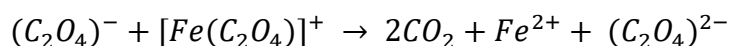
3.1.6 Ferrioxalate actinometry

Ferrioxalate actinometry is a chemical actinometry recommended by IUPAC and considered as a standard tool of photochemical investigations since a century ago[5]. It consists on preparation of potassium ferrioxalate $K_3[Fe(C_2O_4)]_3$ crystals, their dissolution in water, illumination and Fe(II) determination based on color manifestation with 1,10-phenanthroline. The monitored

photoreaction involves the formation of Fe (II), carbon dioxide and free oxalate ion in a formal intracomplex electron transfer reaction following the mechanism below[6-4]:



In normal conditions $(C_2O_4)^{-}$ ions are transformed and produced ferrous ions as described below:



3.1.7 Photonic flux intensity

Intensity defined as photons flux per second and unit area. The incident photon flux received by the actinometric sample is proportional to the number of ferrous ions produced during irradiation and it measured following the protocol below:

In our trials, a volume of 20 ml (V_1) of potassium ferrioxalate solution were firstly irradiated in a fixed times, another volume 1 ml (V_2) taken from the same solution, to which is added 2 ml of acetate buffer and 1.5 ml of 1.10-phenanthroline. The new mixture solution was adjusted with water to 20 ml (V_3). After a half hour in the dark, the absorbance at $\lambda = 510$ nm was measured. Therefore, the number of ferrous ions present in the solution was detected using the following equation:

$$n_{Fe^{2+}} = \frac{N.V_1.V_3.D_{510}}{V_2.L.\epsilon.10^3} \quad \text{Eq(23)}$$

Where:

N : Avogadro constant

V_1 : irradiated actinometric solution volume (mL)

V_2 : Volume taken from V_1 (mL)

V_3 : final volume after dilution (mL)

D_{510} : Absorbance of V_3 at 510 nm

ϵ_{510} : Molar absorption coefficient of complex PNT : Fe^{2+} ($\epsilon = 1,1 \times 10^4$ l.mol⁻¹.cm⁻¹)

L : Optical path length (cm)

The number of ferrous ions calculated permit to calculate the photonic flux incident following the equation:

$$I_0 = \frac{n_{Fe^{2+}}}{\Phi_{AC} t} \quad \text{Eq (24)}$$

Where :

Φ_{AC} represent the known actinometric quantum yield at 254 nm wavelength described by Braun.

t is the irradiated time of actinometric solution.

Irradiation time (min)	Absorbance ($\lambda=510$ nm)
0	0.087
4	0.699
8	0.952
12	2.199

3.1.8 Quantum yield measurement

Quantum yield (Φ) is the measure of efficiency of a photochemical reaction. It is defined as the ratio of the number of photons emitted to the number of photons absorbed.

$$\Phi = \frac{\text{Number of molecules reacting in given time}}{\text{Number of photons absorbed in the same time}}$$

$$\Phi = \frac{\Delta n}{\Delta t \cdot I_0}$$

3.2 Analytical methods

3.2.1 Characterization techniques used for synthesized hematite

3.2.1.1 Powder X-ray Diffraction

Powder X-ray Diffraction (XRD) is a non-destructive qualitative and quantitative technique essential for characterization of solid crystalline materials. XRD allows identification of the crystalline structure, phases, crystal orientations and average grain size [7]. The technique is

based on diffraction phenomenon, the constructive interference of a monochromatic beam of X-rays scattered at specific angles from each set of lattice planes in a sample, generating a unique diffraction pattern that presents several sharp spots, known as Bragg diffraction peaks. The Bragg law relates the XRD wavelength to the interatomic spacing following the equation below[8]:

$$2d \sin\theta = n\lambda \quad \text{Eq (25)}$$

Where d is the perpendicular distance between pairs of adjacent planes, θ is the angle of incidence or Bragg angle, wavelength of the beam and n denotes an integer number, known as order of reflection and is the path difference, in term of wavelength between waves scattered, by adjacent planes atoms as illustrated in figure 24. Nevertheless, only the diffracted waves that satisfy Bragg's law give rise to pattern formation. The diffracted beams can be detected either by surrounding the sample with a strip of photographic film (Debye-Scherrer and Guinier focusing methods) or by means of a movable detector, such as a Geiger counter, connected to a chart diffractometer recorder[9].

The synthesis hematite was characterized using Powder X-ray diffraction (XRD) patterns were carried out on a PANalytical diffractometer with Co $K\alpha$ radiation ($\lambda = 0.1789$ nm, at 40 kV and 40 mA) from 10° to 100° 2θ angles.

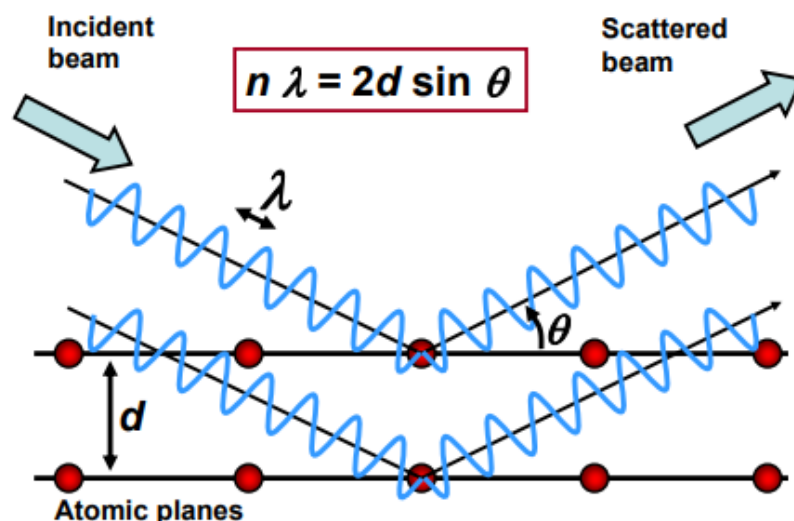


Figure 24:schematic presentation of X-ray diffraction system

3.2.1.2 Fourier Transform Infrared Spectroscopy (FT-IR)

Fourier transform infrared spectroscopy is a technique used to identify chemical composition, and the mineralogical structure of organic, inorganic, and polymeric materials. The FT-IR analysis involves a range array of phenomenon, adsorption, reflection, and emission of light[10]. The analysis consists on the measurement of the decrease in infrared radiation intensity once passing through the sample at specific wavelength range (figure 25). It is considered a qualitative analysis of molecules to investigate the bonds between atoms in order to identify the functional group present in sample. FT-IR is useful in identifying and characterizing unknown materials, detecting contaminants in material, finding additive, and identifying decomposition. In addition, the analysis present wide range for high spectral resolution data collection that is usually between 5000 and 400 cm^{-1} for mid-IR region [11] wavelength, and between 10000 and 4000 cm^{-1} for near-IR region wavelength[12].

In order to investigate the chemical structure of Levafix Blue dye, a FT-IR analysis was performed using Bruker-Tensor 27 spectrometer.

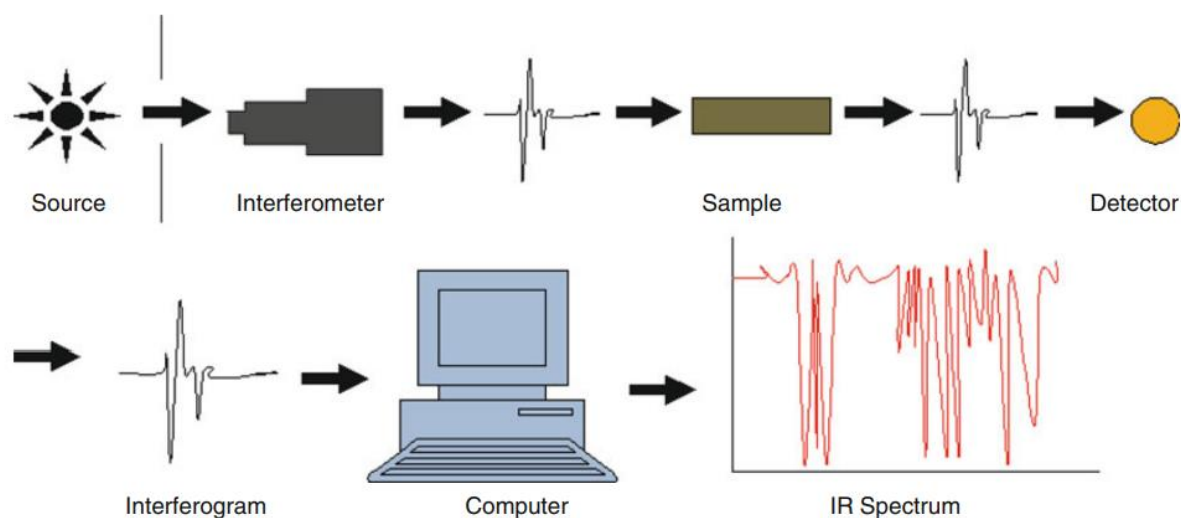


Figure 25: Schematic presentation of FT-IR spectroscopy analysis[10]

3.2.1.3 Brunauer-Emmett Teller (BET)

Brunauer-Emmett Teller (BET) is a technique to analyse the textural properties of materials. The method was designed to measure the specific surface area and pore size of powdered samples [13]. The analysis consists on physical multilayer adsorption system of probing gas molecules at high temperature on a solid surface area that is determined from the volume of Nitrogen gas adsorbed as displayed in figure 26. Nevertheless, the BET method only reflects

the external specific surface area of the analysed materials, this disadvantage is noticed specially once analysing phyllosilicate materials where the internal surface area is much larger than the external one.

The collected BET data is displayed as BET isotherm, which plots the amount of gas of adsorbed against the relative partial pressure[14].

In the present research, the textural properties of hematite were analysed using a Micrometrics TriStar II Plus. Prior to BET, the sample was dried in an oven for 2h at 60°C to remove any trapped moistures.

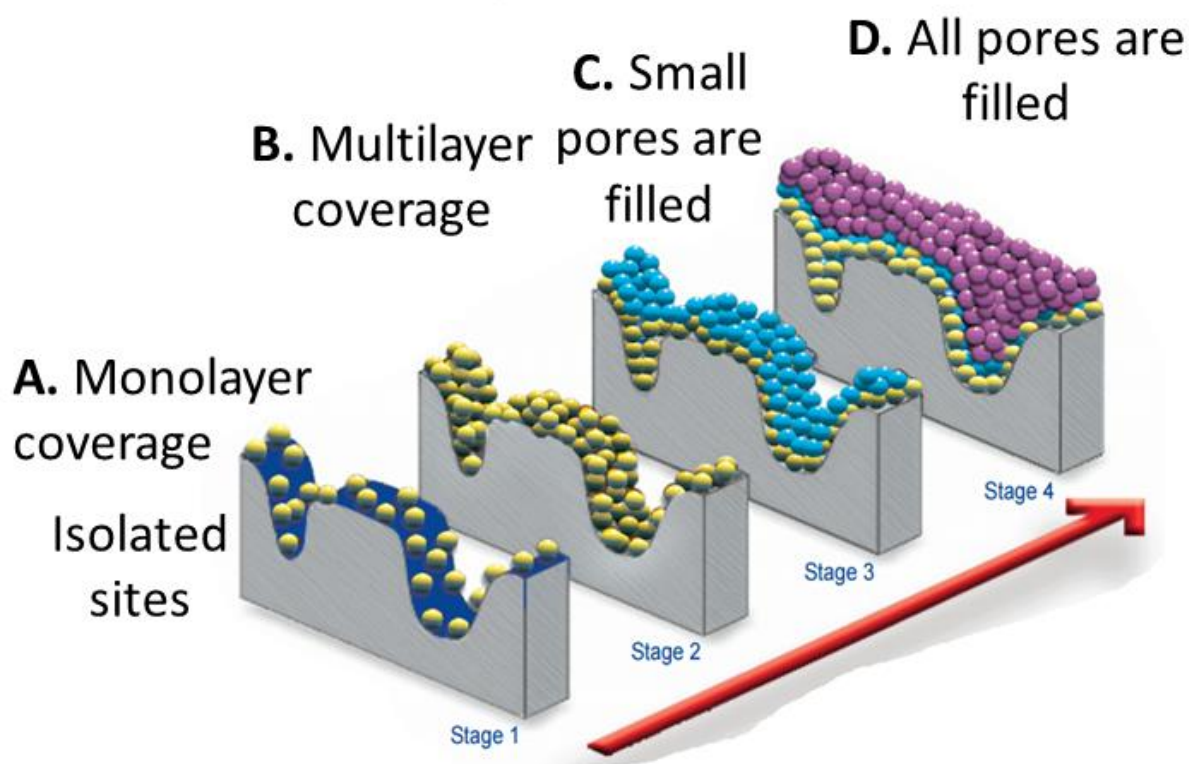


Figure 26: In a gas adsorption measurement, the pores of the sample progressively fill with the adsorptive gas as pressure is increased.

3.2.1.4 UV-Vis Diffuse Reflectance spectroscopy (UV-Vis DRS)

Diffuse reflectance spectroscopy is a surface analytical technique used to determine the optical properties and calculate the band gap energy of materials. When the light propagated through sample, it is scattered and specular reflected from planar surface without defects. Visible light specular reflection occurs from mirror like surface and scattered in all possible directions figure 27. The remaining of light is refracted as it enters the powdered sample, where it is scattered

due to the repeated refraction entry into the sample. DRS were recorded on Perkin-Elmer Lamda 950 spectrophotometer and DRS measurement were carried out in wavelength 200 nm to 800 nm using an integrating sphere. The barium sulfate standard was used as reference spectrum.

The band gap energy represents the energy required for a photon to be absorbed by a material. The absorption of photon and associated energy is equivalent to the difference between the conduction and valence band. The band gap of sample was determined based on the Tauc equation (Eq 26) and the Plot method[15].

$$(\alpha h\nu)^2 = A(h\nu - E_g) \quad \text{Eq(26)}$$

Where α is the absorption coefficient, and A is the proportionality.

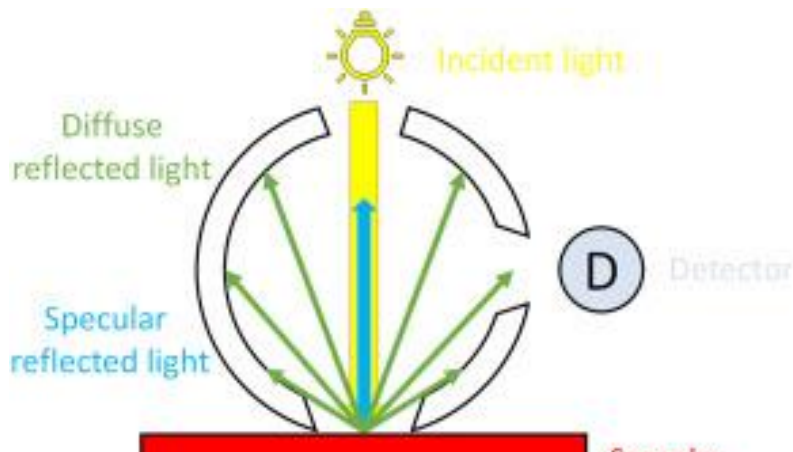


Figure 27:Diffuse reflectance measurement principal

3.2.1.5 Scanning electron microscopy (SEM)

Scanning electron microscopy (figure 28) is a non-destructive technique that provides a high-resolution imaging to investigate the morphology of material at a micro- and nanoscale. The method consists on the use of a focused beam of high-energy electrons that have the ability to scan the surface of studied specimen. The electrons interaction emits a variety of electronic signals that reveal information about the morphology, composition, crystalline structure and the orientation of constitution of analysed material. In our work, SEM analysis was performed by field emission SEM (Hitachi S-4800).

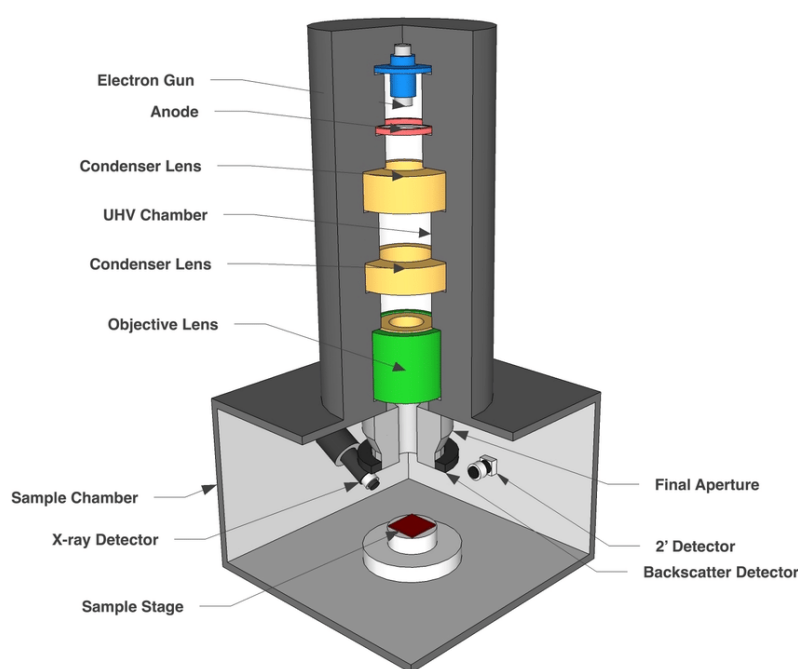


Figure 28: illustration of SEM analysis system

3.2.1.6 Transmission Electron Microscopy (TEM)

Transmission electron microscopy is a widely used characterization analysis technique. TEM consists on transmission of electrons beam condensed and focuses through the objective lenses that passes through the specimen to result a real, highly image recording of sample. The TEM provides detailed information about the crystallographic structure and the composition of studied material[16]. In our work, the hematite TEM images analysis were taken on a Hitachi 7700.

3.2.1.7 Raman spectroscopy

Raman spectroscopy is an analysis tool that provides vibrational electronic properties of material used for material phase identification (figure 29). The technique works based on inelastic scattering phenomenon where the incident photon loose or gain energy by interaction of vibrating molecules. The vibrational energy levels interact with the electromagnetic waves that lead to the shifting of scattered light source from the laser frequency[17]. The hematite Raman spectra were recorded with green laser 514 nm excitation on a RENISHAW in Via Micro-Raman spectrophotometer.

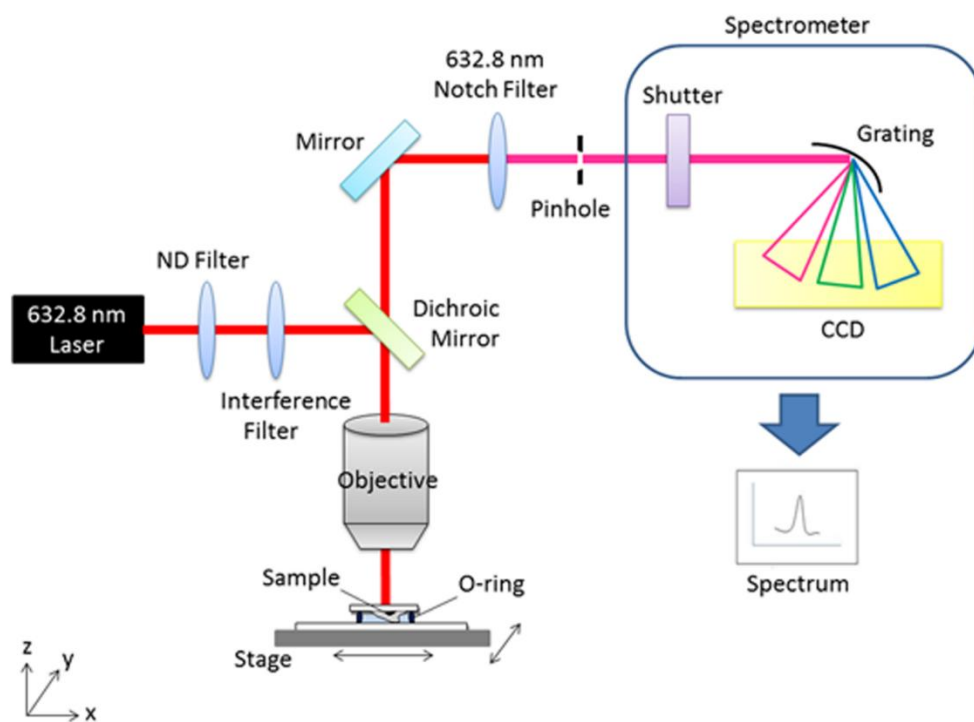


Figure 29: Schimatic explanation of Raman analysis system

3.2.2 Photocatalytic monitoring techniques

3.2.2.1 UV-Vis spectroscopy

Ultraviolet-Visible spectroscopy is an analytical technique denotes absorption in ultraviolet-visible spectral region. The spectrophotometer measures the intensity of light passing through the sample (I), and compares it with the intensity of light passing before through the blank (I_0). The ratio I/I_0 is the transmittance (%T) and the absorbance A of samples are calculated based on transmittance.

The UV-Vis spectroscopy was used for Levafix Blue degradation monitoring. The kinetic study was followed utilizing model Selecta 3100 at $\lambda_{\max} = 613$ nm with a 1cm quartz cells. The removal rate was calculated from the absorbance measurement based on the calibration curve equation figure 30.

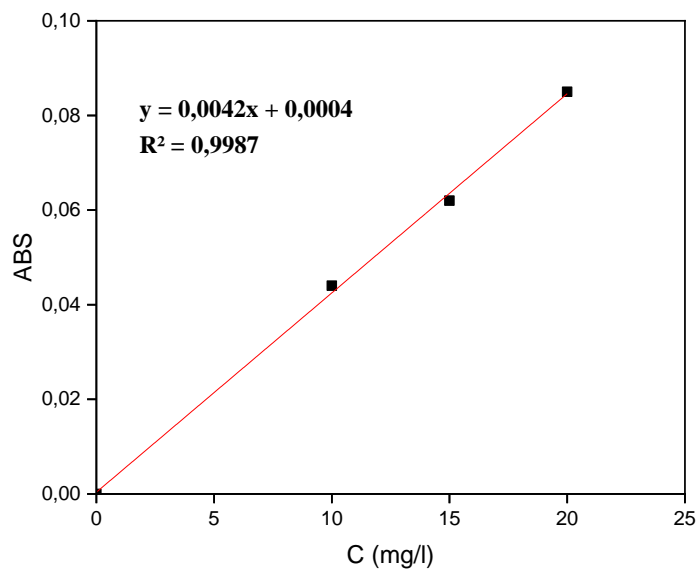


Figure 30:Calibration curve of Levafix Blue dye

3.2.2.2 High Performance Liquid Chromatography (HPLC)

High performance liquid chromatography is an analytical separation and identification technique (figure31). The analysis is based on partitioning of liquid sample between two phases, a mobile phase (solvent/water) and stationary phase (the column packing)[18]. The monitoring of compounds is conditioned by one or more of the following characteristics: high polarity, high molecular weight, thermal instability, and a tendency to ionize in solution. The analysed components are obtained utilizing UV detector coupled to data acquisition. The output data is recorded as chromatogram that present a series of peaks targeting each compound in the sample. The identification of components in the mixture is based on retention time, the time taken for compound to pass through the column. In addition, since the absorption intensity is proportional to the concentration, a calibration curve can be prepared using a standard sample, and the component concentration can be detected by measuring the peak area or height for quantitative analysis.

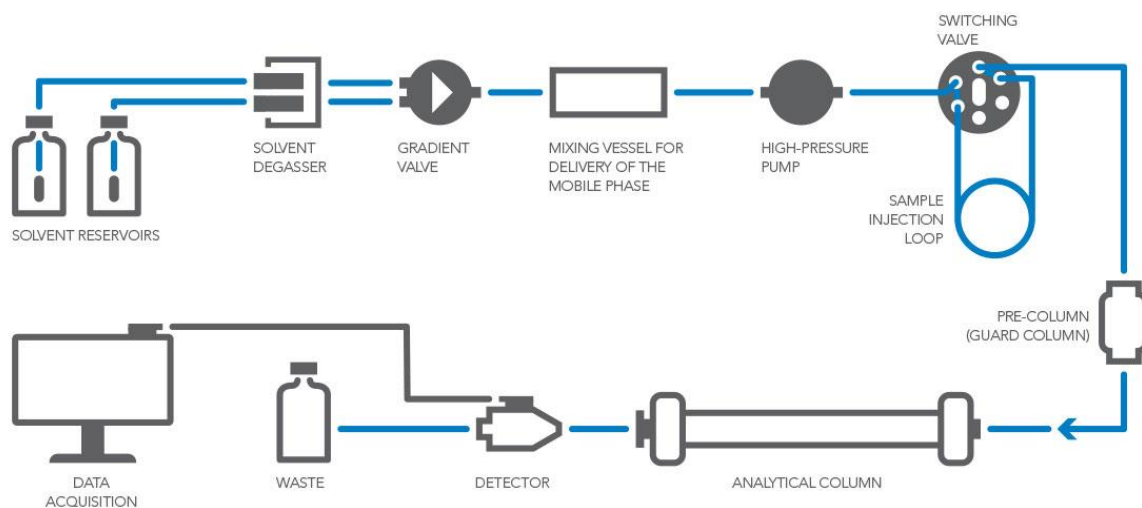


Figure 31: Configuration of HPLC analysis system.

The difenoconazole and acibenzolar-S-methyl degradation was followed with a SHIMADZU HPLC Phenomenex system using C18 Colum (150 mm × 4.6 mm, 5µm). Aliquots of 1 ml were withdrawn at various time intervals and was filtered with a 0.2 µm-size-pore-membrane. For difenoconazole, the Mili-Q water and acetonitrile (ACN) were used as mobile phases (v:v/ 10:90) with an isocratic elution type. The flow rate was adjusted at 1ml/min and 218 nm as a wavelength detector. The total run time for the analysis of DFL samples was 10 min. Moreover, for acibenzolar-S-methyl, the 0.1% Formic acid buffer in water and Methanol (Met) were used as mobile phases (v:v/80:20) with an isocratic elution type. The flow rate was adjusted at 1 ml/min and 254 nm as UV wavelength detector. The total run time for the analysis of ASM samples was 4 min. For the both pesticides, the analysis was performed in duplicate. The removal rate percentage of pesticides in aqueous solution have been calculated following the Eq (27) which is writing as:

$$\text{Removal rate \%} = \frac{(C_0 - C_t)}{C_0} \times 100 \quad (27)$$

Where C_0 and C_t are the pesticides concentration at initial and interval reaction time (min), calculated based on the calibration curves of DFL and ASM respectively (32 & 33).

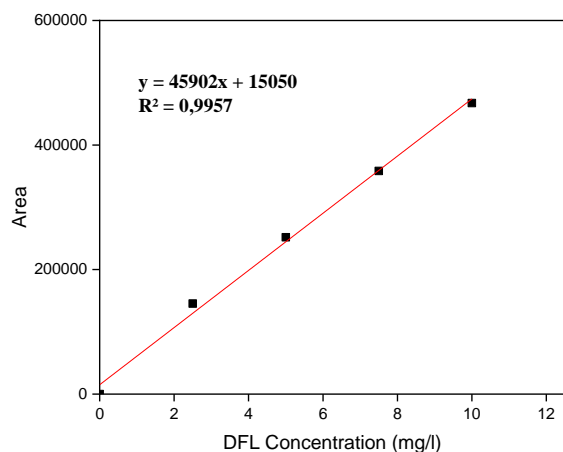


Figure 32:Calibration curve of difenoconazole fungicide

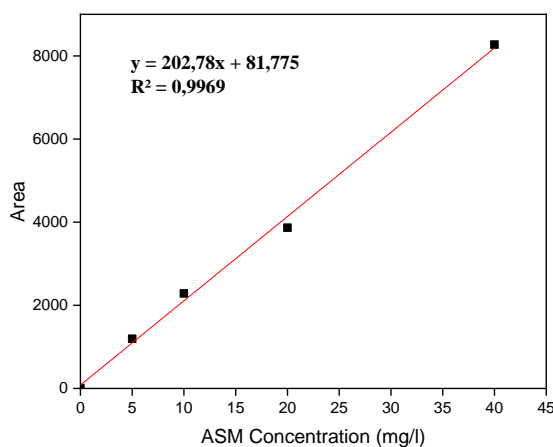


Figure 33:Calibration curve of Acibenzolar-S-Methyl fungicide

3.2.2.3 Gas Chromatography coupled with Mass Spectroscopy (GC/MS)

The gas chromatography combined with mass spectroscopy are analytical platforms to identify different substances within a sample. The samples are propelled firstly by an inert gas usually helium, hydrogen or nitrogen. The separation of each compound from the column occurs at specific time According to the difference in the chemical properties between different molecules and their relative affinity for the stationary phase. Hence, the mass spectrometer capture, ionize and detect the ionized molecules separately that are broken into fragments and are identified according to their mass charge ratio[19]. The analysis was performed to identify the resulted metabolites from the photodegradation of difenoconazole and sonodegradation of acibenzolar-S-methyl with Thermo Scientific™ ISQ™ Quadruple GC/MS systems. The samples were extracted in dichloromethane solution.

3.2.2.4 Total Organic Carbon (TOC)

The total organic carbon is defined as the total amount of carbon species present in liquid sample. The TOC analysis was performed using SHIMADZU TOC Analyser, equipped with an auto sampler. The sample were collected in 9ml vials. The total carbon measurement was repeated twice for each sample.

4. References

- [1] Z. Muñoz and A. Moret, "Sensitivity of *Botrytis cinerea* to chitosan and acibenzolar-S-methyl," *Pest Management Science*, vol. 66, no. 9, pp. 974–979, 2010, doi: 10.1002/ps.1969.
- [2] J. H. Graham and M. E. Myers, "Soil application of SAR inducers imidacloprid, thiamethoxam, and acibenzolar-S-methyl for citrus canker control in young grapefruit trees," *Plant Disease*, vol. 95, no. 6, pp. 725–728, 2011, doi: 10.1094/PDIS-09-10-0653.
- [3] S. Frindy and M. Sillanpää, "Synthesis and application of novel α -Fe₂O₃/graphene for visible-light enhanced photocatalytic degradation of RhB," *Materials and Design*, vol. 188, p. 108461, 2020, doi: 10.1016/j.matdes.2019.108461.
- [4] S. Goldstein and J. Rabani, "The ferrioxalate and iodide-iodate actinometers in the UV region," *Journal of Photochemistry and Photobiology A: Chemistry*, vol. 193, no. 1, pp. 50–55, 2008, doi: 10.1016/j.jphotochem.2007.06.006.
- [5] C. G. Hatchard and C. A. Parker, "A new sensitive chemical actinometer - II. Potassium ferrioxalate as a standard chemical actinometer," *Proceedings of the Royal Society of London. Series A. Mathematical and Physical Sciences*, vol. 235, no. 1203, pp. 518–536, 1956, doi: 10.1098/rspa.1956.0102.
- [6] M. Montalti, A. Credi, L. Prodi, and M. T. Gandolfi, (2006). Handbook of Photochemistry (3rd ed.). CRC Press. <https://doi.org/10.1201/9781420015195>
- [7] V. Vishwakarma and S. Uthaman, *Environmental impact of sustainable green concrete*. Elsevier Inc., 2019. doi: 10.1016/B978-0-12-817854-6.00009-X.
- [8] M. Kaliva and M. Vamvakaki, *Materials Characterization*, vol. 1242. Elsevier Inc., 2010. doi: 10.1002/9780470172919.ch8.
- [9] J. P. Patel and P. H. Parsania, *Characterization, testing, and reinforcing materials of biodegradable composites*. Elsevier Ltd, 2017. doi: 10.1016/B978-0-08-100970-3.00003-1.
- [10] D. D. Joshi, "FTIR Spectroscopy: Herbal Drugs and Fingerprints," in *Herbal Drugs and Fingerprints: Evidence Based Herbal Drugs*, India: Springer India, 2012, pp. 121–146. doi: 10.1007/978-81-322-0804-4_7.
- [11] S. Nasir, M. Z. Hussein, Z. Zainal, N. A. Yusof, S. A. Mohd Zobir, and I. M. Alibe, "Potential valorization of by-product materials from oil palm: A review of alternative and sustainable carbon sources for carbon-based nanomaterials synthesis potential

- valorization of by-product materials from oil palm: A review of alternative and sustaina,” *BioResources*, vol. 14, no. 1, pp. 2352–2388, 2019, doi: 10.15376/biores.14.1.Nasir.
- [12] V. Chevali and E. Kandare, “Rigid biofoam composites as eco-efficient construction materials,” *Biopolymers and Biotech Admixtures for Eco-Efficient Construction Materials*, pp. 275–304, Jan. 2016, doi: 10.1016/B978-0-08-100214-8.00013-0.
- [13] M. Jaroniec, M. Kruk, and A. Sayari, *Adsorption methods for characterization of surface and structural properties of mesoporous molecular sieves*, vol. 117, no. 100. Elsevier Masson SAS, 1998. doi: 10.1016/s0167-2991(98)81008-2.
- [14] S. Palchoudhury, M. Baalousha, and J. R. Lead, *Methods for Measuring Concentration (Mass, Surface Area and Number) of Nanomaterials*, vol. 8. Elsevier, 2015. doi: 10.1016/B978-0-08-099948-7.00005-1.
- [15] J. Tauc and A. Menth, “States in the gap,” *Journal of Non-Crystalline Solids*, vol. 8–10, no. C, pp. 569–585, 1972, doi: 10.1016/0022-3093(72)90194-9.
- [16] P. Senthil Kumar, K. Grace Pavithra, and M. Naushad, *Characterization techniques for nanomaterials*. Elsevier Inc., 2019. doi: 10.1016/B978-0-12-813337-8.00004-7.
- [17] G. S. Bumbrah and R. M. Sharma, “Raman spectroscopy – Basic principle, instrumentation and selected applications for the characterization of drugs of abuse,” *Egyptian Journal of Forensic Sciences*, vol. 6, no. 3, pp. 209–215, 2016, doi: 10.1016/j.ejfs.2015.06.001.
- [18] T. Fornstedt, P. Forssén, and D. Westerlund, “Basic HPLC Theory and Definitions,” *Analytical Separation Science*, pp. 1–24, 2015.
- [19] H. J. Stan, “Chapter 6 GC-MS. I: Basic principles and technical aspects of GC-MS for pesticide residue analysis,” *Comprehensive Analytical Chemistry*, vol. 43, pp. 269–337, 2005, doi: 10.1016/S0166-526X(05)80026-1.

CHAPTER III: Visible light degradation of Levafix
blue dye using Fenton & Photo-Fenton processes

1 Introduction

Blue Levafix (BL) is a synthetic Azo-dye extensively used by the textile industries. The colorful lifestyle nowadays imposes huge dyes manufacturing destined to many sectors (textile, food, cosmetic...etc). Recently, the shortage of water resources is one of the crucial highlighted topics around the world[1]. The human daily requirements enforce the increase of competitive industrial sectors, which generate effluent loaded with micropollutants [2]. Approximately 800.000 tons of dyes per year are exploited and a half of this quantity is discharged in the environment[3-4]. The application of the conventional treatment methods has been tested and proved ineffective in the micropollutants treatment[5-6]. The textile industries are among the sectors responsible of the persistent organic pollutants generation[7]. Homogeneous Fenton-based reaction has proven a high efficiency on organic contaminants removal[8]. Photo-Fenton reaction using UV light [9]or visible radiation[10] have been performed in earlier work. In addition, it has been reported a high efficiency of UV and visible light radiations that remains a sustainable resource[11-13]. The light source accelerates the hydroxyl radicals generation via the ferrous and ferric ions photo-reduction [14]. Both processes were evaluated on diverse contaminants dyes[15] antibiotics [16], pesticides[17] and bacteria[18].

In this work, the effectiveness of photolysis, Fenton and Photo-Fenton processes was investigated. A kinetic study of parameters influencing the reaction was carried out. An optimization of reaction conditions at low concentration of hydrogen peroxide and ferrous ions has also been assessed.

2 Materials & methods

2.1 Photolysis system

The photolysis was conducted in a cylindrical stainless steel container with a Pyrex reactor and four polychromatic (365 nm) low-pressure mercury lamps of 15 W /each installed in symmetric position.

2.2 Fenton and Photo-Fenton processes

The Fenton reaction experiment was operated in 100 ml jacket batch reactor at room temperature. In 100 ml of dye solution 10 mg.L⁻¹, the pH was firstly regulated at 3 with sulfuric acid. Hydrogen peroxide and FeSO₄ were added together. The reaction was performed in the dark and under visible irradiation system. The samples were collected successively at a several time. The kinetic study were followed utilizing a UV-Vis spectrophotometer (model Selecta

3100) at Levafix Blue dye maximum wavelength $\lambda_{\text{max}} = 613 \text{ nm}$ with a 1cm quartz cell. The removal rate was calculated from the absorbance measurement.

3 Results & Discussion

3.1 Spectral characteristics of Levafix Blue

The physico-chemical properties of Levafix Blue dye are not known as the molecule structure is not revealed as mentioned before. Figure 34 illustrated the study of absorption of dye at various pH with 10 ppm of dye concentration at room temperature. As it has been investigated literature[19], the pH would impact the variation of chemical form of the molecule. In our work, we noticed a slight change of the intensity of the different absorbance bands that are related to the measured pH range particularly at 613nm that indicate the high stability of molecule.

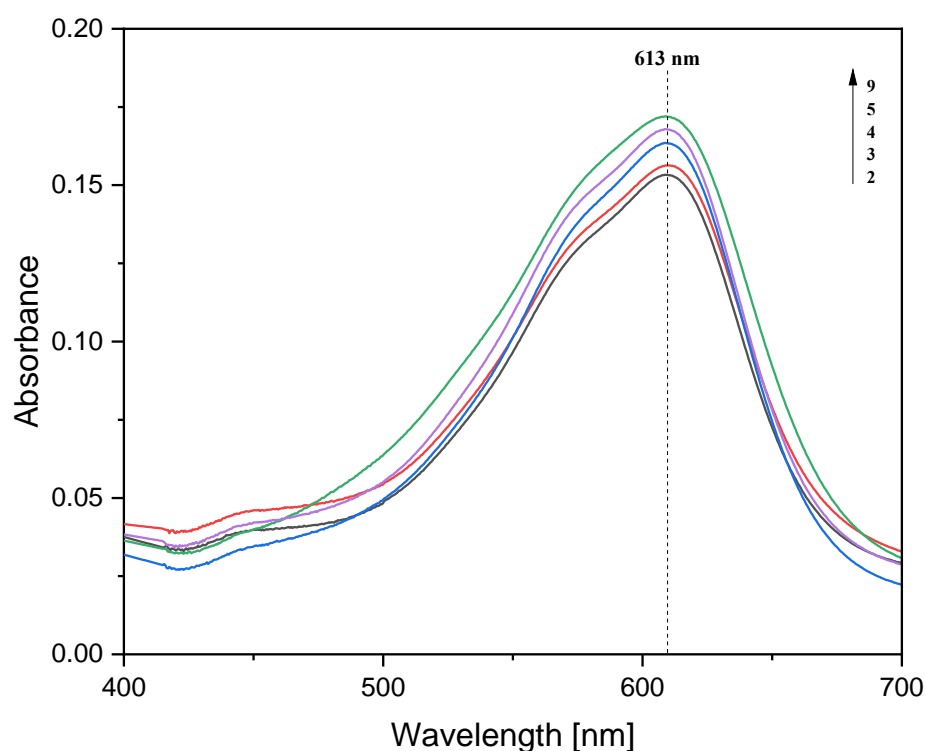


Figure 34: Absorption spectrum of Levafix Blue at different pH, [BL]=10 mg/L

To confirm the stability of molecule in the different pH medium, figure 35 illustrates the dye absorbance versus pH of initial solution. The graph shows a straight line ($R^2=0.9868$) and passing through the origin, which indicate good linear relationship between the absorbance and the pH of medium of the dye.

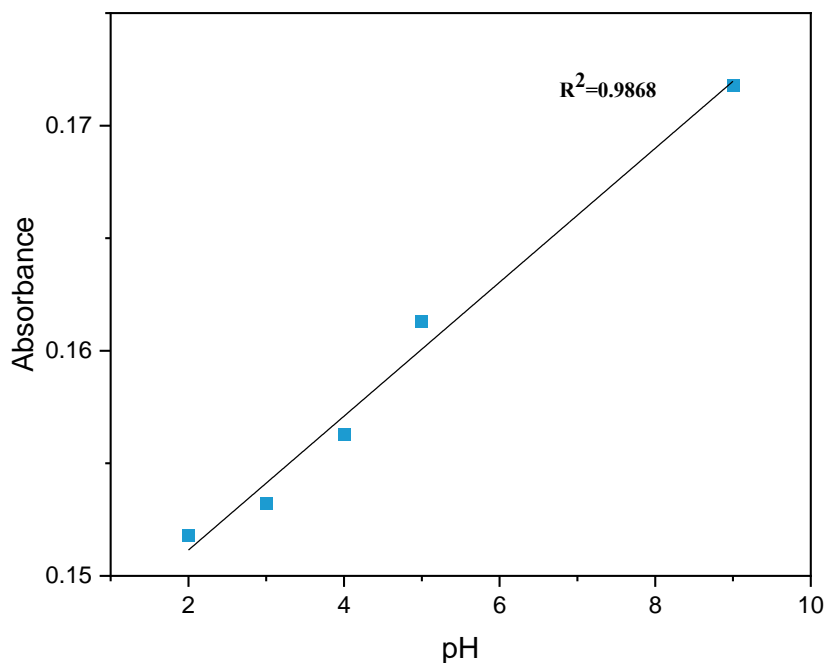


Figure 35: the dye absorbance versus their pH solution

In order to obtain a more precise understanding of the chemical structure of Levafix Blue dye, a FT-IR analysis was performed. As displayed in figure 36, the spectra contain a multitude of bands where the specific bands characteristic of dye are highlighted and assigned as follows:

The FTIR spectra show bands associated with the main classes of organic molecules. The band at 3438 cm^{-1} is characteristic of NH and OH stretching vibrations. The 1751 cm^{-1} band corresponds to the stretching of C=O ester carbonyl or carboxylic acid groups. The 1618 cm^{-1} assigned to the stretching of -N=N azoic functional group. A multitude of bands are located in the region of 1475 cm^{-1} , 1433 cm^{-1} , and 1365 cm^{-1} that originates from the bending vibrations of R-N-R2 group. The 1122 cm^{-1} and 1039 cm^{-1} bands are referred to the stretching vibrations of R-O-R group. The low frequencies bands at 827 cm^{-1} and 682 cm^{-1} are commonly corresponding to the vibrations of the C-H group

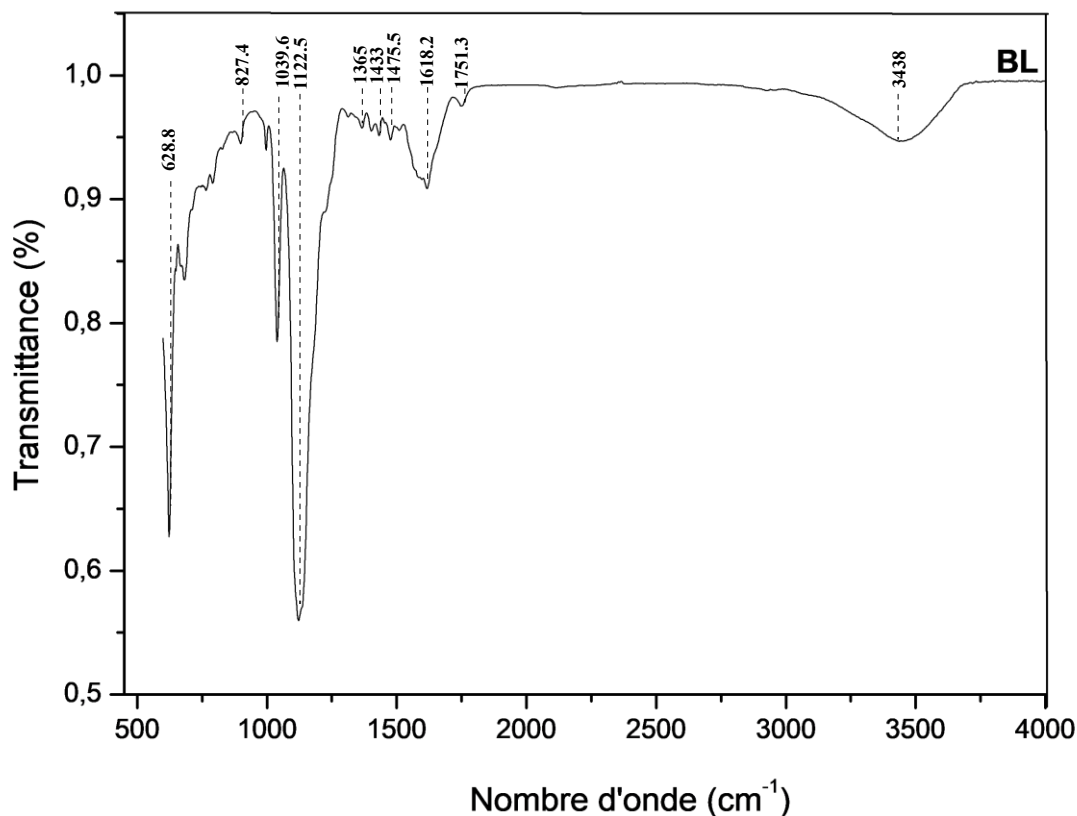


Figure 36: FT-IR spectrum of Levafix Blue dye

3.2 Radiation intensity effect on photolysis

To initiate a photocatalytic process, the light radiation source has to be at certain wavelength range and with specific intensity that the amount of emitted photons could be absorbed easily by the catalyst for high performance of reaction. Light intensity has been one of the important factors influencing the photodegradation rate because light irradiation supplies certain quantity of photons required for the electron transfer from valence band to conduction band of photocatalyst. A high radiations intensity plays an important role in excitation of catalyst for hydroxyl radicals generation that helps in photodegradation of emerging pollutants. In this work, all interacted parts in process were investigated in order to have a solid awareness about the most efficient and economic conditions. Otherwise said, the light source radiations are the second flagship of photocatalysis after the catalyst material properties. It has been proven that visible light resource still the best option as it is near to the sunlight naturel source which present a friendly and an economical choice. In this section, a self-photolysis experiment was carried out under different visible radiation intensities 0.98, 1.97, 2.96, and 3.94 $\mu\text{W}/\text{cm}^2$ to explore its impact on levafix blue dye degradation. Figure 37 indicates that the removal rate of dye is increasing as the intensity of visible radiation increased. After 48 hours of photolysis, and at the lowest intensity, we noticed a slight degradation of dye attained only 22%. However, the

removal rate increase under the highest intensities that achieved 47%, 51%, and 70% respectively. Moreover, the photo-Fenton process was carried out for other parameters investigation under the highest intensity using the four lamps[20].

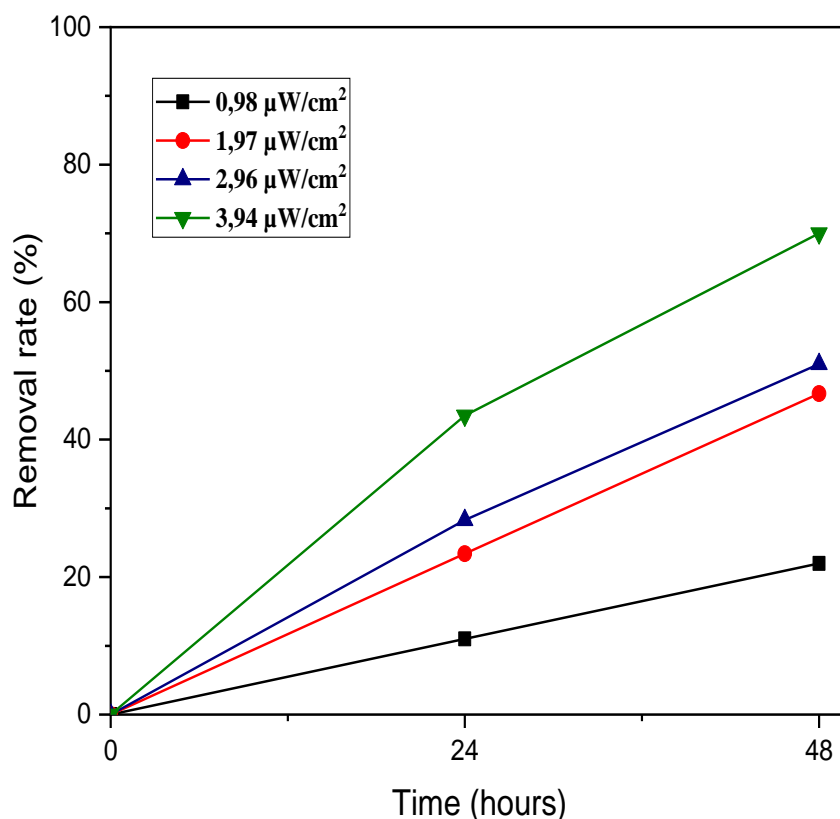


Figure 37: Irradiation intensity effect on BL degradation, pH=5,58, [BL]=10 mg/L

3.3 Photocatalytic discoloration of Levafix Blue dye

Prior to the photocatalytic reaction studies, an investigation was performed to detect whether direct photolysis occurs at initial pH dye solution and 10mg/L of concentration. As displayed in figure 38, it was observed that no significant degradation of the substrate occurs under photolysis treatment alone, since after 60 min only 16% of discoloration rate was achieved. In addition, when dark Fenton reaction was carried out at acidic pH with 10mM of ferrous ions concentration and 0.8M of hydrogen peroxide, there was a slight decrease in discoloration of BL due to hydroxyl radicals generation from the interaction of ferrous ions and hydrogen peroxide. The Fenton reaction in the dark attained 64% of discoloration rate within 60 min prior to turning the light source on. However, the photo-Fenton process has confirmed to be the most

effective treatment that achieved 89% of dye degradation in the first five minutes of treatment to attain the complete discoloration within 20 min. Thus, the result confirm that light irradiation plays crucial role in activation of catalytic reaction via boosting the generation of high potential oxidizing species like hydroxyl radicals in our case. Furthermore, we undertook experiments under various experimental conditions in order to optimize the degradation of Levafix Blue.

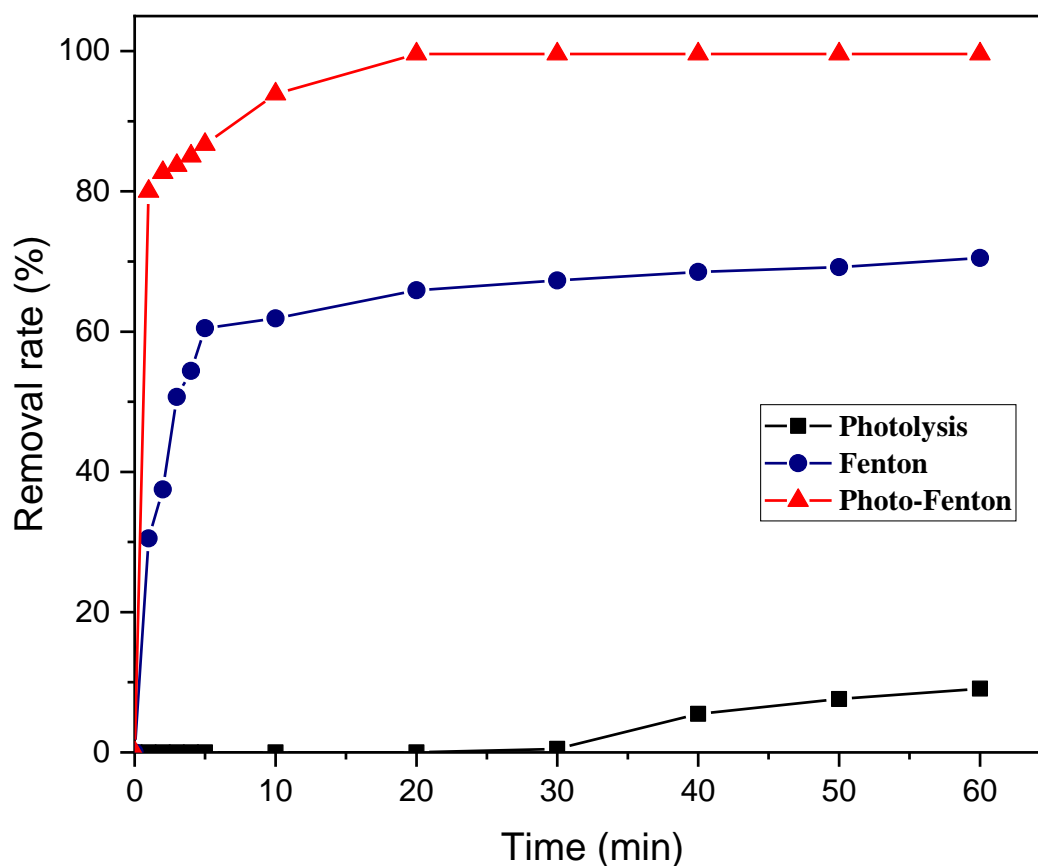


Figure 38: Degradation of BL under different systems, [BL]=10 mg/L, pH=3.0, [Fe²⁺]=10mM, [H₂O₂]=0.8 M.

3.4 Effect of initial pH

The discharged organic wastewater effluents from industries may come out with varied pH. On that account, the initial solution pH is considered as a crucial factor in photocatalytic processing since it impacts the properties of photocatalyst. To investigate the initial pH effect on Fenton and Photo-Fenton processes performance, experiments were realized at various pH conditions: 3, 7, and 9. Figure 39 revealed that for both of processes, the optimum conditions were in acidic medium, namely pH 3. The Levafix Blue removal rate reached 70 % and 98 % for Fenton and Photo-Fenton respectively. However, under neutral and alkaline pH medium have negatively affected the reaction. The instability of ferrous ions and hydrogen peroxide at alkaline pH

decreases the stationary concentration of hydroxyl radicals and thus stimulate the formation of ferric ions complexes that form a block of particles and forbids the light interaction in solution.

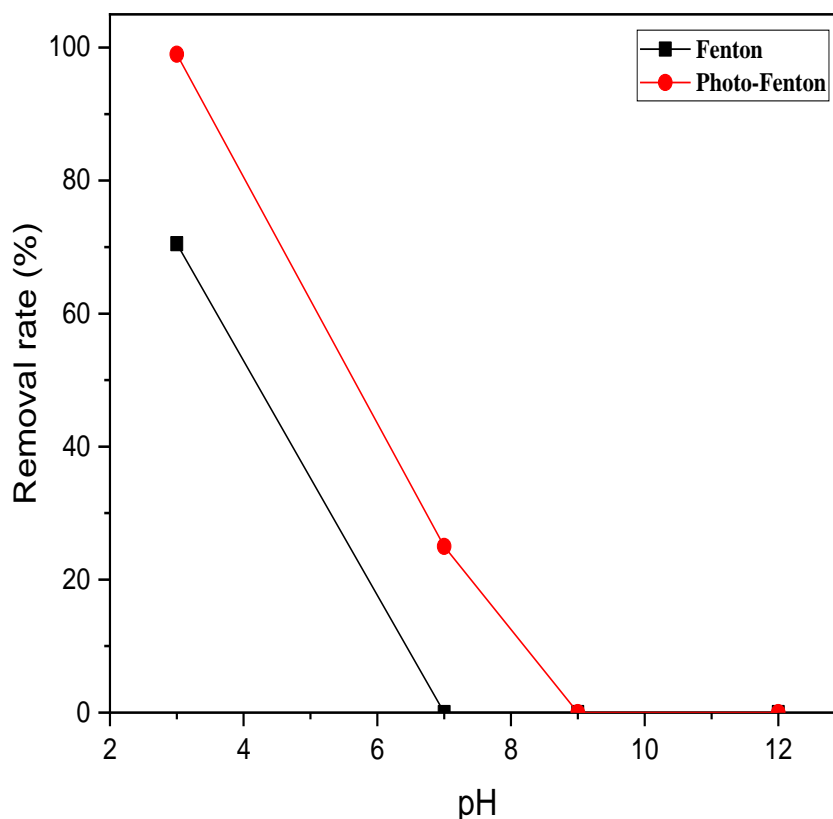


Figure 39: Effect of initial pH of solution, [BL]=10 mg/L, [H₂O₂]=0.8M, and [Fe²⁺]=10mM

3.5 Initial dye concentration effect

The dye concentration is an important parameter for any treatment investigation. At different concentration the solution contains much more amount of organic persistent chemicals. Thus, the photodegradation rate will be related to the interaction of pollutants in the solution with the photocatalytic process. As describes figure 40, the concentration of dye was varied from 10 to 100 mg/l. Both processes have proven a high degradation from 10 to 50 mg/l. However, as the concentration increase, a slight decrease was observed for the Fenton reaction after 50 mg/l. May it due to the molar ratio of oxidant as recorded in similar work before[21]. In high initial dye concentration, minimize the efficiency of the reaction and require oxidant dose increasing[22].

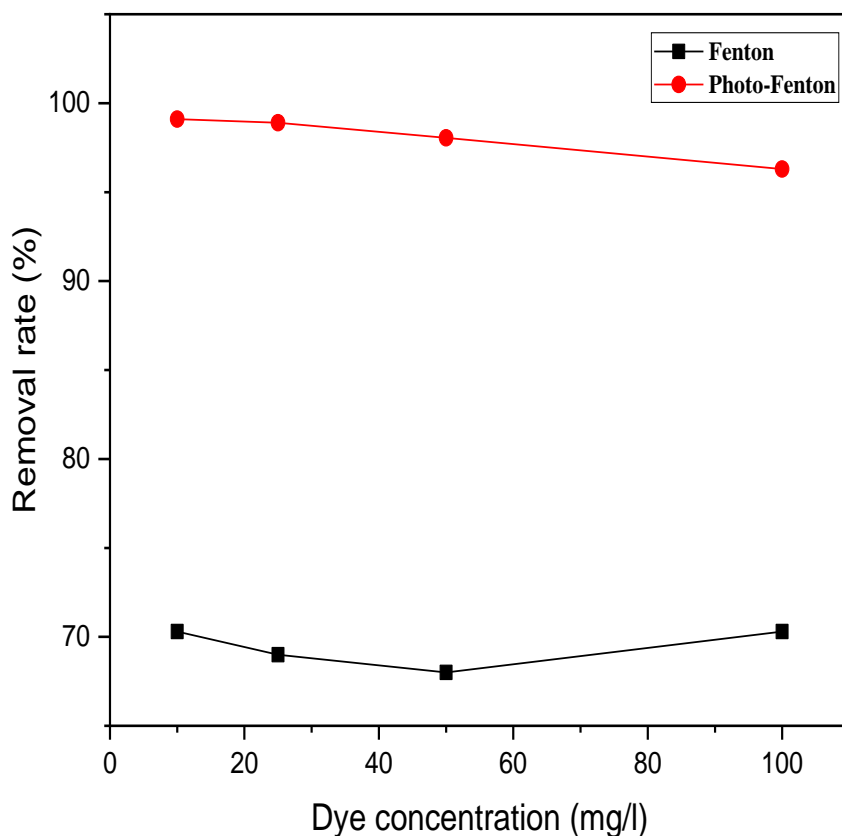


Figure 40: Effect of initial dye concentration, pH=3.0, [H₂O₂]=0.8M, and [Fe²⁺]=10mM

3.6 H₂O₂ concentration effect

Hydrogen peroxide was proven to be effective promotor in photo-initiated oxidation reactions; under UV/Visible light irradiations, hydrogen peroxide (H₂O₂) has the capacity of excitation and undergoing the O-O band scission producing highly reactive radicals[23]. The effect of initial hydrogen peroxide dose versus total removal rate of dye was studied to detect whether to increase the H₂O₂ dose consecutively. Classical Fenton process generally uses high concentration of hydrogen peroxide (<30%). Conversely, in this work, the investigation of influence of hydrogen peroxide were tested at low doses (0.1M, 0.2M, 0.5M, and 0.8M). Figure 41 confirms that process efficiency and the high doses have been risen along together for both processes after 60 min. The hydrogen peroxide plays a powerful role on hydroxyls radicals generations •OH. The radiation source stimulates expeditiously the reaction. The degradation rate difference between the two processes were less noticeable. Contrarily to our result, the high concentration of H₂O₂ may have a negative effect on the reaction whether the oxidant change a behaviour to become a scavenger of hydroxyl radicals[24].

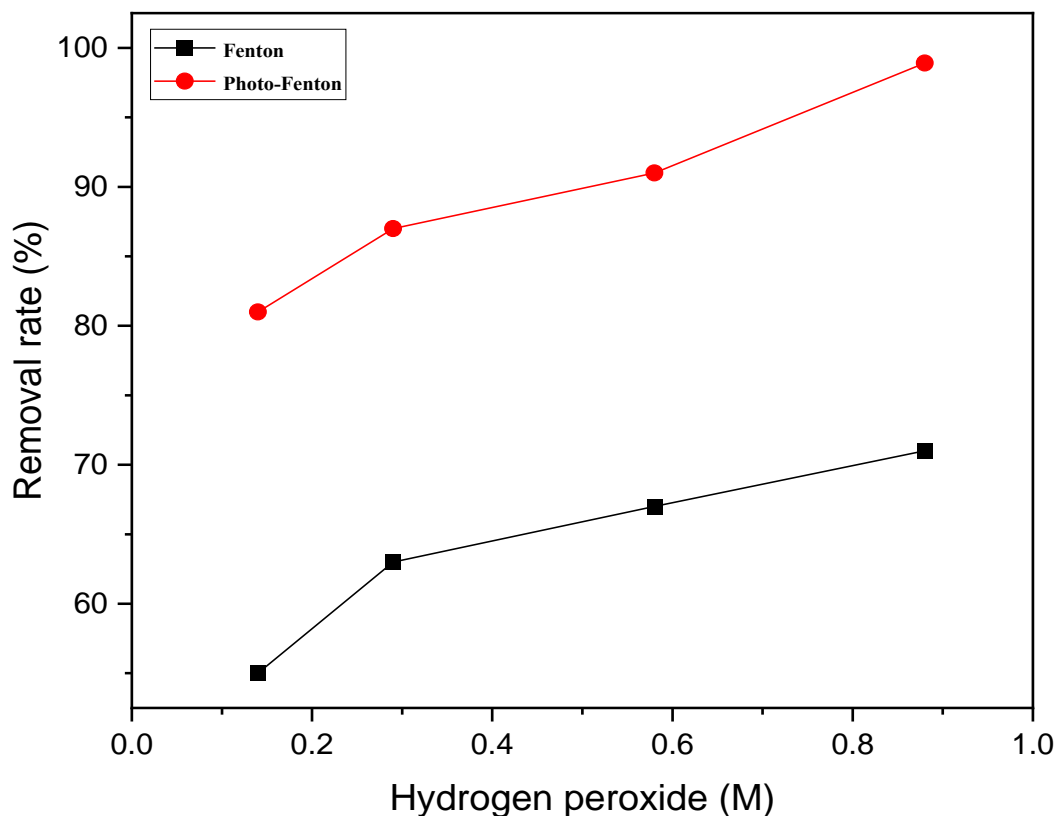


Figure 41: Effect of hydrogen peroxide, [BL]=10 mg/L, pH=3.0, and [Fe²⁺]=10mM

3.7 Ferrous ions concentration effect

Iron is the flagship element of Fenton reaction. Hydrogen peroxide and pH have been steadied at 3% and 3 respectively. Six concentrations of FeSO₄ were tested on Fenton and Photo-Fenton processes 1mM, 10mM, 50mM, 100mM, 150mM and 200mM. As shown in figure 42, a high degradation of Blue Levafix was proven of 70 % from 10mM to 100mM ferrous ions concentration for the Fenton process in the dark. Nevertheless, the degradation via the Photo-Fenton process attended the 98 % at low iron sulfate (II) concentration from 10mM to 100mM. The visible radiation increases the performance of the Fenton reaction. Beyond of 100mM for both processes, an obvious decrease of the removal rate have been observed. Approximately 68% at 150mM to 200mM for Fenton reaction. Whereas, 0% removal rate was recognized for the Photo-Fenton process after 150mM. An excess ferrous ions concentration dose led to an inhibition effect on the processes. The FeSO₄ behave as hydroxyl radicals scavenger in high concentration related to previous studies[25]. The optimum concentration of ferrous ions as was recorded in this study is 50mM for the Fenton reaction in the dark and 10mM for the Photo-Fenton.

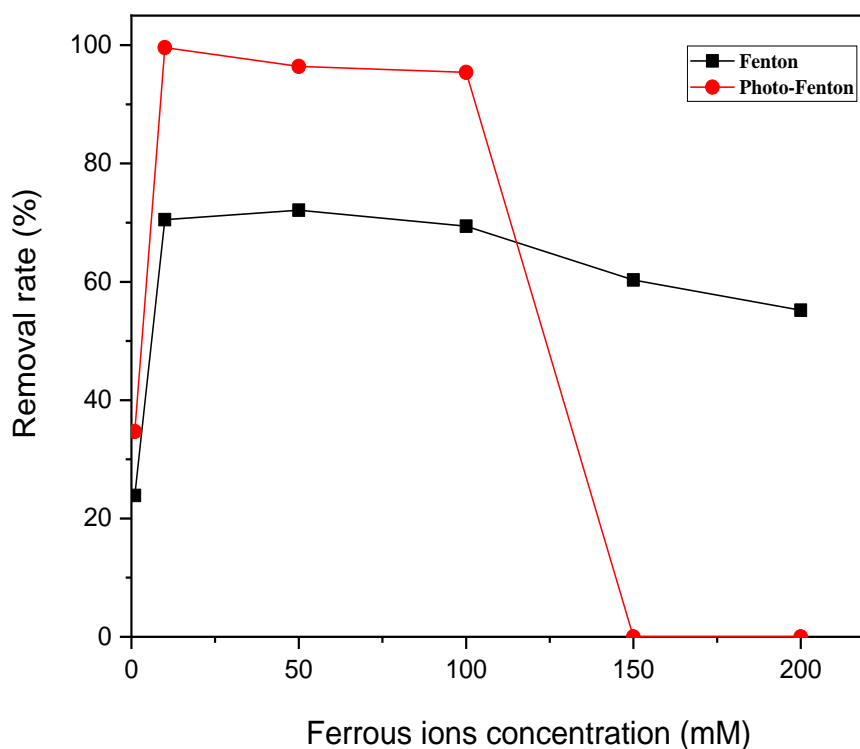


Figure 42: Effect of ferrous ions concentration, [BL]=10 mg/L, pH=3.0, [H₂O₂]=0.8M.

3.8 Humic acid effect

Humic substances were a debated subject for researchers since many years ago. Their chemical structure as macromolecules presents a challenge for many sciences application studies. With carboxylate, phenolic and carbonyl functional group contain, the Humic substances have the capability to form a new complex form with iron[26]. In addition, the humic acids have demonstrated a high catalytic activity in synthesis reaction of some materials[27]–[29]. The effect of these substances on the Fenton and Photo-Fenton processes have been inspected via adding a 50mg/l of humic acid to the reaction. Figure 43 demonstrates that the use of those substances has boosted the removal rate of Blue Levafix. The rate of removal attended 100% of degradation in 10 minutes for Photo-Fenton reaction. However, for the Fenton reaction in the dark, the degradation has reached 83% in 10 minutes and it carried and remain stable for 60 min of reaction. The humic substances adopt photocatalytic behavior under radiation which explain the high proven efficiency of HA/Photo-Fenton system

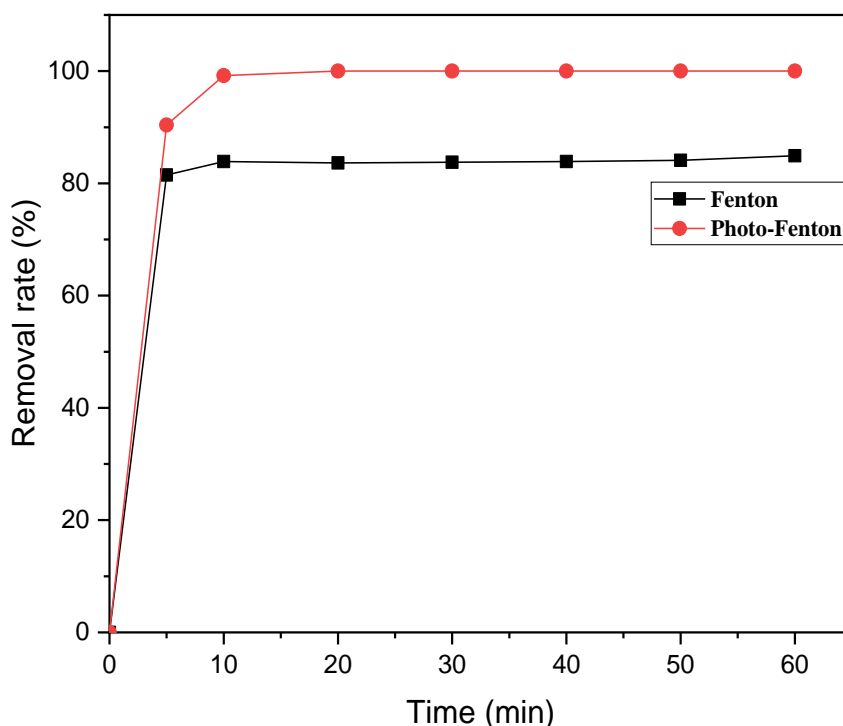


Figure 43: Effect of Humic acid on BL degradation, pH=3.0, [BL]=10 mg/L, [H₂O₂]=0.8M, and [Fe²⁺]=10mM

4 Conclusion

Degradation of BL dye using Fenton in the dark and Photo-Fenton system with visible light have confirmed its high efficiency. Acidic medium, 3% of hydrogen peroxide and low concentration of ferrous ions were demonstrated as optimum conditions for the both oxidation processes. Although, an inhibiting effect was noticed with overdoses of ferrous ions concentrations until a total obstruction of reaction specifically Photo-Fenton reaction. Based on the results, the both of processes ability to remove pollutants as the azo-dye in the present work, permit to considering Fenton and Photo-Fenton as ecological and economical processes to solve the pollution in aquatic medium.

5 References

- [1] P. T. Almazán-sánchez *et al.*, “Treatment of Indigo-Dyed Textile Wastewater Using Solar Photo-Fenton with Iron-Modified Clay and Copper-Modified Carbon,” 2017, doi: 10.1007/s11270-017-3489-z.
- [2] M. C. Cotto-maldonado, J. Duconge, C. Morant, and F. Márquez, “Fenton Process for the Degradation of Methylene Blue using Different Nanostructured Catalysts,” 2017, doi: 10.3844/ajeassp.2017.373.381.
- [3] H. Fan, S. Huang, W. Chung, J. Jan, W. Lin, and C. Chen, “Degradation pathways of crystal violet by Fenton and Fenton-like systems: Condition optimization and intermediate separation and identification,” vol. 171, pp. 1032–1044, 2009, doi: 10.1016/j.jhazmat.2009.06.117.
- [4] L. Elayazi, I. Ellouzi, A. Khairat, S. El Hajjaji & H. Mountacer (2014) Removal of blue levafix dye from aqueous solution by clays. *J. Mater. Environ. Sci*, 5, 2030-2036.
- [5] V. K. Saharan, D. V Pinjari, P. R. Gogate, and B. Pandit, *Advanced Oxidation Technologies for Wastewater Treatment: An Overview*. Elsevier Ltd., 2014. doi: 10.1016/B978-0-08-099968-5.00003-9.
- [6] S. Giray, M. Hakan, and S. Akarsu, “Comparison of classic Fenton with ultrasound Fenton processes on industrial textile wastewater,” *Sustainable Environment Research*, vol. 28, no. 4, pp. 165–170, 2018, doi: 10.1016/j.serj.2018.02.001.
- [7] M. Paola, S. Cotillas, D. Clematis, P. Ca, M. A. Rodrigo, and M. Panizza, “Chemosphere Degradation of dye Procion Red MX-5B by electrolytic and electro- irradiated technologies using diamond electrodes,” vol. 199, pp. 445–452, 2018, doi: 10.1016/j.chemosphere.2018.02.001.
- [8] M. E. Hassan, Y. Chen, G. Liu, D. Zhu, and J. Cai, “Journal of Water Process Engineering Heterogeneous photo-Fenton degradation of methyl orange by Fe₂O₃ / TiO₂ nanoparticles under visible light,” *Journal of Water Process Engineering*, vol. 12, pp. 52–57, 2016, doi: 10.1016/j.jwpe.2016.05.014.
- [9] K. M. Reddy and J. Devaraju, “ScienceDirect Kinetics of Photo Fenton Process and Ag-TiO₂ Photocatalyst under,” *Materials Today: Proceedings*, vol. 17, pp. 235–238, 2019, doi: 10.1016/j.matpr.2019.06.424.
- [10] S. Giannakis, T. M. Le, J. M. Entenza, and C. Pulgarin, “Solar photo-Fenton disinfection of 11 antibiotic-resistant bacteria (ARB) and elimination of representative AR genes. Evidence that antibiotic resistance does not imply resistance to oxidative treatment,” *Water Research*, 2018, doi: 10.1016/j.watres.2018.06.062.
- [11] L. Zhou, J. Lei, L. Wang, Y. Liu, and J. Zhang, “Highly Efficient Photo-Fenton Degradation of Methyl Orange Facilitated by Slow Light Effect and Hierarchical Porous Structure of Fe₂O₃-SiO₂ Photonic Crystals,” *Applied Catalysis B, Environmental*, 2017, doi: 10.1016/j.apcatb.2017.08.039.
- [12] G. Tekin, G. Ersöz, and S. Atalay, “Visible light assisted Fenton oxidation of tartrazine using metal doped bismuth oxyhalides as novel photocatalysts,” *Journal of*

- Environmental Management*, vol. 228, no. August, pp. 441–450, 2018, doi: 10.1016/j.jenvman.2018.08.099.
- [13] Y. Zhu *et al.*, “Heterogeneous photo-Fenton degradation of bisphenol A over Ag / AgCl / ferrihydrite catalysts under visible light,” *Chemical Engineering Journal*, 2018, doi: 10.1016/j.cej.2018.04.073.
- [14] S. R. Pouran, A. R. A. Aziz, W. Mohd, and A. Wan, “Journal of Industrial and Engineering Chemistry Review on the main advances in photo-Fenton oxidation system for recalcitrant wastewaters,” *Journal of Industrial and Engineering Chemistry*, vol. 21, pp. 53–69, 2015, doi: 10.1016/j.jiec.2014.05.005.
- [15] M. M. Rashad, A. A. Ibrahim, D. A. Rayan, M. M. S. Sanad, and I. M. Helmy, “Photo-Fenton-Like Degradation of Rhodamine B Dye from Waste Water Using Iron Molybdate Catalyst under Visible Light Irradiation Graphical abstract,” *Environmental Nanotechnology, Monitoring & Management*, V(8), 175-186. 2017, doi: 10.1016/j.enmm.2017.07.009.
- [16] A. S. Giri and A. K. Golder, “Ciprofloxacin degradation in photo-Fenton and photo-Catalytic processes: Degradation mechanisms and iron chelation,” *Journal of Environmental Sciences*, pp. 1–12, 2018, doi: 10.1016/j.jes.2018.09.016.
- [17] M. Gar, A. Tawfik, and S. Ookawara, “Journal of Water Process Engineering Comparison of solar TiO₂ photocatalysis and solar photo-Fenton for treatment of pesticides industry wastewater : Operational conditions , kinetics , and costs,” *Journal of Water Process Engineering*, vol. 8, pp. 55–63, 2015, doi: 10.1016/j.jwpe.2015.09.007.
- [18] S. Giannakis, S. Watts, S. Rtimi, and C. Pulgarin, “Solar light and the photo-Fenton process against antibiotic resistant bacteria in wastewater : A kinetic study with a Streptomycin-resistant strain,” *Catalysis Today*, no. July, pp. 0–1, 2017, doi: 10.1016/j.cattod.2017.10.033.
- [19] D. Malyshev, R. Öberg, L. Landström, P. O. Andersson, T. Dahlberg, and M. Andersson, “pH-induced changes in Raman, UV–vis absorbance, and fluorescence spectra of dipicolinic acid (DPA),” *Spectrochimica Acta Part A: Molecular and Biomolecular Spectroscopy*, vol. 271, p. 120869, Apr. 2022, doi: 10.1016/J.SAA.2022.120869.
- [20] R. Dina Asrifah *et al.*, “The Effect of Flow Rate Discharge on TDS, pH, TSS, and Cu in Electrocoagulation with Continuous Reactors,” *Yogyakarta Conference Series Proceeding on Engineering and Science Series (ESS)*, vol. 1, no. 1, pp. 737–746, 2020, doi: 10.31098/ess.v1i1.171.
- [21] M. S. Lucas and J. A. Peres, “Decolorization of the azo dye Reactive Black 5 by Fenton and photo-Fenton oxidation,” *Dyes and Pigments*, vol. 71, no. 3, pp. 236–244, 2006, doi: 10.1016/j.dyepig.2005.07.007.
- [22] M. L. Rache, A. R. García, H. R. Zea, A. M. T. Silva, L. M. Madeira, and J. H. Ramírez, “Applied Catalysis B: Environmental Azo-dye orange II degradation by the heterogeneous Fenton-like process using a zeolite Y-Fe catalyst — Kinetics with a model based on the Fermi ’ s equation,” *Applied Catalysis B, Environmental*,” vol. 146, pp. 192–200, 2014, doi: 10.1016/j.apcatb.2013.04.028.

- [23] M. Klavarioti, D. Mantzavinos, and D. Kassinos, "Removal of residual pharmaceuticals from aqueous systems by advanced oxidation processes," *Environment International*, vol. 35, no. 2, pp. 402–417, Feb. 2009, doi: 10.1016/J.ENVINT.2008.07.009.
- [24] J. de Laat, Y. H. Dao, N. Hamdi El Najjar, and C. Daou, "Effect of some parameters on the rate of the catalysed decomposition of hydrogen peroxide by iron(III)-nitrilotriacetate in water," *Water Research*, vol. 45, no. 17, pp. 5654–5664, Nov. 2011, doi: 10.1016/J.WATRES.2011.08.028.
- [25] M. Verma and A. K. Haritash, "Journal of Environmental Chemical Engineering Degradation of amoxicillin by Fenton and Fenton-integrated hybrid oxidation processes," *Journal of Environmental Chemical Engineering*, vol. 7, no. 1, p. 102886, 2019, doi: 10.1016/j.jece.2019.102886.
- [26] F. Wang, Y. Wu, Y. Gao, H. Li, and Z. Chen, "Effect of humic acid , oxalate and phosphate on Fenton-like oxidation of microcystin-LR by nanoscale zero-valent iron," *Separation and Purification Technology*, vol. 170, pp. 337–343, 2016, doi: 10.1016/j.seppur.2016.06.046.
- [27] Z. Wei, J. Li, Z. Wang, P. Li, and Y. Wang, "Synthesis of 1, 4-Dihydropyridine Compounds Catalyzed by Humic Acid," *Chinese Journal of Organic Chemistry*, vol. 37, no. 7, pp. 1835–1838, Jul. 2017, doi: 10.6023/cjoc201612055.
- [28] H. Wang, Y. Wang, Y. Han, W. Zhao, and X. Wang, "Humic acid as an efficient and reusable catalyst for one pot three-component green synthesis of 5-substituted 1: H - tetrazoles in water," *RSC Advances*, vol. 10, no. 2, pp. 784–789, 2019, doi: 10.1039/c9ra08523h.
- [29] M. Kļaviņš, J. Dipāne, and K. Babre, "Humic substances as catalysts in condensation reactions," *Chemosphere*, vol. 44, no. 4, pp. 737–742, 2001, doi: [https://doi.org/10.1016/S0045-6535\(00\)00294-0](https://doi.org/10.1016/S0045-6535(00)00294-0).

CHAPTER IV: Photocatalytic degradation of
fungicide difenoconazole via Photo-Fenton process
using $\alpha\text{-Fe}_2\text{O}_3$

1 Introduction

Over the last decade, the world's priority was to meet human food needs. Pesticides are chemical compounds created to deal with phytopathology for human survival exigency. They are classified depending on their principal target and chemical structure[1]. Insecticides, herbicides, fungicides, and nematicides are a broad array of products utilized every day in crop fields worldwide. Certainly, the agricultural production has been guaranteed, but in return, the treatment rate with those compounds exceeded the threshold to the contamination stage. Previous monitoring studies revealed that pesticides had affected the surface and groundwater quality, and it classed as the second aggrieved part of environment after soils contamination [2-3]. A various Toxicity test strategies were improved to prevent crops contamination, which it had an indispensable rule to detect the ideal used concentration of pesticides and how preliminary test could be a useful approach to minimize the ecotoxicity [4-5]. Since the world has become more environmentally conscious, the governments have been oriented towards enormous investments in green technologies. The Fenton catalysis is known as a low cost and most feasible methods, and the high efficiency of the process has been confirmed on a large variety of pollutants; dyes, pharmaceutical compounds, and pesticides [6-9]. The treatment based on the combination of the hydrogen peroxide and ferrous ions or synthesized semiconductor-based materials in an acidic medium for hydroxyl radical generation[10-11]. Commercial or synthesized, the metal oxides were the principle aim of previous and current studies[12]. Indeed, the wide range of synthesis and doped simple approaches and their treatment efficiency, some research unveiled a negative impact of some chemical source synthesized materials. They recommend the orientation to friendly bioremediation fabrication methods[13]. Hematite is one of the abundant existing metals; it has known via its expanded application in multidisciplinary fields. Water treatment, oncology, material sciences research projects have revealed appealing results of iron oxide activity.

In the present work, we reported the synthesis of α -Fe₂O₃ nanoparticles with the hydrothermal method at 180°C. it manifested as an eco-friendly and economical approach with low-cost reagents and a simple fabrication method. The sample properties were characterized using a range of analytical techniques XRD, SEM, TEM, and RAMAN analysis. The potential photocatalytic activity of α -Fe₂O₃ nanoparticles under UV light source was investigated by monitoring the degradation of difenoconazole (DFL). A possible photocatalytic mechanism pathway was proposed to elucidate the enhancement of DFL photodegradation.

2 Materials & methods

2.1 Synthesis protocol

The described approach by Frindy et al.; was used for hematite synthesis. In 250 ml baker, 80 ml of ferric chloride poured, and 80 ml of the sodium hydroxide NaOH added dropwise to the solution for 15 min until dark brown color appeared. The mixture was vigorously stirred for 30 min. The mixture was transferred in Teflon-lined autoclave and was hydrothermally treated for 24 h at 180 °C. The hydrothermally treated and prepared hematite was washed with deionized water several times as well as ethanol and it was dried at 60 °C for an overnight before further use.

2.2 Characterization of synthesized α -Fe₂O₃

The synthesis hematite was characterized using Powder X-ray diffraction (XRD) patterns were carried out on a PANalytical diffractometer with Co K α radiation ($\lambda = 0.1789$ nm, at 40 kV and 40 mA) from 10° to 100° 2 θ angles. Scanning electron microscopy (SEM) analysis were taken by field emission SEM (Hitachi S-4800). Transmission electron microscopy (TEM) analysis were taken on a Hitachi 7700. Raman spectra were recorded at ambient temperature with a green laser 514 nm laser excitation on a RENISHAW in Via Micro-Raman spectrophotometer. A Micrometrics TriStar II Plus analyser was used to obtain the pore dimension and specific surface area of hematite. UV–vis diffuse reflectance spectra (UV–vis, Perkin-Elmer Lambda 950) were used for the determination of band-gap energy.

2.3 Photochemical degradation activity

The fungicide DFL solution stock 10 mg/L was prepared for the photodegradation activity. At room temperature with pH = 5, 0.5 g/L of the catalyst was added into a 50 ml of pollutant solution using a quartz reaction cell, and the mixture was stirred for 30 min in the darkness. Afterward, a 30 μ l of hydrogen peroxide was poured into the mixture under a UVC lamp irradiation system at 254 nm. The experiments were performed in duplicate. The samples were collected and filtered (syringe filter with nylon membrane 0.2 μ m diameter 25 mm). The kinetic study was monitored using high-performance liquid chromatography (HPLC). All results data were treated via Origin Lab software.

3 Results & discussion

3.1 Characterization of $\alpha\text{-Fe}_2\text{O}_3$

As indicated previously, hematite is the most stable iron oxide under ambient conditions. It has interesting properties that is categorized to be non-toxic, low-cost, high resistant to corrosion. Thus, its utilized in several sectors such as catalysis processes, photoelectrode, battery electrode, gas sensor, pigment, and magnetic materials. A wide variety of chemical and physical strategies have been developed to synthesis iron oxides particles. Sol-gel procedures, hydrothermal synthesis protocol, and laser ablation deposition are among the developed synthesis techniques. In this study, we opted for the simple and rapid synthesis route the hydrothermal technique.

3.1.1 DRS analysis

The optical properties of the synthesized photocatalyst were evaluated using firstly UV-Vis diffuse reflectance spectroscopic studies. Figure 44 present DRS spectra of hematite $\alpha\text{-Fe}_2\text{O}_3$ that indicate the absorption of hematite material within the range 250 nm to 800 nm. Strong band edge was observed from 537 nm to 563nm which is approximate result with previous work [14] and that assigned according Bagheri et al,[15] to the band gap electronic transition.

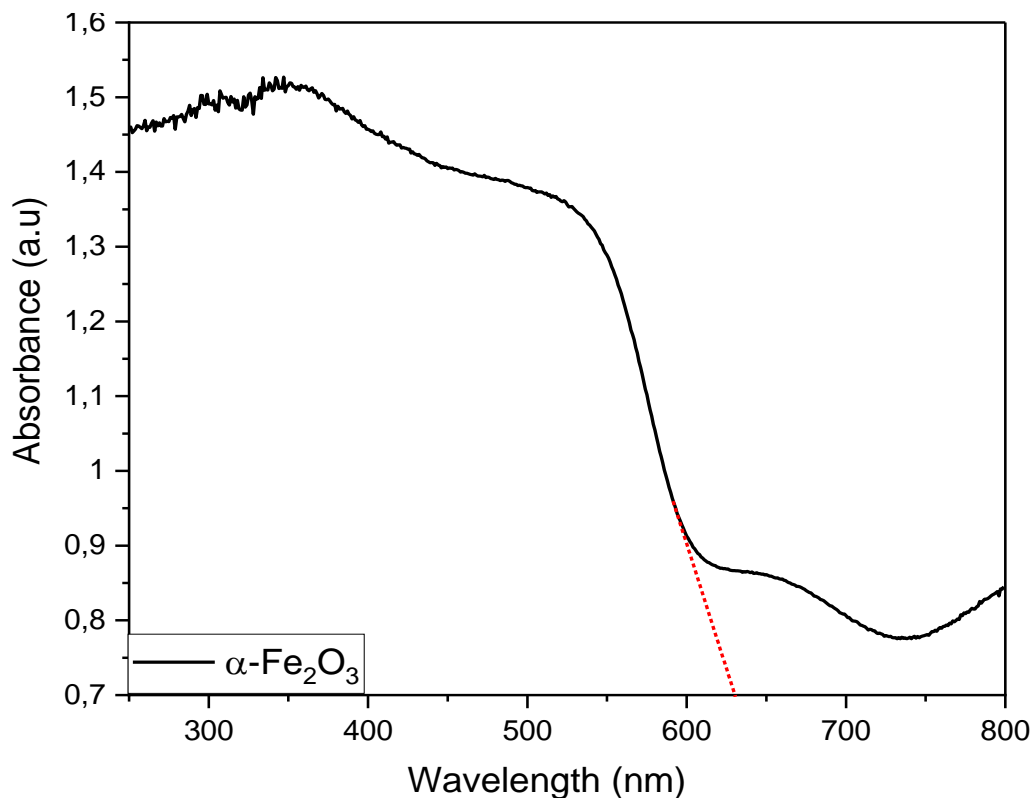


Figure 44: UV-Vis diffuse reflectance spectra of hematite

The bandgap energy of catalysts is commonly calculated using Tauc plot method Eq (24), in which $(\alpha h\nu)^2$ is plotted versus $h\nu$ (photon energy). The intersection between the linear fit and the photon energy axis gives the value of bandgap energy (E_g) of material.

$$(\alpha h\nu)^2 = A(h\nu - E_g) \quad (\text{Eq 24})$$

Where α is the absorption coefficient, and A is the proportionality[16]. The Bandgap value of synthesized hematite is $E_g=1.94$ eV as indicated in figure 45 which is approximately the same as known in literature[17].

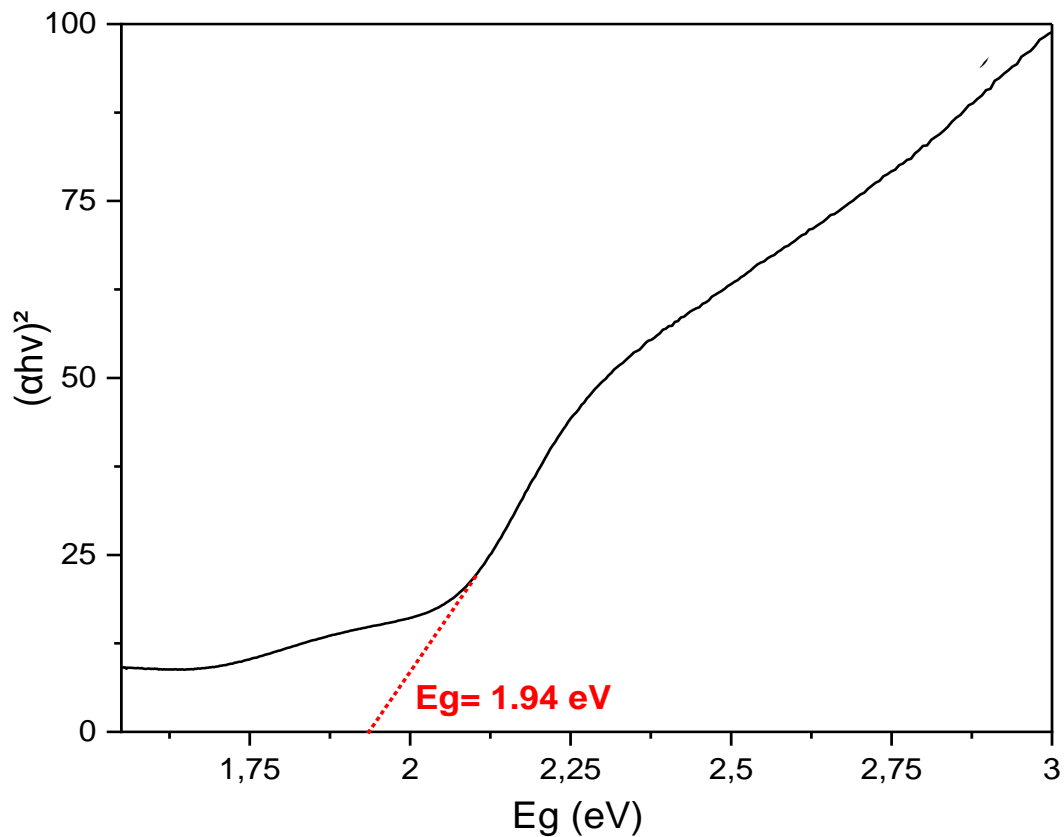


Figure 45: Tauc plot for hematite bandgap determination

3.1.2 BET analysis

The Brunauer-Emmet-Teller technique was carried out to determine the specific surface area of the photocatalyst. As plotted in figure 46, the Nitrogen adsorption-desorption was found to be an isotherm type IV with an H3 hysteresis loop according to adsorption isotherms IUPAC classification, which occurs as a mesoporous structure of $\alpha\text{-Fe}_2\text{O}_3$. A dilated pores have been noticed in prepared material as described by Dahbi et al; which is caused due to the presence

of hysteresis cycle at high pressure level. Table 7 describes the obtained structural data of hematite, surface area, volume of pores surface.

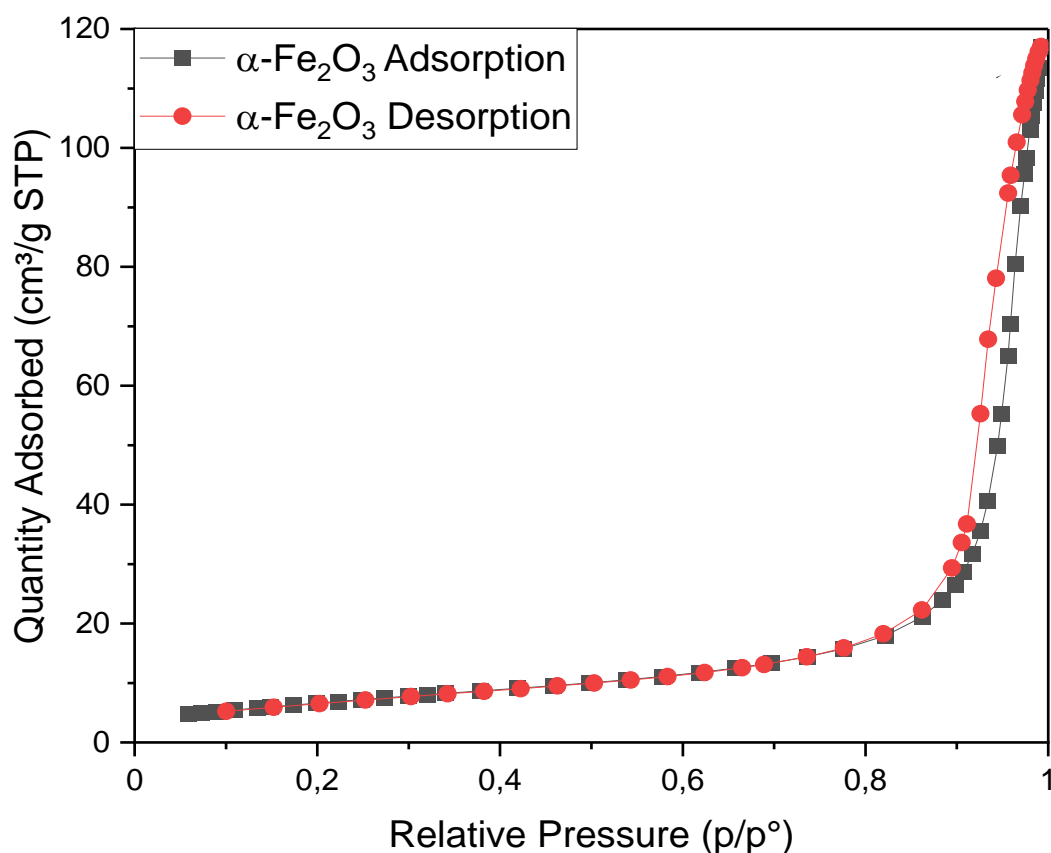


Figure 46: Nitrogen adsorption-desorption spectra

Table 9: Textural characteristic of hematite

Material	S _{BET}	Pore volume	E _g	Size
$\alpha\text{-Fe}_2\text{O}_3$	24.82 m ² .g ⁻¹	0.132 cm ³ .g ⁻¹	1.94	27nm

3.1.3 X-ray diffraction analysis

The X-ray diffraction (XRD) pattern of synthesized hematite $\alpha\text{-Fe}_2\text{O}_3$ is illustrated in figure 47 shows a strong, pure phase by comparing the obtained peaks with JCPDS-ICCD file No (33-0664). The diffraction peaks at 23.92°, 32.22°, 35.53°, 40.65°, and 49.22° assigned to (012),(114),(110),(113), and (024) respectively. The high intensity of peak 104 is the same as described in the hematite XRD data standard as it was proven in similar work[18]. The crystal unit cell of the catalyst expressed a rhombohedral structure. The diffraction peaks are limited

to those corresponding to the pure hematite with no impurity's peaks have been observed which designate the good quality of synthesized material. Average crystallite size has been calculated 27 nm by Debye Scherrer equation $D = K \lambda / \beta \cos \theta$, where $K=0.9$, λ is the XRD wavelength radiation and β is the half peak width at specific Bragg angle θ .

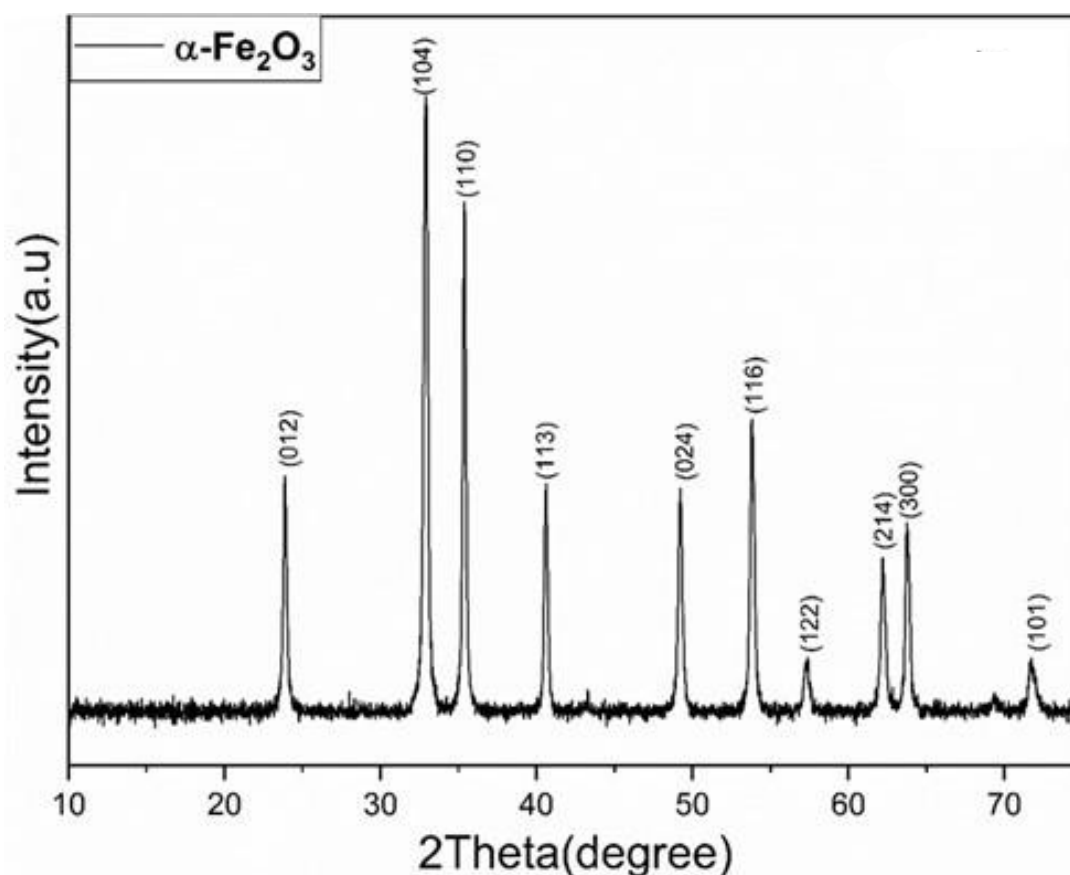


Figure 47: X-ray diffraction pattern of hematite $\alpha\text{-Fe}_2\text{O}_3$.

3.1.4 SEM & TEM analysis

The morphology of hematite surface was recorded using SEM and TEM images analysis, as is shown in figure 48. A uniform size distribution of $\alpha\text{-Fe}_2\text{O}_3$ nanoparticles is presented in the micrographs. The sample composed of crystals with semi-spherical shape. The growth direction of hematite $\alpha\text{-Fe}_2\text{O}_3$ and the particle size were obtained from the TEM micrograph. The grain size of the monodisperse nanoparticles is about 52nm.

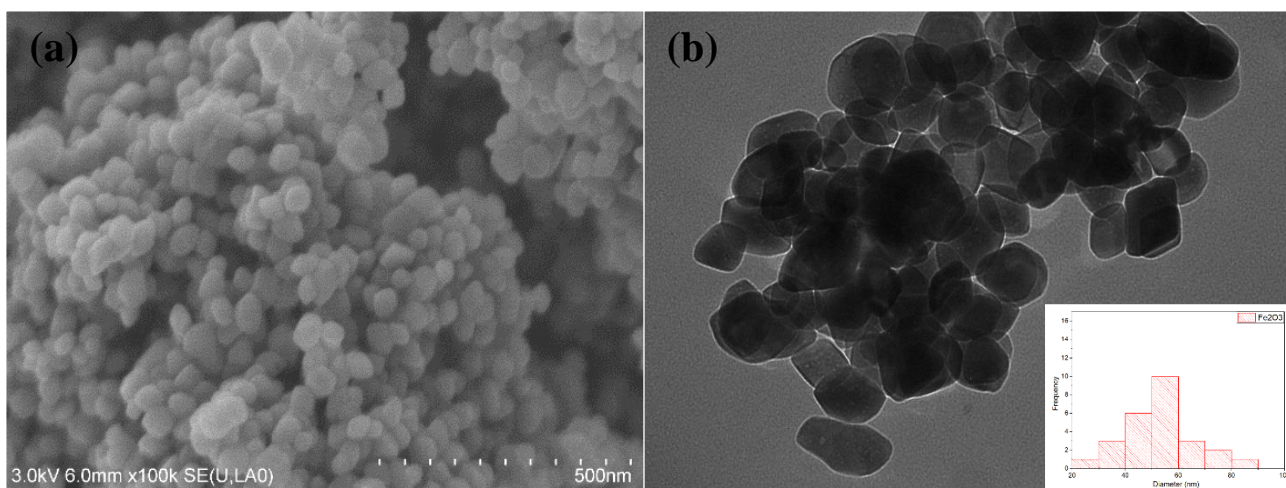


Figure 48: SEM & TEM micrographs of hematite

3.1.5 Raman analysis

Figure 49 displays the Raman spectrum of hematite $\alpha\text{-Fe}_2\text{O}_3$ that exhibit the presence of seven strong resonant spectral signature deemed for hematite analysis. The peaks seen at 221 cm^{-1} and 287 cm^{-1} are assigned to A_{1g} modes. The other five peaks at $246, 308, 400, 494$ and 603 cm^{-1} are assigned to the E_g modes. The peaks positions are in good agreement with the commonly observed from $\alpha\text{-Fe}_2\text{O}_3$ nanoparticles. In addition, as an antiferromagnetic material, the hematite knows an excitation in the magnon state. The magnon are the spin wave quantum, are excitation modes related to the flip of a single spin. Moreover, another intense peak noticed at approximately 1296 cm^{-1} that is explained in literature by the interaction of two magnons created at nearest spin sites[19].

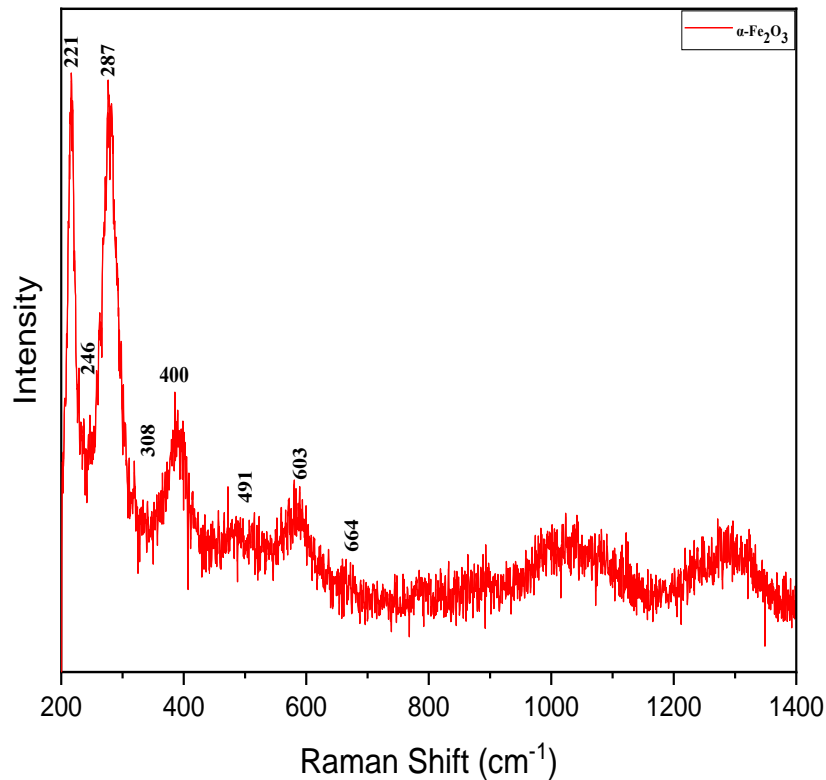


Figure 49: RAMAN spectra of α -Fe₂O₃

3.2 Photocatalytic activity

3.2.1 Photodegradation under different systems

In the beginning, DFL photodegradation was performed under different systems: direct photolysis, UV/H₂O₂, UV/ α -Fe₂O₃, Fenton in the dark, and Photo-Fenton process. As shown, in figure 50, Photo-Fenton process was observed to be the most effective over other methods, achieving a total removal 100% within 20 min. Contrarily, DFL removal via Fenton in the dark and under UV/ α -Fe₂O₃ system were completed only 37% and 78% removal rate, respectively in 20 min, which describes irradiation's influential role in improving the reaction conditions. Moreover, the absence of hydrogen peroxide in UV photolysis reaction demonstrated a crucial act on DFL degradation with only 49%.

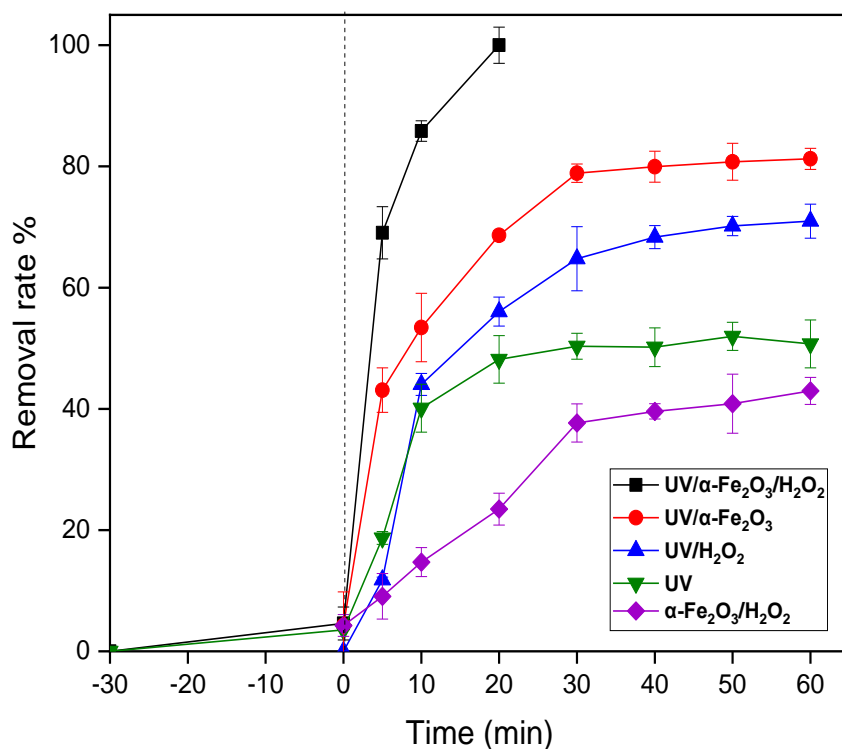


Figure 50: Photodegradation of DFL under different system (UV/α- Fe₂O₃/ H₂O₂, UV/α- Fe₂O₃, UV/ H₂O₂, UV, and α- Fe₂O₃/ H₂O₂), pH=5, [H₂O₂]=9.79 M, [α- Fe₂O₃]=0.5 g/l

3.2.2 pH effect

The pH effect is one of evident parameters for Photo-Fenton reaction. The Photo-Fenton process, as known in literature, usually is more effective in acidic medium pH=3. In the present investigation, it was observed that the optimum pH that manifested an effective treatment as mentioned in figure 51 was pH=5, which was the initial pH of pollutant solution attending a removal rate of 100% in 20 min. However, the experiences that were tested in neutral pH=7 and alkaline pH conditions pH=10 and pH=12 led to decrease the process efficiency attending a removal rate of 73%, 32%, and 29%, respectively. The instability of ferrous ions and hydrogen peroxide at alkaline pH decrease the regeneration of hydroxyl radicals and stimulate the formation of ferric ions complexes.

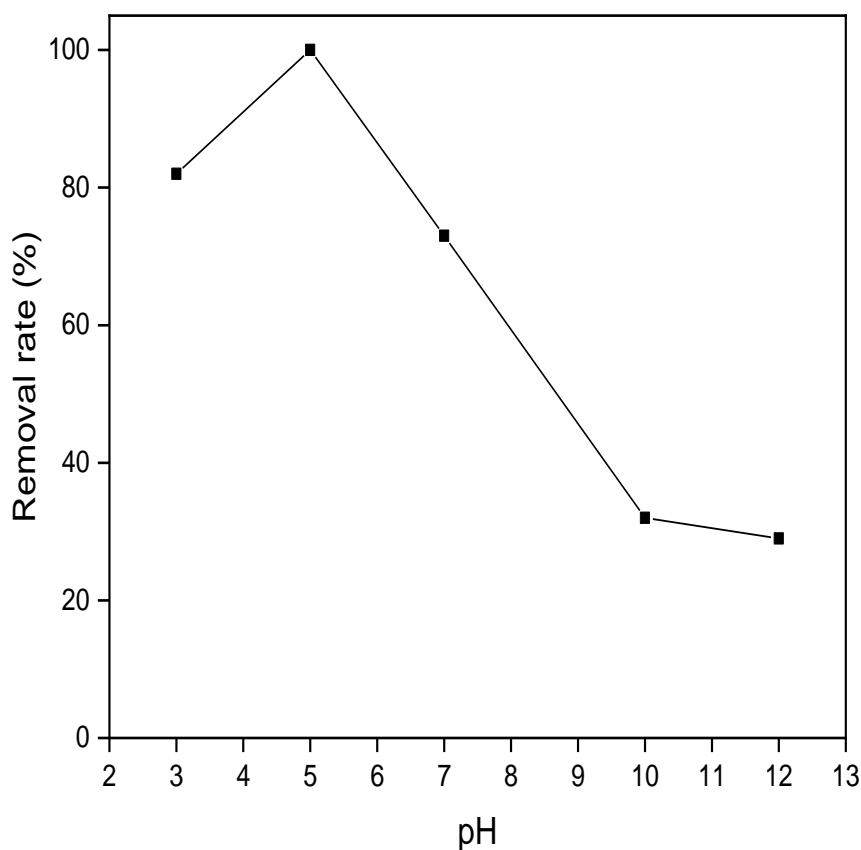


Figure 51: pH effect, at 20 min of reaction, $[H_2O_2]=9.79M$, $[\alpha-Fe_2O_3]=0.5$ g/l, UV

3.2.3 Hydrogen Peroxide concentration effect

The hydrogen peroxide is one of the most potent oxidants for wastewater treatment processes; it is a hydroxyl radicals generation stimulator. Many previous works have shown that hydrogen peroxide concentration has a significant effect on Photo-Fenton reaction[20]. Hence, the impact of H_2O_2 concentration was carried out in the present work figure 52 at initial pollutant solution pH= 5 with 0.5 g/L amount of $\alpha-Fe_2O_3$ catalyst. Total oxidation of DFL has been achieved within 20 min at the highest hydrogen peroxide concentration 9.79M, whereas, at low concentration of H_2O_2 , Photo-Fenton process efficiency decreased (i.e., 70%, 65%, and 56% at 6.52 M, 3.25 M and 1.63 M, accordingly). Otherwise, in an anterior investigation, it has been proven that a high amount of hydrogen peroxide induces inhibition of reaction and it was noticed as an auto-scavenger of the reaction, which was contrarily to our study case[21].

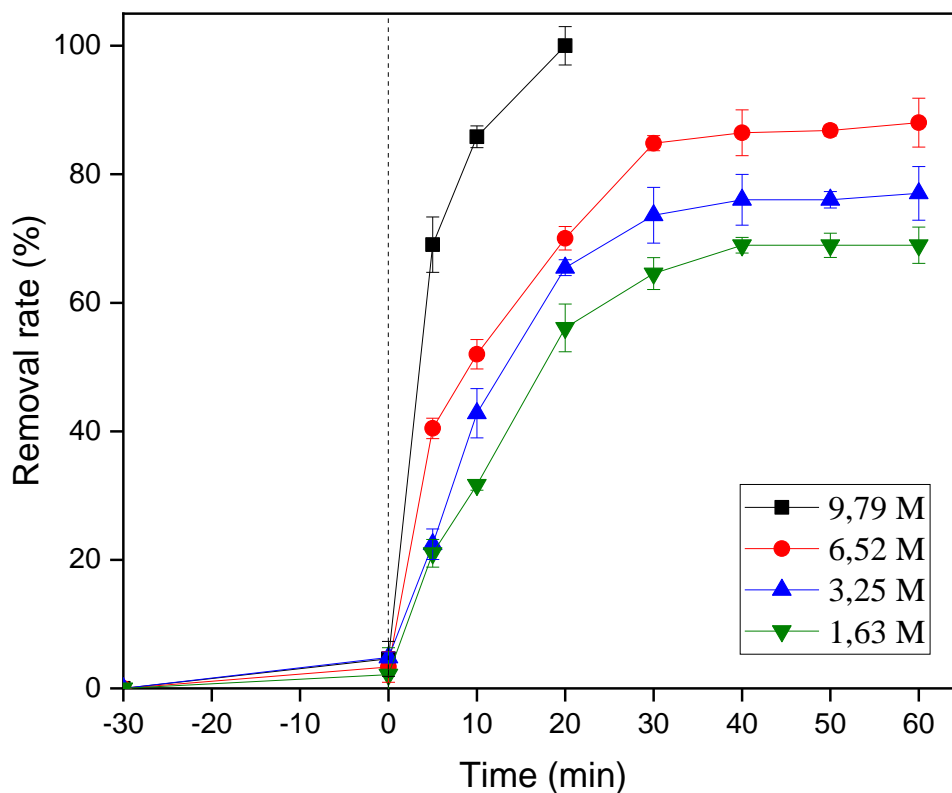


Figure 52: Hydrogen peroxide effect, pH=5, [α -Fe₂O₃]=0.5 g/l ,UV

3.2.4 The effect of catalyst dosage.

To optimize the Photo-Fenton reaction conditions, a series of experiments with different catalyst concentration has been realized. As displayed in figure 53, the optimum amount for a high removal rate of 100% was 0.5 g/L which improves an important efficiency compared to other photocatalysts[22]. At the lowest catalyst concentration of 0.2 g/L, efficiency has been decreased to 72% within 20 min after UV irradiation. Furthermore, the highest catalyst concentration of 1 g/L and 1.5 g/L attended only 60% and 57% removal rate, respectively. These results have been explained in similar previous work by the fact that a high amount of catalyst condenses and forms a barrier, which limits the photon absorption ability[23].

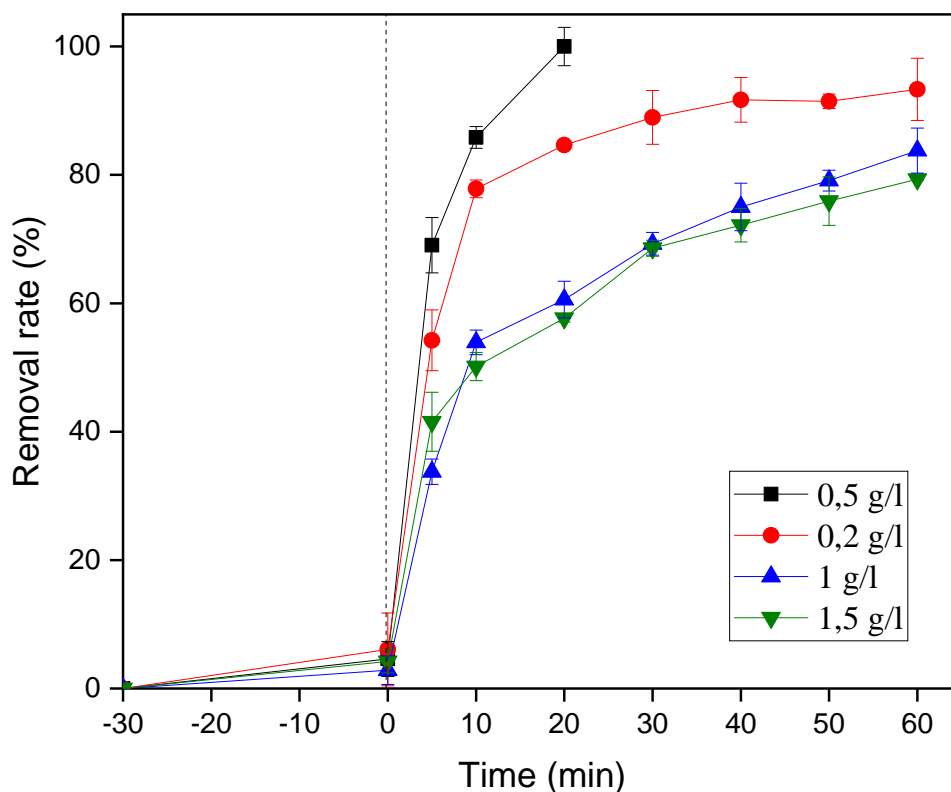
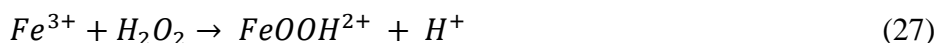


Figure 53: Effect of catalyst dosage, pH=5, [H₂O₂]=9.79 M, UV.

3.2.5 Scavenger study

The scavenger study has maintained with the commonly used quenchers, isopropanol, EDTA, and benzoquinone as a captive of OH[•], h⁺ and [•]O₂ radicals, respectively. The importance of scavengers reflected on uncovering the reaction process by reducing the reaction rate[24]. In the presence of benzoquinone and EDTA in the reaction process separately, the rate of photodegradation slightly declined from 100% to 91% and 72% respectively figure 54. While, with the addition of isopropanol, the removal rate reported a substantial decrease of 52% compared to the reaction process without scavengers. Hence, the result indicated that the O₂ has less significant influence on process, and both species h⁺, OH[•] were found to be the responsible radicals in difenoconazole photodegradation process. As reported in previous researches, the following equations describe the mechanism of the removal of Difenoconazole by the Photo-Fenton process[25].



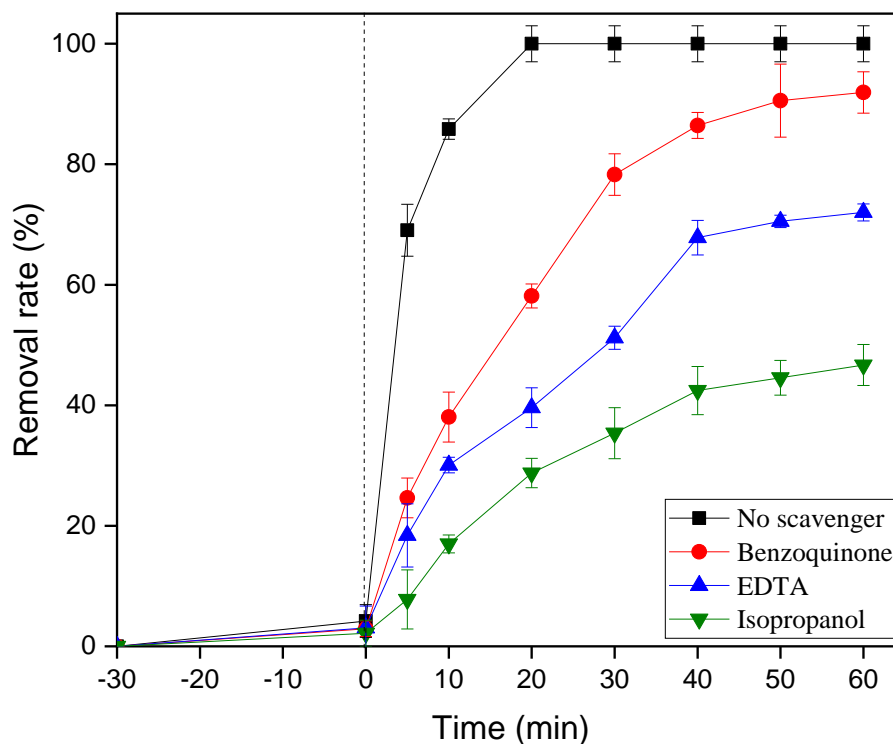


Figure 54: pH=5, $[H_2O_2] = 9.79$ M, $[\alpha\text{-}Fe_2O_3] = 0.5$ g/L, scavengers study

3.2.6 Reusability efficiency

The hematite $\alpha\text{-}Fe_2O_3$ was collected and was reused as a photocatalyst twice after the first use under the same photodegradation conditions. As shown in figure 55, the reusability test revealed that in every reuse cycle, the photocatalyst loses up its absorption capacity. The photodegradation rate of DFL displayed a slight decrease comparing to the first use, within 20 min, the removal rate attended 97% and 93% for the second and third use respectively. The result demonstrated that the synthesized photocatalyst has a good absorption ability several times even with the meager loss compared to other catalysts reuse efficiency, which demonstrated a significant loss of 30% of their efficiency[26]. The decrease of catalyst efficiency after several uses was explained by the loss of chemical stability of material induced by the photocorrosion phenomenon[27].

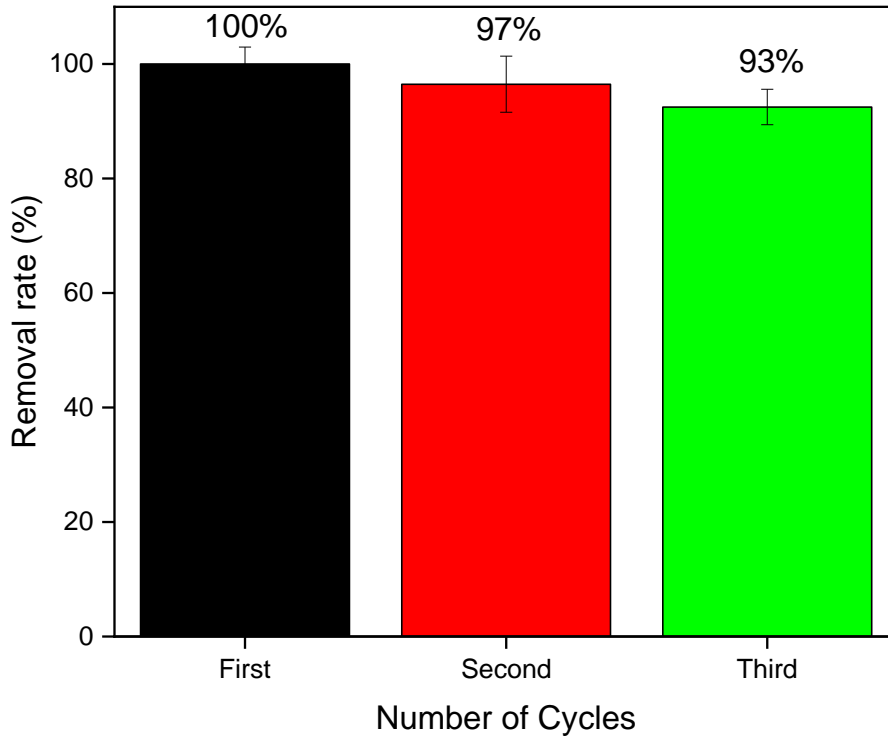


Figure 55: reusability of catalyst.

3.2.7 Kinetic analysis

To indicate the kinetic degradation details of DFL, the n -order of reaction, and constant rate k , the following equations (31) & (32) were used.

$$r = -\frac{dC}{dt} = k_{App}C \quad (31)$$

Where k_{App} is the degradation constant rate of the reaction,

$$\ln\left(\frac{C_0}{C}\right) = k_{App}t \quad (32)$$

Figure 56 indicates the plots of $\ln(C_0/C)$ versus time for the various degradation systems, UV Photolysis, UV/H₂O₂, UV/ α -Fe₂O₃, and UV/H₂O₂/ α -Fe₂O₃. As clearly described, the results represent straight lines. Hence, the photocatalytic degradation processes followed the pseudo-first-order kinetics. The heterogeneous photocatalysis as presented by the Photo-Fenton was revealed as most effective for DFL removal ($K_{app}= 0.124\text{min}^{-1}$).

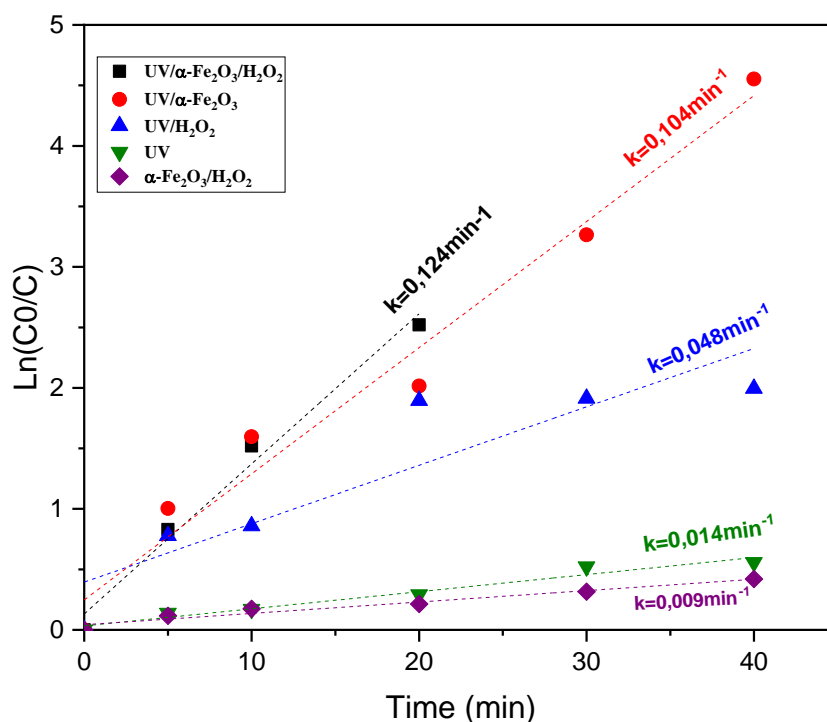


Figure 56: pH=5, [H₂O₂]=9.79 M, [α -Fe₂O₃]=0.5 g/L, kinetic study $\text{Ln}(C_0/C)=f(\text{time})$

3.2.8 Quantum yield

In order to quantifying the photocatalytic process efficiency, the quantum yield has been calculated using the ferrioxalate actinometer method. The potassium ferrioxalate $\text{K}_3[\text{Fe}(\text{C}_2\text{O}_4)_3]$ prepared following the method described by Goldstein and al;[28]. The prepared sample has been confirmed with the α -phenanthroline test that manifests a full red color. The experiments started with V_1 of ferrioxalate $6 \cdot 10^{-3}\text{M}$ irradiated at time t . Then V_2 of the same samples mixed with 2 ml of α -phenanthroline (0.1%), 1.5ml prepared acetate buffer solution (0.1N sulphuric acid, 0.1N sodium acetate), and mixtures adjusted to V_3 with deionized water. The final samples stirred for 30min in the dark. Absorbance readings were recorded with UV-Vis spectra at 510 nm. Hence, the conversion has been calculated.

Where N is the Avogadro constant, ABS_{510} is the absorbance of the mixture, l is the quartz cell surface, and k is the slope obtained from the Iron calibration curve using Hartchard & Parker method[29]. The value of quantum yield was estimated to be $\Phi = 0.17 \text{ mol. Einstein}^{-1}$.

3.3 Identification of photoproducts of Difenconazole photodegradation

The degradation of toxic organic compounds by oxidation processes may generate intermediates that may be sometimes be more toxic than the studied molecule itself. Therefore, the identification of the result degradation products is a necessary section in advanced oxidation

processes study. Firstly, figure 57 displays firstly HPLC chromatogram of difenoconazole substance detected at 2.020 min of analysis.

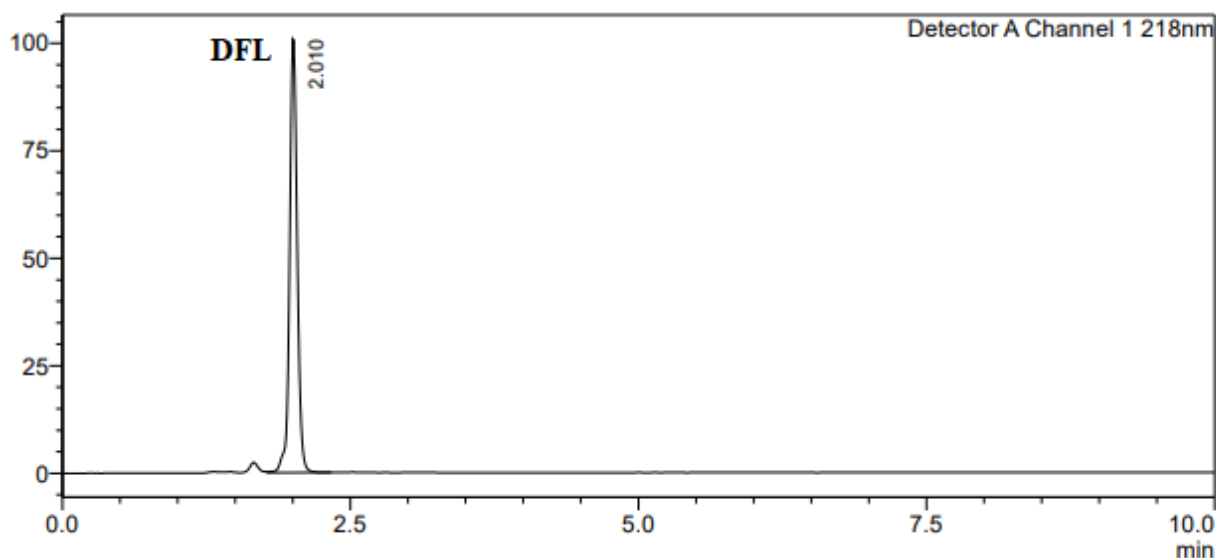


Figure 57: Representative HPLC chromatogram of Difenoconazole

Figure 58 illustrates the HPLC chromatogram of difenoconazole after 60 min of photo-Fenton process treatment. It is obvious from the obtained chromatogram that photocatalytic degradation of difenoconazole under photo-Fenton using hematite generates a series of five photoproducts appeared at different retention time before of the studied compound.

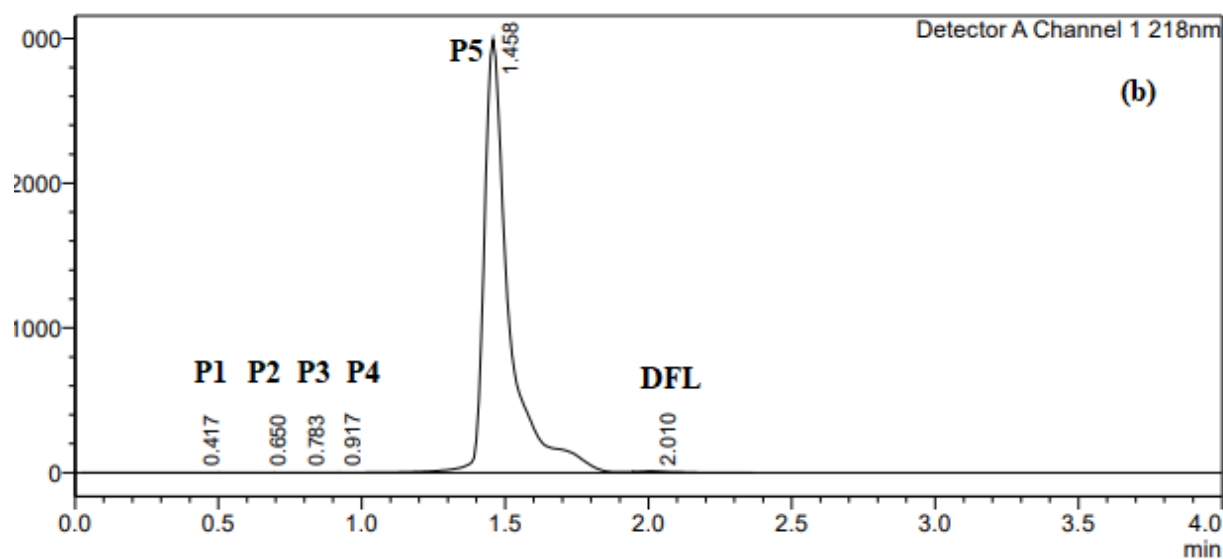


Figure 58: HPLC chromatogram of photoproductes generated from the photocatalytic degradation of difenoconazole

In order to determine precisely the oxidized products formed during the photocatalytic reaction, GC/MS analysis has been performed before and after Photo-Fenton. All photoproducts were formed during the photocatalytic process, as they were not detected in initial sample without treatment.

Under the chromatographic conditions, the parent product Difenoconazole was eluted at a retention time of 15.76 As displayed in Figure 59.

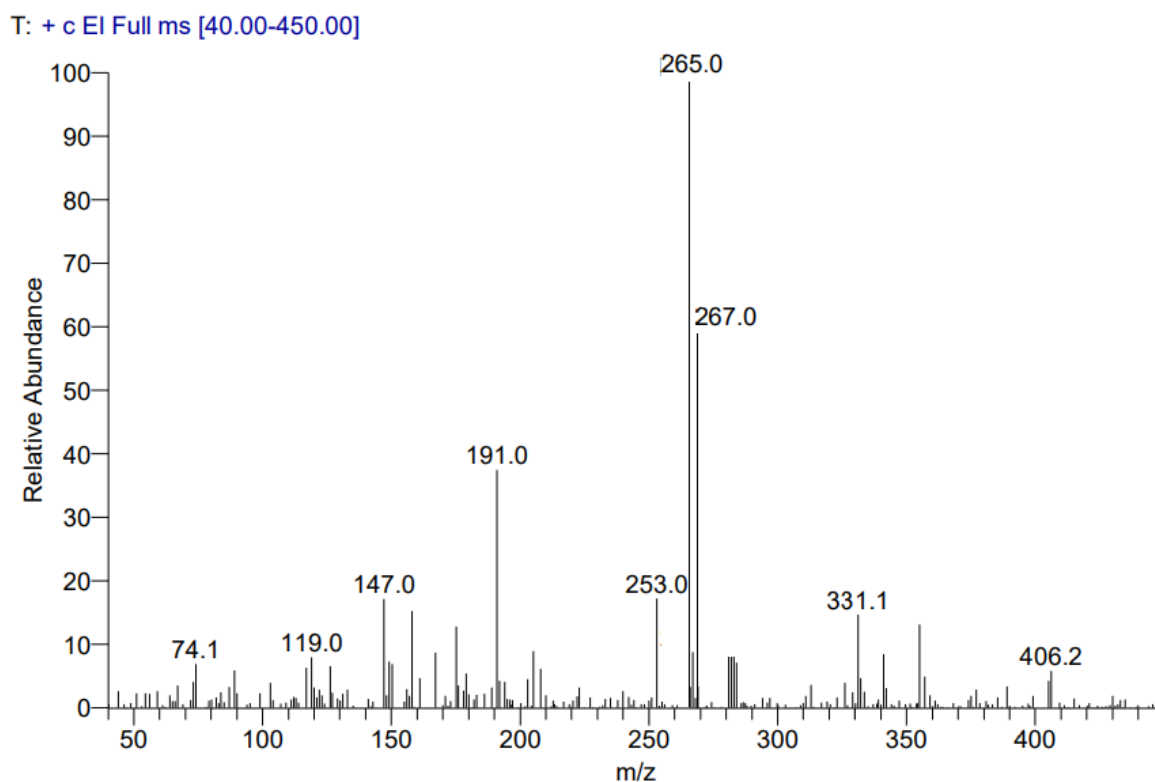


Figure 59: Mass spectrum of Difenoconazole at 15.76 min.

A Photoproducts were detected at different retention time as illustrated in figure 60. Although several positions of the identified photoproducts have been found. However, we believe that a dominant position would be the most involved. These products are likely to arise from the direct excitation of Difenoconazole in the presence of hydroxyl radicals.

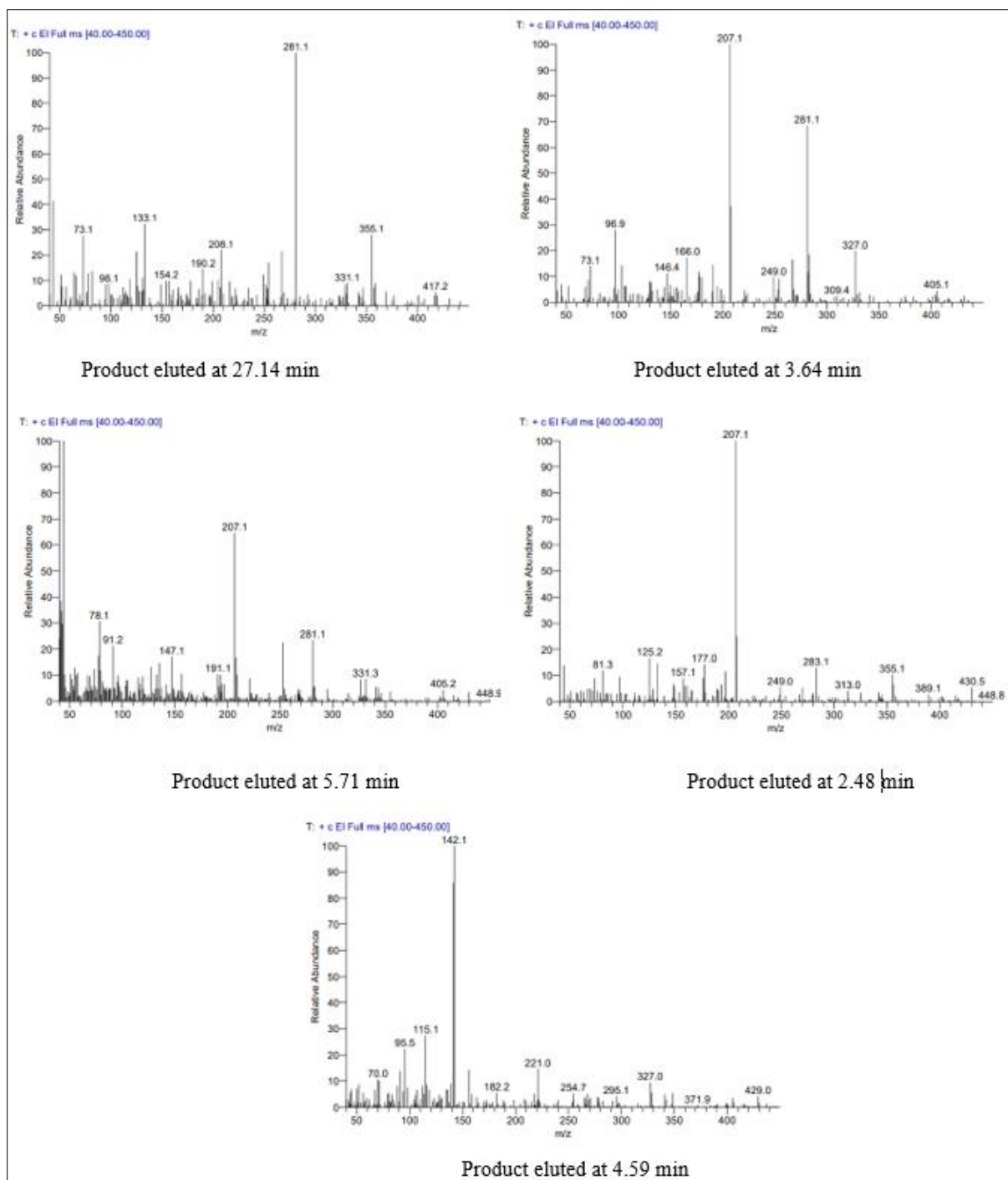
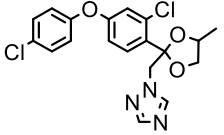
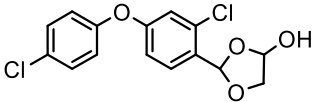
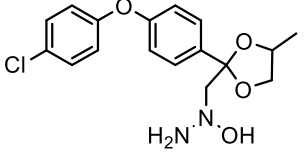
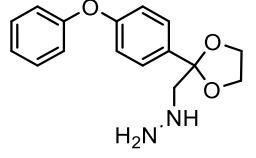
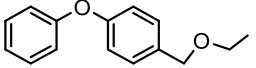
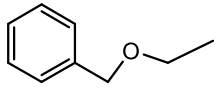


Figure 60: Mass spectrum of different identified photoproducts at various retention time.

It is important to note that other photoproducts, with larger molecular weights, were observed at long retention times. They probably correspond to dimeric forms of the parent product, Difenoconazole.

The degradation photoproducts of difenoconazole fungicide have been identified from their chromatographic profile according to the molecular ion and mass spectrometry fragmentation peaks. Table 10 describes in details of elemental composition of each photoproduct.

Table 10: The photoproducts generated from difenoconazole fungicide degradation obtained by GC/MS analysis

Compounds	Molecular structure	m/z	Molecular weight	Retention Time
DFL		405.06	406	15.76
P1		328.01	324	27.14
P2		352.10	350	3.64
P3		287.14	286	5.71
P4		224	228	2.48
P5		139.09	136	4.59

According to obtained metabolites, a proposed transformation pathway has been illustrated in figure 61. The schematic diagram indicates that the photodegradation process follows two possible pathways by either DFL were strongly oxidized by hydroxyl radicals leading to cleavage of C-N bond that freed the triazole group and yielded the first photoproduct P1 2-(2chloro-(4chlorophenoxy) phenyl)-4-methyl, 3-dioxolane. The photoproduct P2/P2' 1-((2-

(4-(4-chlorophenoxy)phenyl)-4-methyl-1,3-dioxolan-2-yl)methyl)-1-hydroxyhydrazine yielded via dechlorination and ring opening polymerization of triazole group. Moreover, as the reaction proceeds, the P1 generated dechlorinated intermediate P4 1-(ethoxymethyl)-4-phenoxybenzene. The photoproduct P2/P2' has again undergone dechlorination and generated the photoproduct P3. The photoproduct P5 was formed with the involvement of the homolytic scission of C-O bond that freed the benzene group from the compound.

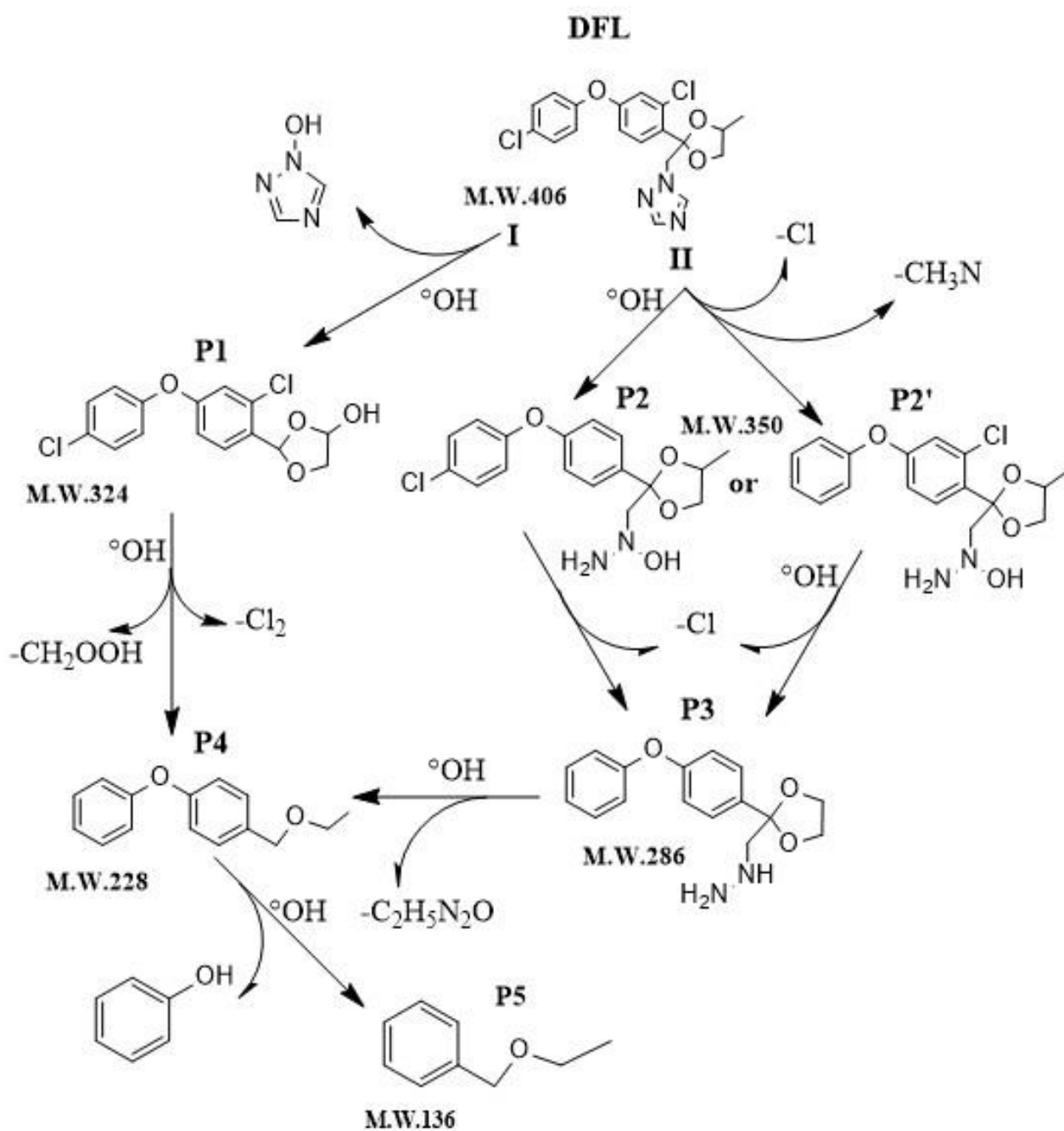


Figure 61: Proposed transformation pathway of difenoconazole under Photo-Fenton process treatment.

3.4 Mineralization study

The intermediates products are a result of all treatment processes. It could be toxic or highly toxic than the treated compound as revealed in previous research. Furthermore, figure 62 shows the mineralization of DFL under all investigated processes. At 60 min, it has been found that UV photolysis, UV/catalyst and UV/H₂O₂ mineralized 18.53%, 52.37% and 42.69% respectively. Otherwise, the combined process UV/ α -Fe₂O₃/H₂O₂ detected to be the highest TOC removal rate of 83.67%.

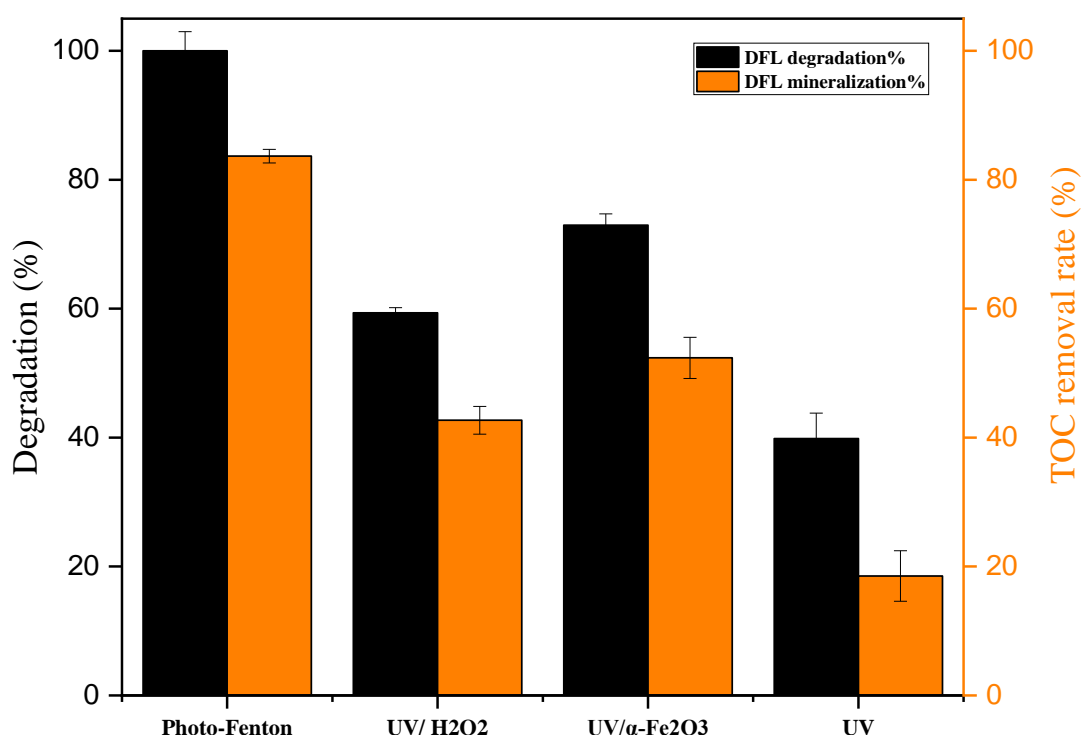


Figure 62: Degradation and TOC removal rate under different used systems.

4 Conclusion

Micropollutants were the aim of many research studies since the environmental and health contamination alert. Innovative technologies were established to deal with the wastewater treatment. Our study was focused on heterogeneous photocatalysis process. A hydrothermal process was used to synthesis α -Fe₂O₃, an abundant and low-cost naturel and synthesized metal oxide. The result sample has been characterized in detail with XRD, TEM, SEM, and RAMAN spectra to detect its physic-chemical material properties. The Photocatalytic activity of powder was tested on a widely used fungicide, Difenoconazole that targeted as a toxic compound in overdoses. A duplicated series of experiments under different systems have been realized as a way to investigate the practical process for photodegradation of pollutant. The Photo-Fenton-

like process has been proven a high efficiency among all tested methods with a high removal rate detection in only 20 min of treatment. Hence, the conditions of different parameters of Photo-Fenton reaction were optimized. The hydroxyl radicals are found to be responsible for the photodegradation reaction as a result of reaction scavenger study.

5 References

- [1] A. Marican and E. F. Durán-Lara, “A review on pesticide removal through different processes,” *Environmental Science and Pollution Research*, vol. 25, no. 3, pp. 2051–2064, 2018, doi: 10.1007/s11356-017-0796-2.
- [2] M. H. Rasoulifard, M. Akrami, and M. R. Eskandarian, “Degradation of organophosphorus pesticide diazinon using activated persulfate: Optimization of operational parameters and comparative study by Taguchi’s method,” *J Taiwan Inst Chem Eng*, vol. 57, pp. 77–90, 2015, doi: 10.1016/j.jtice.2015.05.014.
- [3] M. A. Camacho-González, M. Quezada-Cruz, G. I. Cerón-Montes, M. F. Ramírez-Ayala, L. E. Hernández-Cruz, and A. Garrido-Hernández, “Synthesis and characterization of magnetic zinc-copper ferrites: Antibacterial activity, photodegradation study and heavy metals removal evaluation,” *Materials Chemistry and Physics*, vol. 236, no. June, 2019, doi: 10.1016/j.matchemphys.2019.121808.
- [4] M. Abbas *et al.*, “*Vibrio fischeri* bioluminescence inhibition assay for ecotoxicity assessment: A review,” *Science of the Total Environment*, vol. 626, pp. 1295–1309, 2018, doi: 10.1016/j.scitotenv.2018.01.066.
- [5] M. Iqbal, “*Vicia faba* bioassay for environmental toxicity monitoring: A review,” *Chemosphere*, vol. 144, pp. 785–802, 2016, doi: 10.1016/j.chemosphere.2015.09.048.
- [6] L. Chu, J. Wang, J. Dong, H. Liu, and X. Sun, “Treatment of coking wastewater by an advanced Fenton oxidation process using iron powder and hydrogen peroxide,” *Chemosphere*, vol. 86, no. 4, pp. 409–414, 2012, doi: 10.1016/j.chemosphere.2011.09.007.
- [7] I. Carra, J. A. Sánchez Pérez, S. Malato, O. Autin, B. Jefferson, and P. Jarvis, “Performance of different advanced oxidation processes for tertiary wastewater treatment to remove the pesticide acetamiprid,” *Journal of Chemical Technology and Biotechnology*, vol. 91, no. 1, pp. 72–81, 2016, doi: 10.1002/jctb.4577.
- [8] T. Mandal, S. Maity, D. Dasgupta, and S. Datta, “Advanced oxidation process and biotreatment: Their roles in combined industrial wastewater treatment,” *Desalination*, vol. 250, no. 1, pp. 87–94, 2010, doi: 10.1016/j.desal.2009.04.012.
- [9] B. Bethi, S. H. Sonawane, B. A. Bhanvase, and S. P. Gumfekar, “Nanomaterials-based advanced oxidation processes for wastewater treatment: A review,” *Chemical Engineering and Processing: Process Intensification*, vol. 109, pp. 178–189, 2016, doi: 10.1016/j.cep.2016.08.016.
- [10] K. K. Das, S. Patnaik, B. Nanda, and A. C. Pradhan, “ZnFe₂O₄-Decorated Mesoporous Al₂O₃ Modified MCM-41 : A Solar-Light-Active Photocatalyst for the Effective Removal of Phenol and Cr (VI) from Water,” pp. 1806–1819, 2019, doi: 10.1002/slct.201803209.
- [11] M. J. Lima, C. G. Silva, A. M. T. Silva, J. C. B. Lopes, M. M. Dias, and J. L. Faria, “Homogeneous and heterogeneous photo-Fenton degradation of antibiotics using an

- innovative static mixer photoreactor,” *Chemical Engineering Journal*, vol. 310, pp. 342–351, 2017, doi: 10.1016/j.cej.2016.04.032.
- [12] R. Arshad *et al.*, “Degradation product distribution of Reactive Red-147 dye treated by UV/H₂O₂/TiO₂ advanced oxidation process,” *Journal of Materials Research and Technology*, vol. 9, no. 3, pp. 3168–3178, 2020, doi: 10.1016/j.jmrt.2020.01.062.
- [13] I. Bibi *et al.*, “Green synthesis of iron oxide nanoparticles using pomegranate seeds extract and photocatalytic activity evaluation for the degradation of textile dye,” *Journal of Materials Research and Technology*, vol. 8, no. 6, pp. 6115–6124, 2019, doi: 10.1016/j.jmrt.2019.10.006.
- [14] G. K. Pradhan and K. M. Parida, “Fabrication, Growth Mechanism, and Characterization of alpha-Fe₂O₃ Nanorods,” vol. 3, no. 2, pp. 317–323, 2011, doi: <https://doi.org/10.1021/am100944b>.
- [15] S. C. K. G. ; S. B. A. H. Bagheri, “Generation of Hematite Nanoparticles via Sol-Gel Method,” *Research Journal of Chemical Sciences*, vol. 3, no. 7, pp. 62–68, 2013.
- [16] J. Tauc and A. Menth, “States in the gap,” *Journal of Non-Crystalline Solids*, vol. 8–10, no. C, pp. 569–585, 1972, doi: 10.1016/0022-3093(72)90194-9.
- [17] S. Piccinin, “The band structure and optical absorption of hematite (α -Fe₂O₃): a first-principles GW-BSE study,” *Phys. Chem. Chem. Phys.*, vol. 21, no. 6, pp. 2957–2967, 2019, doi: 10.1039/b000000x.
- [18] X. M. Liu, S. Y. Fu, H. M. Xiao, and C. J. Huang, “Preparation and characterization of shuttle-like α -Fe₂O₃ nanoparticles by supermolecular template,” *Journal of Solid State Chemistry*, vol. 178, no. 9, pp. 2798–2803, 2005, doi: 10.1016/j.jssc.2005.06.018.
- [19] B. Zhao, G. Mele, I. Pio, J. Li, L. Palmisano, and G. Vasapollo, “Degradation of 4-nitrophenol (4-NP) using Fe-TiO₂ as a heterogeneous photo-Fenton catalyst,” *Journal of Hazardous Materials*, vol. 176, no. 1–3, pp. 569–574, 2010, doi: 10.1016/j.jhazmat.2009.11.066.
- [20] E. E. Ebrahiem, M. N. Al-Maghrabi, and A. R. Mobarki, “Removal of organic pollutants from industrial wastewater by applying photo-Fenton oxidation technology,” *Arabian Journal of Chemistry*, vol. 10, pp. S1674–S1679, 2017, doi: 10.1016/j.arabjc.2013.06.012.
- [21] A. Tabasum *et al.*, “Uv-accelerated photocatalytic degradation of pesticide over magnetite and cobalt ferrite decorated graphene oxide composite,” *Plants*, vol. 10, no. 1, pp. 1–18, 2021, doi: 10.3390/plants10010006.
- [22] R. Mohite and A. Garg, “Performance of Supported Copper Catalysts for Oxidative Degradation of Phenolics in Aqueous Medium: Optimization of Reaction Conditions, Kinetics, Catalyst Stability, Characterization, and Reusability,” *Industrial and Engineering Chemistry Research*, vol. 59, no. 29, pp. 12986–12998, 2020, doi: 10.1021/acs.iecr.0c02211.
- [23] F. Torrades and J. García-Montaña, “Using central composite experimental design to optimize the degradation of real dye wastewater by Fenton and photo-Fenton reactions,”

- Dyes and Pigments*, vol. 100, no. 1, pp. 184–189, 2014, doi: 10.1016/j.dyepig.2013.09.004.
- [24] P. P. Marcinowski, J. P. Bogacki, and J. H. Naumczyk, “Cosmetic wastewater treatment using the Fenton, photo-Fenton and H₂O₂/UV processes,” *Journal of Environmental Science and Health - Part A Toxic/Hazardous Substances and Environmental Engineering*, vol. 49, no. 13, pp. 1531–1541, 2014, doi: 10.1080/10934529.2014.938530.
- [25] B. Weng, M. Y. Qi, C. Han, Z. R. Tang, and Y. J. Xu, “Photocorrosion Inhibition of Semiconductor-Based Photocatalysts: Basic Principle, Current Development, and Future Perspective,” *ACS Catalysis*, vol. 9, no. 5, pp. 4642–4687, 2019, doi: 10.1021/acscatal.9b00313.
- [26] A. Delavaran Shiraz, A. Takdastan, and S. M. Borghei, “Photo-Fenton like degradation of catechol using persulfate activated by UV and ferrous ions: Influencing operational parameters and feasibility studies,” *Journal of Molecular Liquids*, vol. 249, pp. 463–469, 2018, doi: 10.1016/j.molliq.2017.11.045.
- [27] S. Goldstein and J. Rabani, “The ferrioxalate and iodide-iodate actinometers in the UV region,” *Journal of Photochemistry and Photobiology A: Chemistry*, vol. 193, no. 1, pp. 50–55, 2008, doi: 10.1016/j.jphotochem.2007.06.006.
- [28] C. G. Hatchard and C. A. Parker, “A new sensitive chemical actinometer - II. Potassium ferrioxalate as a standard chemical actinometer,” *Proceedings of the Royal Society of London. Series A. Mathematical and Physical Sciences*, vol. 235, no. 1203, pp. 518–536, 1956, doi: 10.1098/rspa.1956.0102.

CHAPTER V: Photochemical and sonochemical
removal of Acibenzolar-S-Methyl fungicide:
transformation mechanism pathway.

1 Introduction

Agriculture sector is one of the pillars that plays a crucial role in human being life, it considered a powerful motor of economies of developing and industrialized countries [1]. However, since many years, this sector dealt with phytopathology issues, which affect the food production industry[2]. A million of people around the whole world are suffering from famine crisis, a severe food insecurity causing high level of mortality[3]. Hence, a series of chemical compounds have been created to cope with a large variety of plant diseases [4]. Those products are classified according to their target pests. Herbicides, nematicides, insecticide and fungicides contribute to increasing agricultural yield. Certainly, pesticides were a brilliant creativity to ensure the agriculture productivity for world food security.

Nevertheless, the mismanagement of these chemicals generates a range of problems that are not taken into account, a severe contamination of food[5], soil[6], human health[7] and environment[8]. As is popularly known, the dose make poison which was the case of the excessive use of pesticides[9]. It has been revealed that agrochemicals affect also the non-target organisms and it has been detected in animals and human blood and body tissues, it was confirmed also that those chemicals are associated with some types of cancer disease[10-12]. The pesticides alter the pedological characteristics of soil to pollution stage[13]. Hence, the surface and groundwater sources confronted a serious threat of contamination by soil drainage process[14]. In addition, the chemicals found their way to wastewater effluents from the agro-food-industries[15].

Within the framework of sustainable water resources management strategies, the implementation of wastewater treatment plants (WWTP) was an evolutionary step to cope with water pollution[16]. Firstly, those WWTP worked with simple biological and chemical processes. Subsequently, with the detection of new generation of pollutants that are more persistent and harder to remove with the existing conventional methods, the world of research has known a technological revolution that led to the appearance of new approaches[17]. Advanced oxidation processes (AOPs) are defined as wide range of treatment methods, simple or combined processes, they are all based on the hydroxyl radicals ($\bullet\text{OH}$) generation[18]. AOPs are promising, effective technologies, photochemical, electrochemical, sonochemical and Fenton process have proven high removal efficiency of organic pollutants with non-selectivity[19]. Having capacity to generate the strongest oxidant ($\bullet\text{OH}$), AOPs have attracted the researcher's attention that end up with an important publication in this field [20-22].

Among those processes, the ultrasound irradiation (US) that is recognized as clean and low-power process, the US has the capacity of producing hydroxyl radicals ($\bullet\text{OH}$) with the active cavitation bubbles[23]. The sono-Fenton process is one of the integrated hybrid oxidation processes, it has been revealed that the process accelerates the oxidant production which leads to the increase in the pollutant removal rate[24].

In the present work, we explore the performance of Fenton-related processes for removal of Acibenzolar-S-methyl. The degradation of ASM was investigated under various treatment processes including sonolysis, photolysis, Fenton ($\text{Fe}^{2+}/\text{H}_2\text{O}_2$), photo-Fenton ($\text{UV}/\text{Fe}^{2+}/\text{H}_2\text{O}_2$), and sono-Fenton system ($\text{US}/\text{Fe}^{2+}/\text{H}_2\text{O}_2$). Afterwards, the focus of the study was oriented to comparison between photo-Fenton and sono-Fenton processes. In addition, the main factors influencing both processes were carried out (pH, oxidant concentration, and Ferrous ions dosage). ASM's photochemical and sonocatalytic degradation was monitored using high-performance liquid chromatography (HPLC).

2 Materials & methods

2.1 Experimental Design

All degradation processes of ASM consisted of laboratory scale. Figure 1 illustrates the photochemical and sonochemical reactors. The photo-Fenton method was carried out with a UV Philips lamp 254 nm (8 W) fixed at the top of a rectangular enclosure. Ultrasonic experiments were performed with (Sonic & Materials, Inc., 750 VCX) sonicator at 20 kHz of the frequency with a titanium alloy probe with a tip diameter of 13 mm and maximum power output of 125 W. At room temperature, for both processes, a quartz reactor was filled with 100 mL of fungicide ASM solution stock (10 mg/L), the pH of the reaction was adjusted by sulfuric acid and sodium hydroxide, an amount of 10 mmol/L ferrous sulphate and 3.25 M hydrogen peroxide were added for the Fenton reaction.

2.2 Analytical Methods

All experiments were carried out at room temperature. Aliquots of 1 mL were withdrawn at various time intervals and filtered with a 0.2 μm -size-pore-membrane. The obtained samples were analyzed utilising high-performance liquid chromatography SHIMADZU with a C18 Colum (150 mm \times 4.6 mm, 5 μm , Phenomenex). 0.1% Formic acid buffer in water and Methanol were used as mobile phases (v:v/80:20) with an isocratic elution type. The flow rate was adjusted at 1 mL/min and 254 nm as a UV wavelength detector. The total run time for the

analysis of ASM samples was 4 min. Therefore, the samples were analyzed twice. All collected data were treated by Origin Lab software.

3 Results & Discussion

3.1 Spectral characteristic of ASM

The UV-Vis spectra of Acibenzolar-S-Methyl (pH= 4.8, C=6mg/L) is shown in figure 63 to highlight the overlap of its absorption with the UV-C emission spectrum. The spectrum of ASM shows one absorption peak defined as $\lambda_{\max}=257$ nm ($\epsilon=4503$ L.mol⁻¹.cm⁻¹). In this figure, it can be seen that there is a significant overlap between emission spectrum of UV-C and the absorption spectrum of ASM. According to the European Directive 94/37/EC, the phototransformation of micropollutants must be taken into account once the molar absorption coefficient exceeds 10 L.mol⁻¹.cm⁻¹ at $\lambda=290$ nm. Hence, in our case the ASM molar extinction coefficient at $\lambda=290$ nm is $\epsilon=1608$ L.mol⁻¹.cm⁻¹ which confirm that our molecule has the ability to be degraded under irradiation and must be a subject of a photochemical investigation.

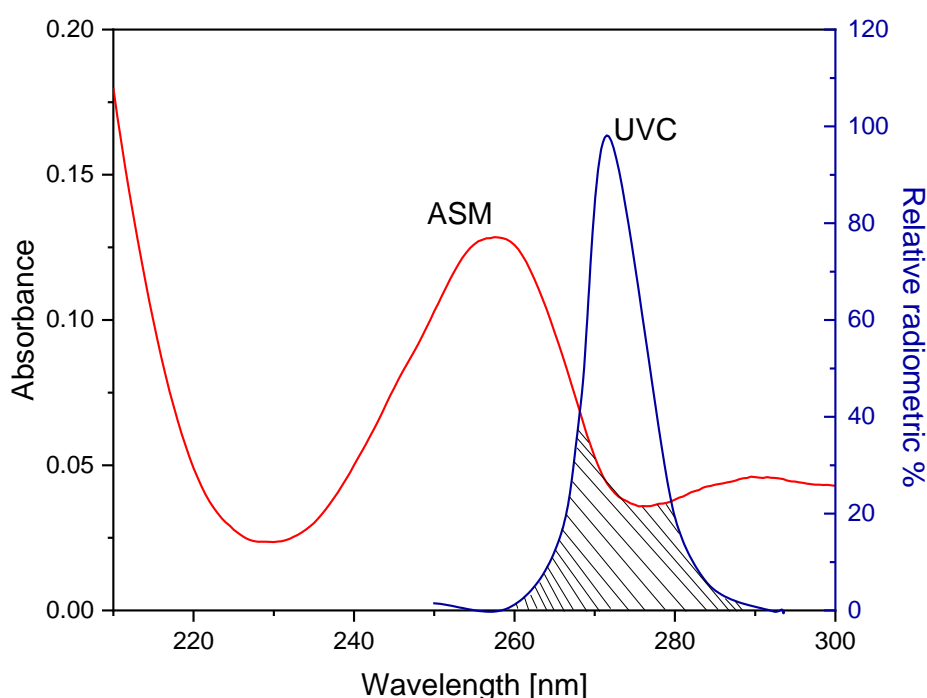


Figure 63: Intersection between ASM UV-Vis spectra and UV-C emission spectrum

3.2 Degradation of ASM by various processes

In order to investigate the most efficient degradation process of ASM, a preliminary degradation tests under various treatment processes including ultrasound irradiation, photolysis, Fenton ($\text{Fe}^{2+}/\text{H}_2\text{O}_2$) and Photo-Fenton ($\text{UV}/\text{Fe}^{2+}/\text{H}_2\text{O}_2$), and Sono-Fenton ($\text{US}/\text{Fe}^{2+}/\text{H}_2\text{O}_2$) were conducted Figure 64. The sonolysis and photolysis treatments showed no significant ASM degradation, after 60 min of reaction the both treatments reached 25% and 67% removal rate respectively. The Fenton in the dark, were achieved to quantify the oxidative potential of process in absence of sonocatalytic or photocatalytic activities, the treatment attained 72% of ASM removal rate after 60 min. As it was proven in many previous researches, Fenton oxidation system attributed also to the hydroxyl radicals generation[25]. Moreover, under Photo-Fenton and sono-Fenton processes, ASM degradation was powerfully accelerated and reached 100% within 30 min of treatment for photo-Fenton and 20 min for sono-Fenton. The sono-Fenton was assigned to be more effective than other tested processes. The enhancement removal rate explained by formation of extra hydroxyl radicals from ultrasound irradiation source.

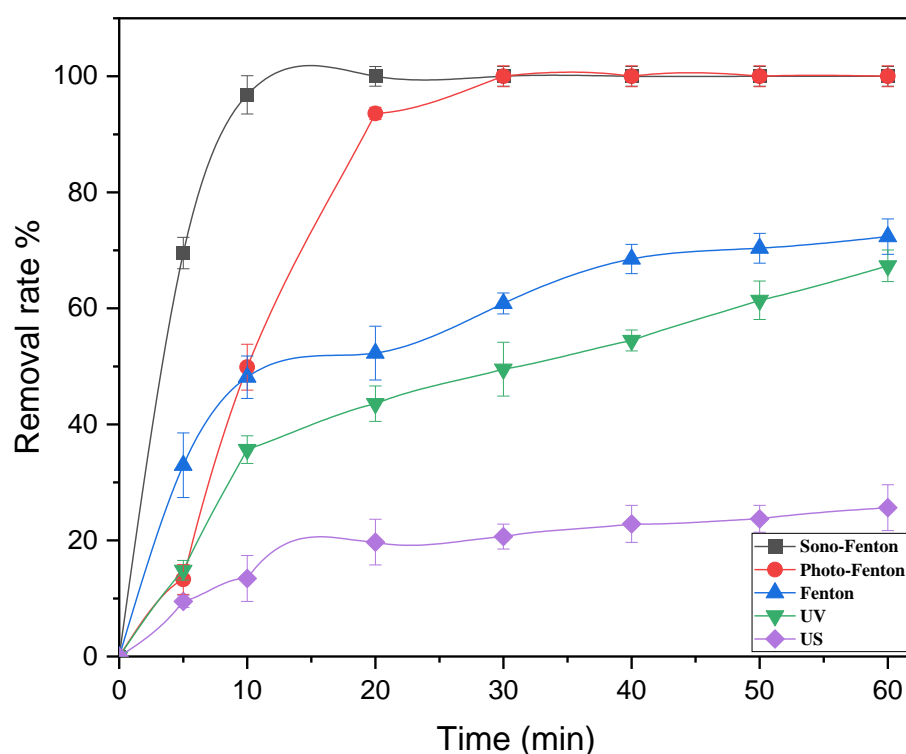


Figure 64: ASM removal under different processes Photolysis, Sonolysis, Fenton (pH= 3.0, $[\text{H}_2\text{O}_2]=3.25$ M, $[\text{Fe}^{2+}]=10$ mmol/L), Photo-Fenton & Sono-Fenton.

3.3 pH effect

The initial solution pH is a crucial parameter influencing the Fenton-based reaction. Hence, in order to detect the optimum pH medium for ASM degradation methods, a series of experiments of Photo-Fenton and Sono-Fenton processes were tested with various initial solution pH 3, 7 and 10 which constitute extreme values for catalytic degradation. Figure 65 describes the behaviour of reaction in acidic, neutral, and alkaline medium for both processes. The results clearly indicates that both treatments were reached the high effectiveness in acidic medium. However, the photo-Fenton process also occurs in neutral and alkaline medium even with significant decrease of efficiency the removal rate was decreased to 51% and 14%, respectively which was contrarily to Sono-Fenton process with no reaction in alkaline medium. The decrease of efficiency and the total inhibition of reaction in alkaline medium was explained by the instability of ferrous ions and hydrogen peroxide oxidant that led to the loss of activity and its decomposition to oxygen and water in those pH mediums, the decrease of hydroxyl radicals generation[26]. While, the acidic medium assigned to be the reasonable choice as it had no significant effect on the ASM degradation that reached the maximum value.

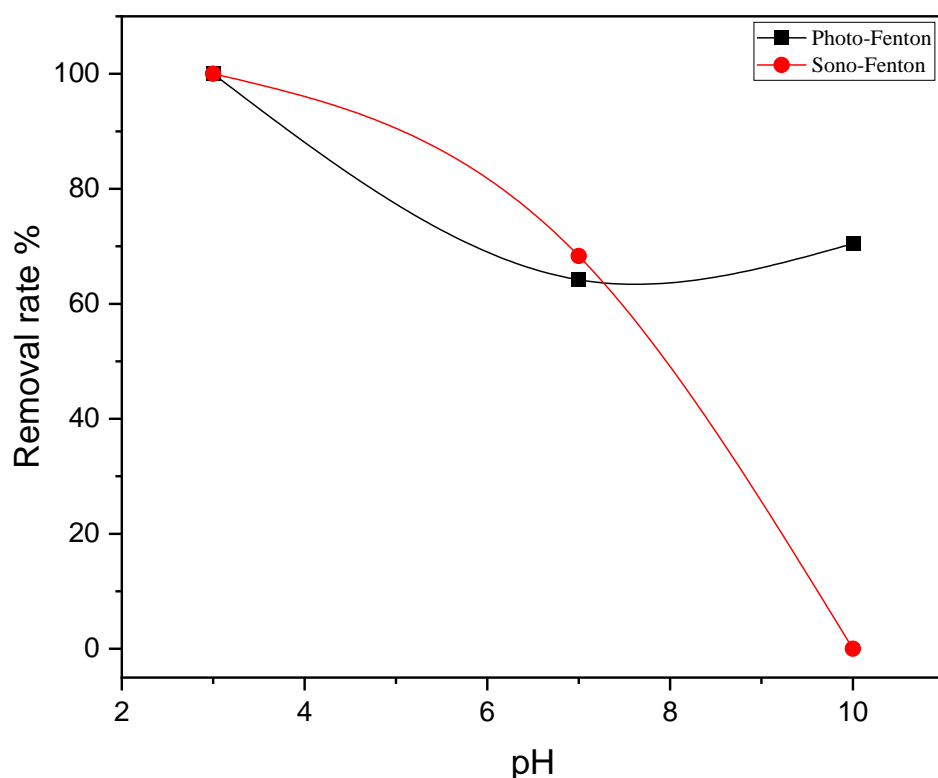


Figure 65: Effect of initial solution pH on Photo-Fenton and Sono-Fenton processes,
[H₂O₂]=3.25 M, [Fe²⁺]= 10 mmol/L.

3.4 Effect of hydrogen peroxide concentration

The effect of hydrogen peroxide concentration was an important step in degradation study of ASM via sono-Fenton process. To obtain the optimum amount, the investigation was carried out with various H₂O₂ concentrations Figure 66. The series of experiments were conducted in acidic medium pH=3.0 at room temperature. The strongest effect of ASM removal was recorded with 3.25 M of hydrogen peroxide concentration for both methods. Whereas, in low dose of 1.63M, a high decrease was observed, the degradation rate reached 5% and 39% for Photo-Fenton and Sono-Fenton treatment respectively. It has been proven that the oxidant agent increases the degradation of pollutant to achieve the maximum degradation level [27]. In contrast, the increase of hydrogen peroxide concentration to 6.52 M and 9.76 M slowed down the ASM degradation reaction. It was explained that the oxidizing agent at exceeded amount for some molecules behave as scavenger for hydroxyl radicals and plays an important role in auto-decomposition to oxygen and water molecules [28].

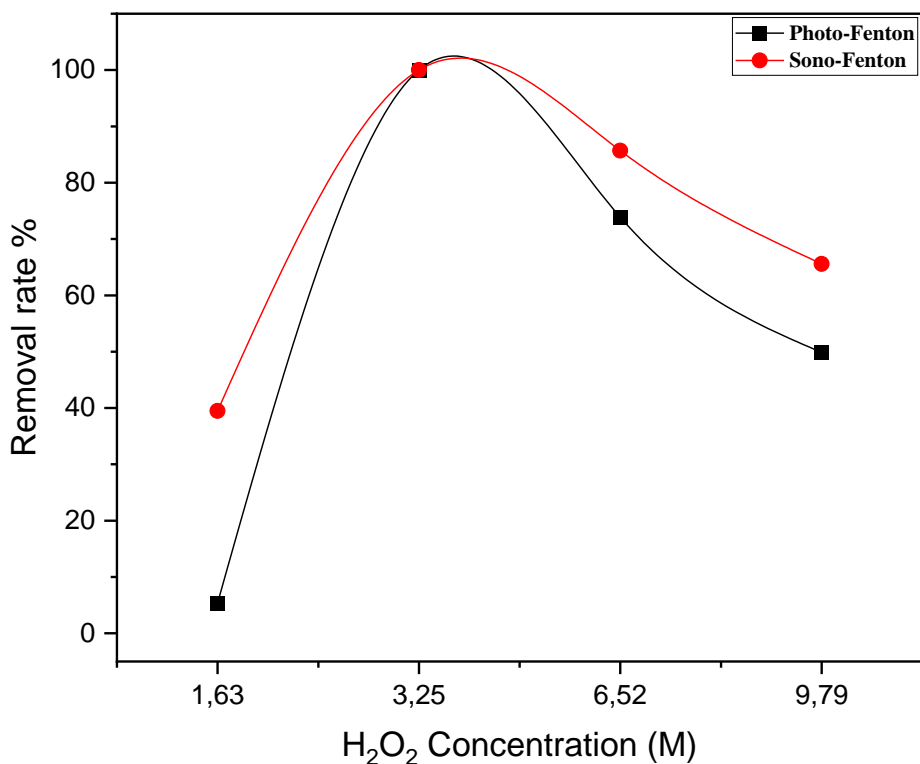


Figure 66: Hydrogen peroxide concentration effect, pH= 3.0, [Fe²⁺]= 10 mmol/L.

3.5 Ferrous ions concentration effect

Ferrous ions and its interaction with oxidant are the basis of Fenton-based reaction. In order to investigate the ideal Fe²⁺ concentration for ASM oxidation a series of experiment were carried out at pH=3.0 and 3.25M hydrogen peroxide concentration Figure 67. As illustrated, the concentration of ferrous ions was varied from 3 mmol/L and 14mmol/L. It was observed that with the lowest concentration, the photo-Fenton occurs after 20min of reaction, and both processes have revealed a significant decrease of degradation performance of ASM. In addition, a meaningful enhancement of ASM removal has been observed for photo-Fenton process at 7mmol/L and 14mmol/L iron concentration achieving the complete degradation of ASM, and a slight decrease of reaction rate was attained at 10 mmol/L. However, for Sono-Fenton, the complete degradation was observed at 10 mmol/L with significant decrease of removal rate of reaction at low and high doses of ferrous ions. In literature, it is revealed that high concentration of ferrous ions boosted the hydroxyl radicals •OH production [29]. However, the rise of ferrous ions dose affected negatively the reaction and decreased the degradation rate that achieved 41% after 20 min. The presence of iron in excess doses changed its behaviour from catalyst to inhibitor of the process reaction via auto-scavenging of the produced hydroxyl radicals [30-31].

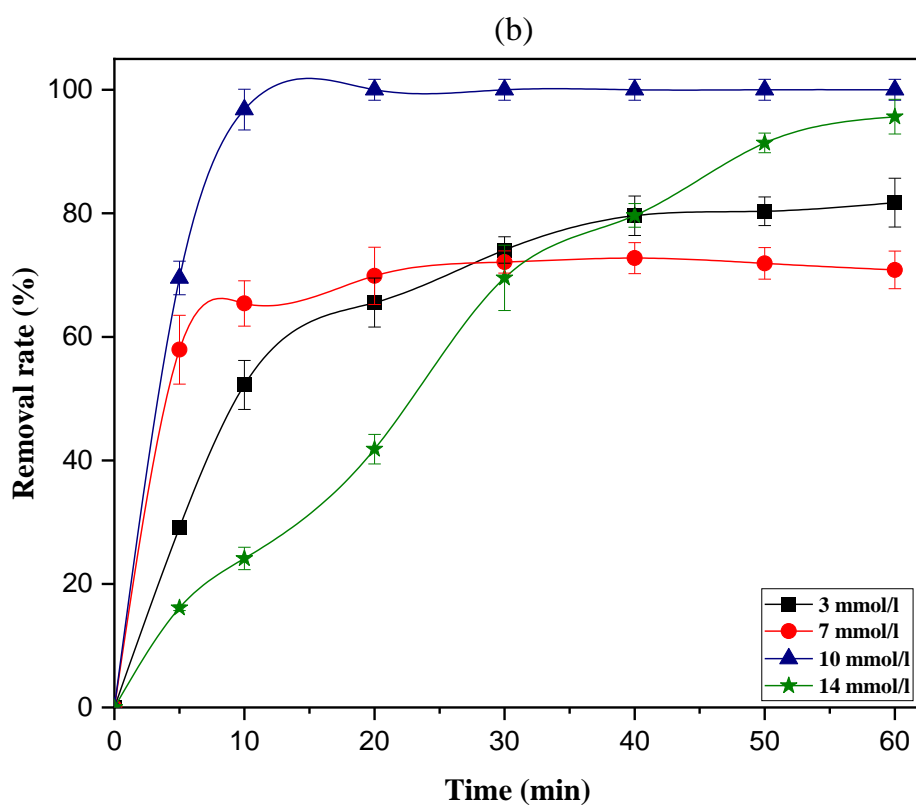
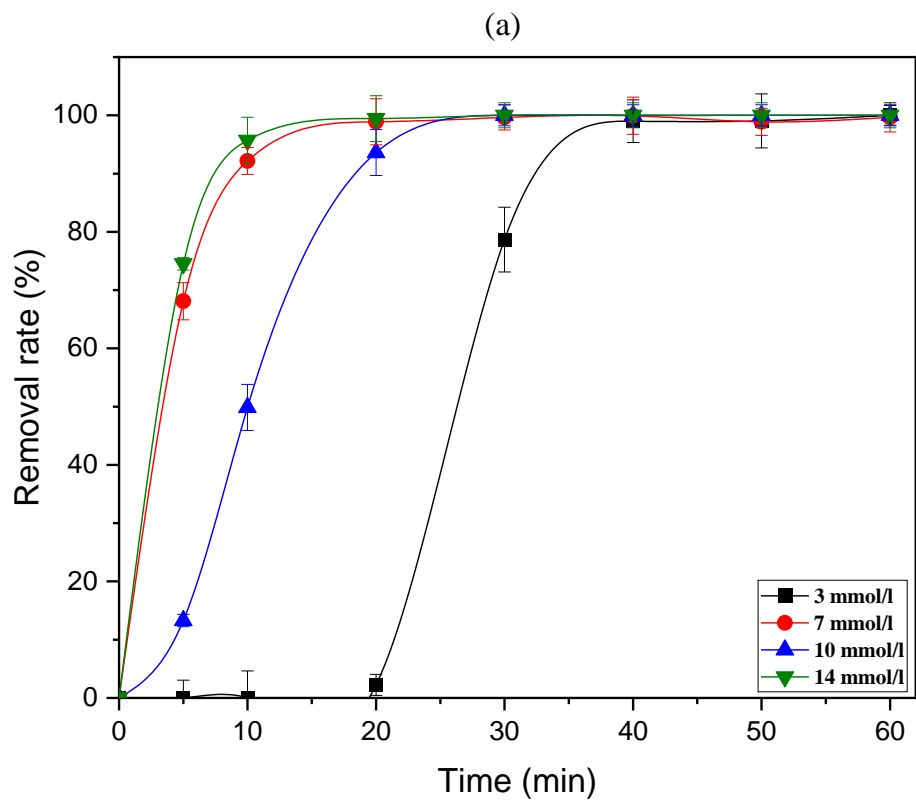


Figure 67: Ferrous ions concentration effect on pH= 3.0, [H₂O₂]=3.25 M. (a) Photo-Fenton process (b) Sono-Fenton.

3.6 Kinetic analysis

To demonstrate the kinetic reaction details including n-order, and constant rate k, figure 68 displays the $\ln(C_0/C)$ versus time plot of all used treatments following the equations bellow:

$$r = -\frac{dC}{dt} = K_{App}C \quad (2)$$

Where K_{App} is the degradation constant rate of the reaction.

$$\ln\left(\frac{C_0}{C}\right) = K_{App}t \quad (3)$$

Photolysis, sonolysis, Fenton, photo-Fenton, and Sono-Fenton process represent straight lines. Therefore, it confirms that all degradation processes followed the pseudo-First-order kinetics. The photo-Fenton and sono-Fenton revealed as most effective treatments for ASM degradation with $K_{App}=0.184 \text{ min}^{-1}$ and 0.481 min^{-1} respectively.

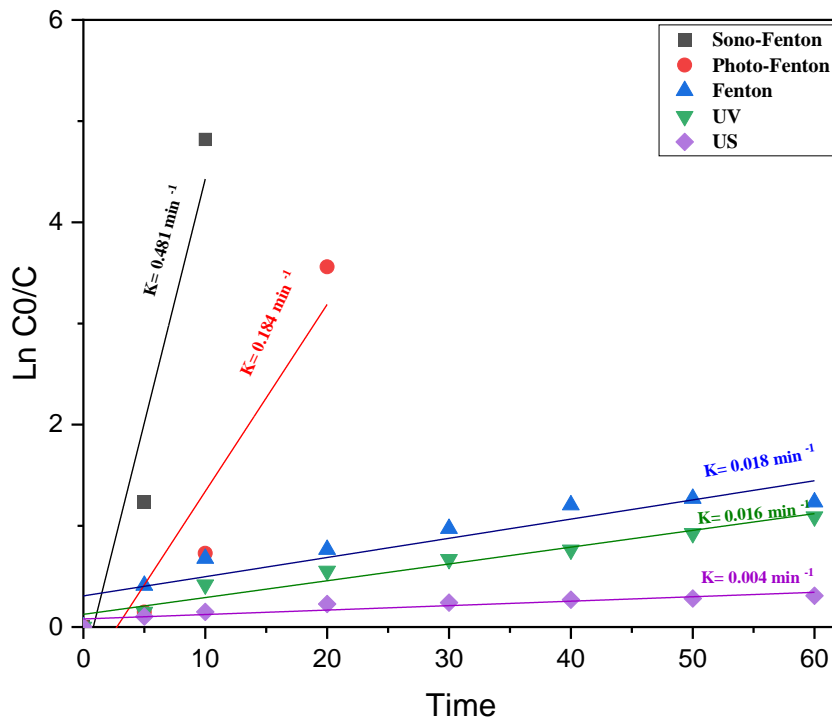


Figure 68: kinetic study $\ln(C_0/C)= f(\text{time})$

3.7 Proposed mechanism of ASM degradation by Sono-Fenton reaction

As mentioned before, the oxidation treatment should crucially be followed by a monitoring and identification of metabolites to more understanding, and having clear idea about their chemical composition and their toxicity. After 60 min of sono-Fenton treatment, the samples were

extracted with dichloromethane and the metabolites were detected using gas chromatography coupled with mass spectrometry (GC/MS). Figure 69 displays the mass spectrum of Acibenzolar-S-Methyl detected at 9.87 min.

T: + c EI Full ms [40.00-450.00]

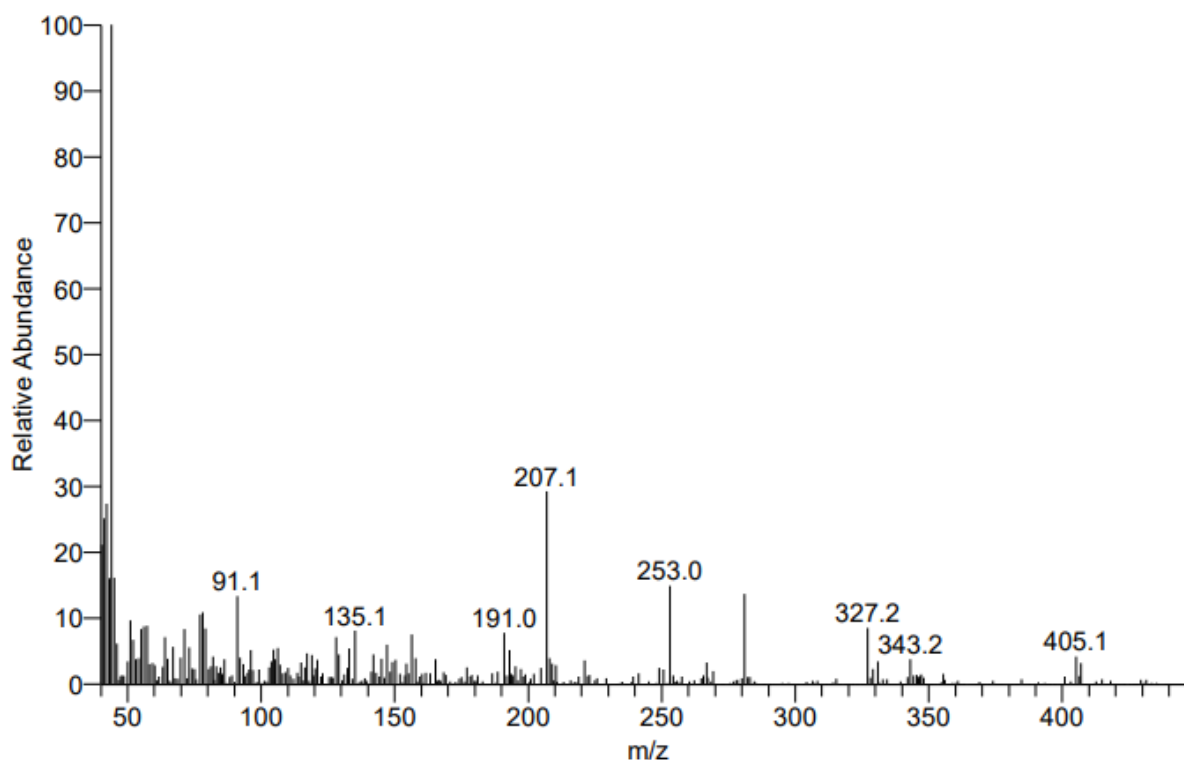


Figure 69: Mass spectrum of ASM eluted at 9.87 min

A sonoproducts were detected at different retention time as illustrated in figure 70. Although several positions of the identified sonoproducts have been found. However, we believe that a dominant position would be the most involved. These products are likely to arise from the direct excitation of Acibenzolar-S-Methyl in the presence of hydroxyl radicals.

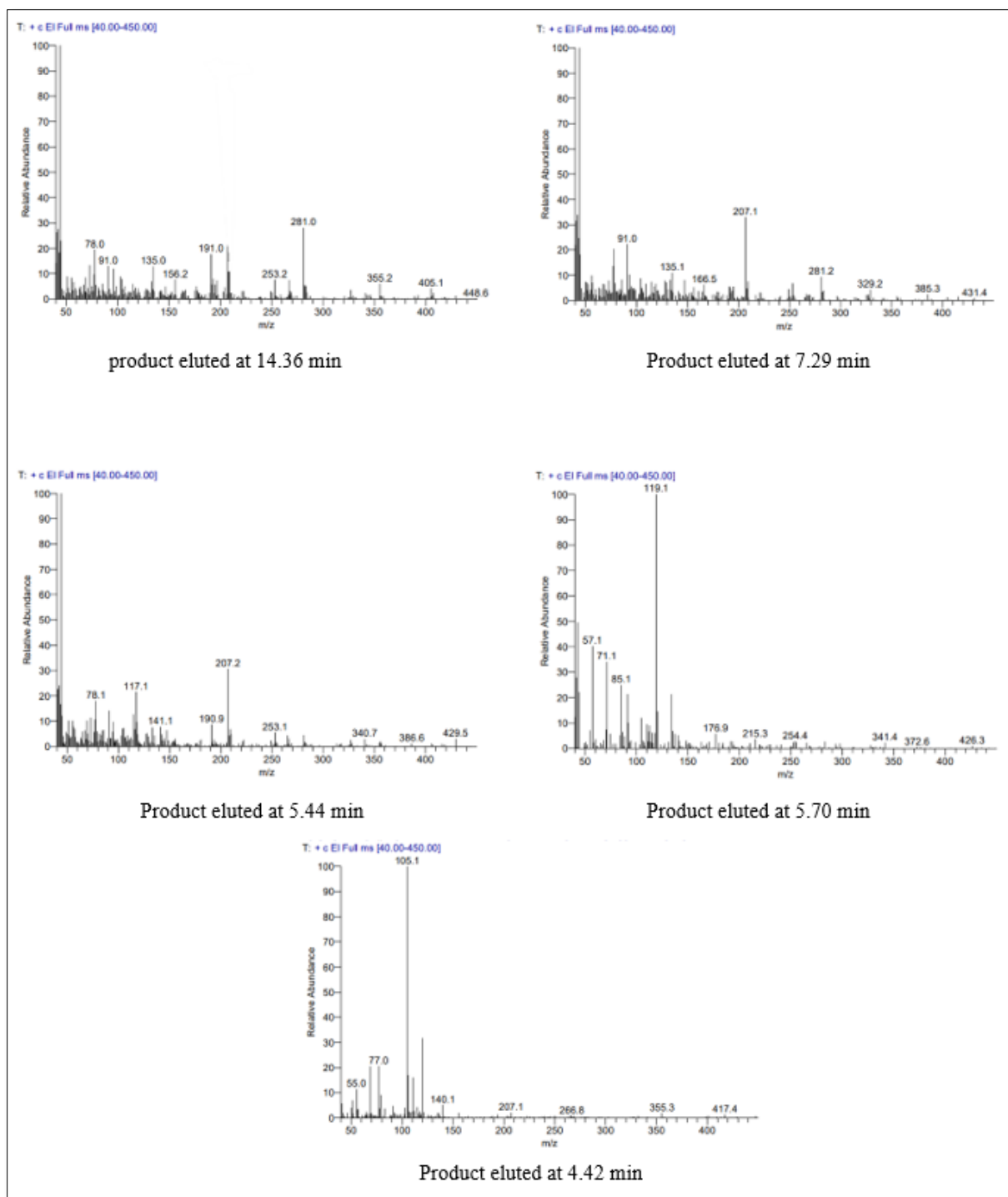
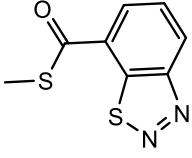
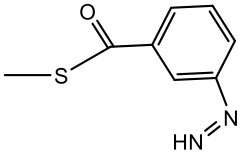
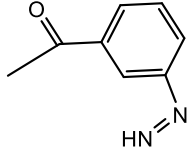
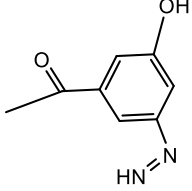
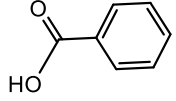
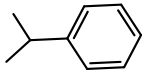


Figure 70: Mass spectrum of different identified Sonoproducts at various retention time.

For more details about metabolites of Acibenzolar-S-Methyl sonocatalytic degradation, Table 11 describes in details the elemental composition of each product that have been identified from their chromatographic profile and according to the molecular ion and mass spectrometry fragmentation peaks.

Table 11: Metabolites of sono-Fenton degradation of ASM according to GC/MS analysis

Compounds	Molecular structure	m/z	Molecular weight	Retention time
ASM		211.99	210	9.87
P1		182.05	180	14.36
P2		148.06	148	7.29
P3		165.06	151	5.44
P4		123.04	122	5.70
P5		121.04	120	4.42

According to the identified intermediates, a possible sonocatalytic degradation pathway of ASM was suggested in Figure 71. The ASM transformation involves an oxidation via hydroxyl radicals. The first step of sonodegradation, the $\bullet\text{OH}$ attacked the sulfate group that yielded the first sonoproduct (benzo[d][1,2,3]thiadiazole-7-carbaldehyde). The P1 oxidized and lost the second sulfate group that produced the P2 (1-(3-diazenylphenyl)ethan-1-one). Afterwards, the compound caught OH that led to five isomers. Moreover, the hydroxyl radicals attacked on the nitrate group and produced P4 Benzoic acid. Hence, the Benzoic acid underwent a deoxygenation that yielded P5 (1-Methylethyl) benzene(propan-2-yl)benzene.

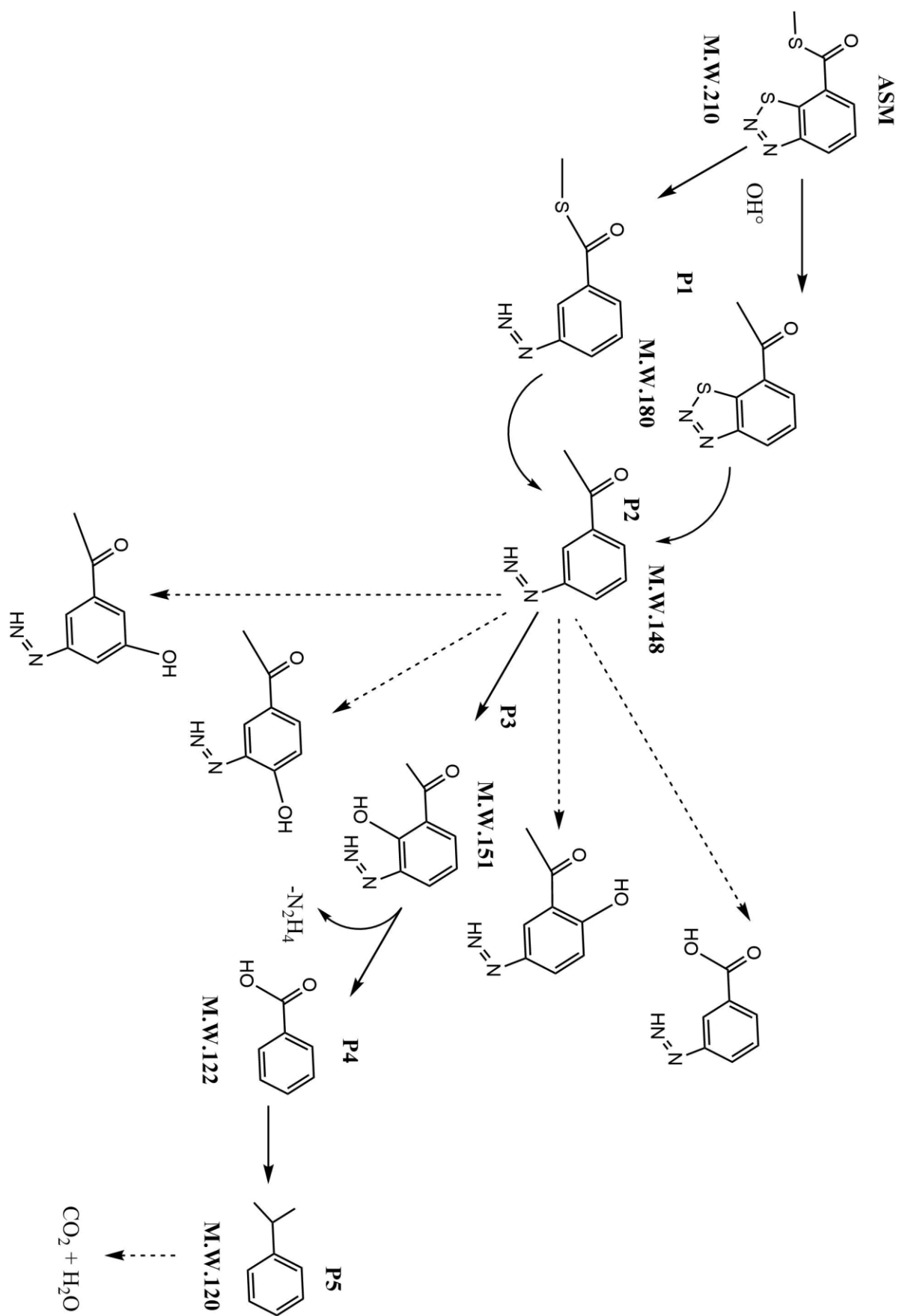


Figure 71: Proposed pathway of sonochemical transformation of ASM

4 Conclusion

The photochemical and sonochemical removal performance of Acibenzolar-S-methyl were investigated under different conditions. The kinetic study was monitored with HPLC analysis technique. The sono-Fenton process found to be the most effective for compound removal (100% within 20 min) compared to other used treatments. The performance was obviously affected by physic-chemical parameters, including pH medium, oxidant dosage and ferrous ions concentration. Finally, based on the extracted samples analysed with GC/MS technique, a series of metabolites were observed that lead to suggest the ASM sonochemical transformation pathway mechanism.

5 References

- [1] N. Valizadeh and D. Hayati, *Journal of Environmental Pollution*. Elsevier Ltd, 2020. doi: 10.1016/j.jclepro.2020.123797.
- [2] F. P. Carvalho, “Pesticides, environment, and food safety,” *Food and Energy Security*, vol. 6, no. 2, pp. 48–60, 2017, doi: 10.1002/fes3.108.
- [3] E. A. Frongillo, H. T. Nguyen, M. D. Smith, and A. Coleman-Jensen, “Food Insecurity Is More Strongly Associated with Poor Subjective Well-Being in More-Developed Countries than in Less-Developed Countries,” *Journal of Nutrition*, vol. 149, no. 2, pp. 330–335, 2019, doi: 10.1093/jn/nxy261.
- [4] D. Valbuena, M. Cely-Santos, and D. Obregón, “Agrochemical pesticide production, trade, and hazard: Narrowing the information gap in Colombia,” *Journal of Environmental Management*, vol. 286, no. March, 2021, doi: 10.1016/j.jenvman.2021.112141.
- [5] M. Shammi *et al.*, “Pesticide exposures towards health and environmental hazard in Bangladesh: A case study on farmers’ perception,” *Journal of the Saudi Society of Agricultural Sciences*, vol. 19, no. 2, pp. 161–173, 2020, doi: 10.1016/j.jssas.2018.08.005.
- [6] V. Silva, H. G. J. Mol, P. Zomer, M. Tienstra, C. J. Ritsema, and V. Geissen, “Pesticide residues in European agricultural soils – A hidden reality unfolded,” *Science of the Total Environment*, vol. 653, pp. 1532–1545, 2019, doi: 10.1016/j.scitotenv.2018.10.441.
- [7] H. Budzinski and M. Couderchet, “Environmental and human health issues related to pesticides: from usage and environmental fate to impact,” *Environmental Science and Pollution Research*, vol. 25, no. 15, pp. 14277–14279, 2018, doi: 10.1007/s11356-018-1738-3.
- [8] E. T. Rodrigues, M. F. Alpendurada, F. Ramos, and M. Â. Pardal, “Environmental and human health risk indicators for agricultural pesticides in estuaries,” *Ecotoxicology and Environmental Safety*, vol. 150, no. October 2017, pp. 224–231, 2018, doi: 10.1016/j.ecoenv.2017.12.047.
- [9] A. Sharma *et al.*, “Worldwide pesticide usage and its impacts on ecosystem,” *SN Applied Sciences*, vol. 1, no. 11, pp. 1–16, 2019, doi: 10.1007/s42452-019-1485-1.
- [10] V. L. Zikankuba, G. Mwanyika, J. E. Ntwenya, A. James, and F. Yildiz, “Pesticide regulations and their malpractice implications on food and environment safety,” *Cogent Food & Agriculture*, vol. 5, no. 1, p. 1601544, 2019, doi: 10.1080/23311932.2019.1601544.
- [11] A. M. Taiwo, “A review of environmental and health effects of organochlorine pesticide residues in Africa,” *Chemosphere*, vol. 220, pp. 1126–1140, 2019, doi: 10.1016/j.chemosphere.2019.01.001.

- [12] M. Ye, J. Beach, J. W. Martin, and A. Senthilselvan, "Pesticide exposures and respiratory health in general populations," *Journal of Environmental Sciences (China)*, vol. 51, pp. 361–370, 2017, doi: 10.1016/j.jes.2016.11.012.
- [13] M. Tudi *et al.*, "Agriculture development, pesticide application and its impact on the environment," *International Journal of Environmental Research and Public Health*, vol. 18, no. 3, pp. 1–24, 2021, doi: 10.3390/ijerph18031112.
- [14] D. la Cecilia, G. M. Porta, F. H. M. Tang, M. Riva, and F. Maggi, "Probabilistic indicators for soil and groundwater contamination risk assessment," *Ecological Indicators*, vol. 115, no. April, p. 106424, 2020, doi: 10.1016/j.ecolind.2020.106424.
- [15] M. C. Campos-Mañas, P. Plaza-Bolaños, A. B. Martínez-Piernas, J. A. Sánchez-Pérez, and A. Agüera, "Determination of pesticide levels in wastewater from an agro-food industry: Target, suspect and transformation product analysis.," *Chemosphere*, vol. 232, pp. 152–163, 2019, doi: 10.1016/j.chemosphere.2019.05.147.
- [16] M. Salgot and M. Folch, "Wastewater treatment and water reuse," *Current Opinion in Environmental Science and Health*, vol. 2, pp. 64–74, 2018, doi: 10.1016/j.coesh.2018.03.005.
- [17] A. Taboada-Santos *et al.*, "Assessment of the fate of organic micropollutants in novel wastewater treatment plant configurations through an empirical mechanistic model," *Science of the Total Environment*, vol. 716, p. 137079, 2020, doi: 10.1016/j.scitotenv.2020.137079.
- [18] R. Guillosoou *et al.*, "Organic micropollutants in a large wastewater treatment plant: What are the benefits of an advanced treatment by activated carbon adsorption in comparison to conventional treatment?," *Chemosphere*, vol. 218, pp. 1050–1060, 2019, doi: 10.1016/j.chemosphere.2018.11.182.
- [19] M. hui Zhang, H. Dong, L. Zhao, D. xi Wang, and D. Meng, "A review on Fenton process for organic wastewater treatment based on optimization perspective," *Science of the Total Environment*, vol. 670, pp. 110–121, 2019, doi: 10.1016/j.scitotenv.2019.03.180.
- [20] K. Paździor, L. Bilińska, and S. Ledakowicz, "A review of the existing and emerging technologies in the combination of AOPs and biological processes in industrial textile wastewater treatment," *Chemical Engineering Journal*, vol. 376, no. December 2018, p. 120597, 2019, doi: 10.1016/j.cej.2018.12.057.
- [21] I. Carra, J. A. Sánchez Pérez, S. Malato, O. Autin, B. Jefferson, and P. Jarvis, "Performance of different advanced oxidation processes for tertiary wastewater treatment to remove the pesticide acetamiprid," *Journal of Chemical Technology and Biotechnology*, vol. 91, no. 1, pp. 72–81, 2016, doi: 10.1002/jctb.4577.
- [22] A. S. Giri and A. K. Golder, "Ciprofloxacin degradation in photo-Fenton and photo-Catalytic processes: Degradation mechanisms and iron chelation," *Journal of Environmental Sciences*, pp. 1–12, 2018, doi: 10.1016/j.jes.2018.09.016.
- [23] R. Yin *et al.*, "Enhanced peroxymonosulfate activation for sulfamethazine degradation by ultrasound irradiation: Performances and mechanisms," *Chemical Engineering Journal*, vol. 335, no. October 2017, pp. 145–153, 2018, doi: 10.1016/j.cej.2017.10.063.

- [24] E. Baştürk and A. Alver, “Modeling azo dye removal by sono-fenton processes using response surface methodology and artificial neural network approaches,” *Journal of Environmental Management*, vol. 248, no. April, 2019, doi: 10.1016/j.jenvman.2019.109300.
- [25] A. Asghar, A. A. A. Raman, and W. M. A. W. Daud, “Advanced oxidation processes for in-situ production of hydrogen peroxide/hydroxyl radical for textile wastewater treatment: A review,” *Journal of Cleaner Production*, vol. 87, no. 1, pp. 826–838, 2015, doi: 10.1016/j.jclepro.2014.09.010.
- [26] H. S. El-desoky, M. M. Ghoneim, R. El-sheikh, and N. M. Zidan, “Oxidation of Levafix CA reactive azo-dyes in industrial wastewater of textile dyeing by electro-generated Fenton ’ s reagent,” vol. 175, pp. 858–865, 2010, doi: 10.1016/j.jhazmat.2009.10.089.
- [27] A. Dargahi, M. Pirsahab, S. Hazrati, M. Fazlzadehdavil, R. Khamutian, and T. Amirian, “Evaluating efficiency of H₂O₂ on removal of organic matter from drinking water,” *Desalination and Water Treatment*, vol. 54, no. 6, pp. 1589–1593, 2015, doi: 10.1080/19443994.2014.889608.
- [28] M. Y. Ghaly, G. Härtel, R. Mayer, and R. Haseneder, “Photochemical oxidation of p-chlorophenol by UV/H₂O₂ and photo-Fenton process. A comparative study,” *Waste Management*, vol. 21, no. 1, pp. 41–47, 2001, doi: 10.1016/S0956-053X(00)00070-2.
- [29] C. Wang and Y. Shih, “Degradation and detoxification of diazinon by sono-Fenton and sono-Fenton-like processes,” *Separation and Purification Technology*, vol. 140, pp. 6–12, 2015, doi: 10.1016/j.seppur.2014.11.005.
- [30] A. Delavaran Shiraz, A. Takdastan, and S. M. Borghei, “Photo-Fenton like degradation of catechol using persulfate activated by UV and ferrous ions: Influencing operational parameters and feasibility studies,” *Journal of Molecular Liquids*, vol. 249, pp. 463–469, 2018, doi: 10.1016/j.molliq.2017.11.045.
- [31] L. G. Devi, S. G. Kumar, K. S. A. Raju, and K. E. Rajashekhar, “Photo-Fenton and photo-Fenton-like processes for the degradation of methyl orange in aqueous medium: Influence of oxidation states of iron,” *Chemical Papers*, vol. 64, no. 3, pp. 378–385, 2010, doi: 10.2478/s11696-010-0011-0.

GENERAL CONCLUSION

The purpose of this dissertation is to give an overview of potential impacts of micropollutants use and exposure, and their hazardous effect on environment. In addition, it was necessary to shed light on wastewater treatment technologies precisely the advanced oxidation processes which provide a large variety of methods. In this work, we focused on photochemical and sonochemical removal of three selected micropollutants, with the aim of optimizing the used processes.

In the first instance, the study of Levafix Blue dye degradation using Fenton and visible light photo-Fenton processes demonstrated a high efficiency. The reaction involves hydroxyl radicals that have been clearly identified and quantified during the treatments. It has been revealed also that the processes depend to different reaction parameters, irradiation intensity, acidic medium, hydrogen peroxide concentration, and low ferrous ions concentration, limiting factors that play crucial role in enhancing or inhibiting the reaction.

In the second part of this research work, we interested in the Fenton-related process for the photocatalytic degradation of one of the selected fungicides, the difenoconazole, a triazole group hazardous chemical used for disease control in fruits, vegetables, and cereals in crops. In this part, we used the Photo-Fenton process based on Ultraviolet light source and synthesized hematite material as photocatalyst. Furthermore, the physico-chemical properties of material were studied based on a series of characterization analysis involving the material particle's structure and size. The photocatalytic performance of process under UV source were tested on degradation of difenoconazole compound monitoring via HPLC analysis, the metabolites have been also identified by GC/MS analysis. The result demonstrates the efficiency of photo-Fenton process at pH 5 with low concentration of hydrogen peroxide and hematite. The study involves the kinetic model of all used treatments, and a scavenger study to confirm the hydroxyl radicals as the main species responsible for oxidation process, also a part dedicated to the quantum yield calculation using the basic ferrioxalate actinometry method.

The final part of our research assessed a comparative study between photochemical and sonochemical process on degradation of fungicide acibenzolar-s-methyl. The photo-Fenton and sono-Fenton processes have confirmed to be efficient under strict conditions of pH, hydrogen peroxide and ferrous ions concentration. The kinetic reaction has been monitoring by HPLC analysis. The Sono-Fenton process has been chosen as the most relevant process, the sono-products have been identified and a transformation mechanism pathway of reaction could be suggested.

This research has investigated a various issues related to Fenton process. Furthermore, additional aspects for future work are recommended below:

The elaboration of new photocatalyst for Fenton-related process based on green resources to minimise the toxicity level of used chemicals. The investigation of photocatalytic performance of these process on a mixture of micropollutants, heavy metals, and/or on real wastewater effluents. The monitoring of transformation mechanism of the mixture will be an interesting part that will reveal the efficacy of treatment on complete mineralization of these hazardous compounds.

SCIENTIFIC CONTRIBUTIONS

1 List of publications

H. Lamkhanter, S. Frindy, Y. Park, M. Sillanpää, and H. Mountacer, “Photocatalytic degradation of fungicide difenoconazole via photo-Fenton process using α -Fe₂O₃,” *Materials Chemistry and Physics*, vol. 267, p. 124713, Jul. 2021.

<https://doi.org/10.1016/J.MATCHEMPHYS.2021.124713>

H. Lamkhanter, F. Z. Ankouri, L. Elayazi, and H. Mountacer, “Visible light degradation of levafix blue dye using Fenton and photo-Fenton processes,” *J. Wat. Env. Sci*, vol. 5, p. 664, 2021 <https://revues.imist.ma/index.php/jwes/article/view/26459/17092> .

H. Lamkhanter, S. Frindy, Y. Park, M. Sillanpää, and H. Mountacer, “Study of Photochemical and Sonochemical Processes Efficiency for Degradation of Acibenzolar-S-Methyl Fungicide in Aqueous Solution,” *Chemistry Africa*, Apr. 2022,

<https://doi.org/10.1007/s42250-022-00355-y> .

2 List of communications

Study of Photochemical and Sonochemical Processes Efficiency for Degradation of Acibenzolar-S-Methyl Fungicide in Aqueous Solution, 3rd International Online-Conference on Nanomaterials, 25th April to 10th May 2022 MDPI platform (*poster*)

Photocatalytic degradation of fungicide difenoconazole via photo-Fenton process using α -Fe₂O₃, Green Chemistry Postgraduate Summer School, 4-9th July 2021, Venice, Italy (*oral*).

Degradation of blue levafix dye under irradiations using Fenton and Photo-Fenton processes, the 6th International Symposium Environment & Sustainable Development, October 2nd-3rd, 2019, Rabat, Morocco (*oral*).

Kinetic Study of Elimination of Blue LEVAFIX Dye from wastewater by Photochemical Process, 5th edition of the national scientific day of Environment and Health, April 18th 2019, Faculty of Sciences & Techniques, Mohammedia, Morocco (*oral*).

Direct and indirect degradation of Blue Levafix dye from aqueous solution using Fenton and Photo -Fenton processes, 2nd edition of The International Conference on Advances in Energy Technologies, Environmental Engineering and Materials Science (AETEEMS), ENSA, December 13– 14th, 2018, El Jadida, Morocco (*poster*).

Removal of Sudan dye from wastewater using Fenton process, 6th edition of "Doctoral Day", Faculty of Sciences and Techniques 05 April 2018, Settat, Morocco (*poster*).

Photochemical Elimination of Some Micropollutants in Aqueous Solution, 5th edition of "Doctoral Day", Faculty of Sciences and Techniques 07 March 2017, Settat, Morocco (*poster*).